Stock assessment of Indian Ocean Bigeye tuna (*Thunnus obsesus*) using Stock Synthesis (2025)

Genevieve A.C. Phillips¹, Giancarlo M. Correa², Agurtzane Urtizberea Ijurco², Gorka Merino² and Dan Fu¹



- 1. Indian Ocean Tuna Commission Secretariat, FAO
- 2. AZTI, Spain, European Union.

CONTENTS

| C | ontents | | 2 |
|----|--|---|----------|
| Li | st of Fi | gures | 4 |
| Li | st of Ta | bles | 7 |
| Ez | xecutive | e summary | 8 |
| | Method Results Catch. Catch t Key se | rates ensitivities enendations for future assessments | |
| A | cknowl | edgements | 13 |
| 1. | Intro | oduction | 14 |
| 2. | Bac | kground | 16 |
| | 2.1. 2.2. 2.3. | Stock structure | 17 |
| 3. | Data | a inputs | 19 |
| | 3.1. 3.2. 3.3. 3.4. 3.5. 3.6. 3.7. 3.8. | General notes Spatial stratification Temporal stratification Definition of model fleets Catch data Abundance indices Length frequency data Tagging data | |
| 4. | Mod | del Description | 41 |
| | 4.1. 4.2. 4.3. | Population dynamics | 46 |
| 5. | Ass | essment model runs | 48 |
| | 5.1. 5.2. 5.3. | Base model | 52 |
| 6. | Mod | delling Results | 55 |
| | 6.1. 6.2. 6.3. 6.4. | Continuity runs from 2022 model Model fits Model estimates. Diagnostics | 57 66 |
| 7. | Sen | sitivity Runs | 76 |
| | 7.1. 7.2. 7.3. | Non-biological parameters Biological parameters Proposed final model options for grid / ensemble | 76 |
| 8. | | ck Status | |

| 8. | 1. | Current status and yields. | 86 |
|------|-------|--|-----|
| 9. | Disc | cussion | 92 |
| 9. | 1. | Recommendations for future assessments | 93 |
| 10. | Refe | erences | 94 |
| 11. | App | endix A: | 99 |
| 12. | App | endix B: CPUE comparison | 105 |
| 12 | 2.1. | Introduction | 105 |
| | | Data and methods | |
| 12 | 2.3. | Catch and effort data | 105 |
| | 2.4. | | |
| 13 | 3.1. | References | |
| Appe | endix | C: Diagnostic table for M sensitivity runs | 114 |
| Appe | endix | D: Diagnostic table for grid models | 115 |

LIST OF FIGURES

| Figure i: Output from the KOBE plots from the ensemble of models in the grid9 |
|--|
| Figure ii: Management outputs from the ensemble of models (grid) used in 2025. Bounds around the |
| main darker line represent the highest and lowest values from the grid of models. The grey band on the |
| |
| catch graph represents estimated optimal catch at MSY (80 % confidence interval). The horizontal rec |
| lines indicate limit or reference points for SSB/SSB _{MSY} and F/F _{MSY} . The red vertical line shows the |
| current year (2025) |
| Figure iii: Estimated raised catches for the Indian Ocean bigeye tuna fishery from 1975-2024 11 |
| Figure 1: Spatial stratification of the Indian Ocean for the four-region assessment model |
| Figure 2: Fishery catches (x 1000 metric tonnes) aggregated by model region and coloured according |
| to fishing fleet in the model24 |
| Figure 3: Fishery catches (metric tonnes) aggregated by year. Note the y-axes differ between plots. Rec |
| lines are catches used in the 2022 assessment. The differences in catch are mainly due to the revision |
| of catch data by Indonesia, although some changes will be due to general improvements in the data |
| quality over time |
| Figure 4: Standardized CPUE series produced in 2019 (red), 2022 (blue), and 2025 (black) |
| Operational-level data were used in the 2019 and 2025 analyses, while aggregated data were used in |
| |
| 2022. Figure taken from Kitakado et al. (2025) |
| Figure 5: Comparison of 2022 (grey) and 2025 (purple) CPUE indices from the joint longline indices |
| from Taiwan (China), Korea, and Japan. |
| Figure 6: Quarterly standardized CPUE index for the long and short time series superposed (Figure |
| taken from Correa et al., 2025) |
| Figure 7: The availability of length sampling data from each fishery by year. The grey circles denote |
| the presence of samples in a specific year (the size indicate number of quarters being sampled). The rec |
| horizontal lines indicate the time period over which each fishery operated |
| Figure 8: Length compositions of bigeye tuna samples aggregated by model fishery34 |
| Figure 9: Mean length (fork length, cm) of bigeye sampled from the principal fisheries by year quarter |
| The grey line represents the fit of a loess smoother to the dataset |
| Figure 10: Location of releases (green) and density of recoveries for the bigeye tuna RTTO-IO tag |
| Program |
| Figure 11: Number of tag releases by quarter and age class (year) included in the assessment data set |
| |
| All tag releases occurred in region 1S. Ages (year) were assigned based on the length of the fish, and |
| updated growth model from Eveson et al. (2025) |
| Figure 12: Bigeye tag recoveries by year/quarter and fishery included in the assessment model. Purse |
| seine tag recoveries have not been corrected for reporting rate |
| Figure 13: Fixed growth functions for bigeye tuna from the 2022 and 2025 assessments (0_base_2022) |
| and <i>4_update_growth</i> respectively) by Farley et al. 2021 and Eveson et al. 2025 (left), and length-based |
| maturity Ogive following Shono et al (2009) (RHS). For the growth functions, the shaded distributions |
| represent the assumed variability of mean size-at-age in the assessment models |
| Figure 14: The different instantaneous rates of natural mortality (M) used in the 2022 ("0 base 2022" |
| "6f_Mbase") and 2025 reference model. The 2025 model uses the Hamel & Cope model, using 14.7 |
| years as the Age _{max} . Age in the graph is in quarters as this is how it is structured in the model45 |
| Figure 15: Spawning biomass trajectories for IO bigeye tuna from the stepwise model updates. (from |
| the 2022 assessment reference model '0 base 2022'). |
| Figure 16: Fits to the joint regional frozen longline CPUE indices (1979-2024) and PS'short' (2010- |
| 2024) in the large and delice models there? |
| 2024) in the base model '6_update_bias'. |
| Figure 17: Standardised residuals from the fits to the CPUE indices from the base mode |
| '6_update_bias' |
| Figure 18: Observed (grey bars) and predicted (red line) length compositions (in 4 cm intervals) for |
| each fishery of bigeye tuna aggregated over time for the base model '6_update_bias'61 |
| Figure 19: A comparison of the observed (grey points) and predicted (red points and line) average fish |
| length (FL, cm) of bigeye tuna by fishery for the main fisheries with length data for the base mode |
| '6_update_bias'62 |

| Figure 20: Estimated age-based (quarters) selectivity for model fleets within the base mode '6 update bias' |
|---|
| Figure 21: Observed and predicted number of tags recovered by quarter for the PSLS fishery in region 1S (PSLS 1S). Only tags at liberty after the four quarter mixing period are included. Tag recoveries are |
| aggregated for each release group. Base model '6_update_bias'64 |
| Figure 22: Observed and predicted number of tags recovered by year/quarter time-period (left), by ago |
| (mid), and by time at liberty (in quarters, right) for main Purse seine and longline fisheries in region 1N |
| and 1S (PSLS 1S, 1N, PSFS 1S, 1N, and LL 1S, 1N) from '6 update bias'. Only tags at liberty after |
| the four-quarter mixing period are included. Tag recoveries are aggregated for each of the regional |
| fisheries |
| Figure 23: Recruitment deviates from the SRR with 95% confidence interval from the base mode |
| '6 update bias' |
| Figure 24: Estimated age specific movement parameters for the base model '6 update bias'69 |
| Figure 25: Tag reporting rates for each fishery from the base model '6 update bias'. Purse seine |
| reporting rates were fixed at a value of 1.0. Reporting rates for the other fisheries were estimated. The |
| grey lines represent the 95% confidence interval for the estimated values |
| Figure 26: Estimated spawning biomass trajectories for the individual model regions from the base |
| model '6 update bias'70 |
| Figure 27: Estimated spawning biomass trajectories for the whole stock from the base mode |
| '6 update bias'70 |
| Figure 28: Trends in fishing mortality (yearly) by fleet for the base model '6_update_bias'71 |
| Figure 29: ASPM analysis for the base model '6 update bias': ASPMfixed (no recruitment deviations) |
| and ASPMrec (recruitment deviates from the reference model added back). Both runs excluded the |
| length composition data and fixed the selectivity parameters |
| Figure 30: Retrospective analysis summary for SSB estimates (t) from the base model '6_update_bias' |
| 74 Fig. 21 Detection of the second of the se |
| Figure 31: Retrospective analysis summary for fishing mortality estimates from the base mode |
| '6_update_bias' |
| Figure 32: Retrospective analysis summary for recruitment estimates from the base mode '6 undete bios' |
| '6_update_bias' |
| Figure 33: SSB (1000 t) estimates from all sensitivity models |
| Figure 35: Retrospectives for all M sensitivity models, for estimates in spawning stock biomass (t) |
| showing Mohn's Rho. Five years of data are removed in these analyses |
| Figure 36: Retrospectives for all M sensitivity models, for fishing mortality (F), showing Mohn's Rho |
| Five years of data are removed in these analyses. |
| Figure 37: Retrospectives for all M sensitivity models, for estimated recruitment, showing Mohn's Rho |
| Five years of data are removed in these analyses. |
| Figure 38: Likelihood profiling (change in -log(likelihood)) for M for one of the models where M was |
| estimated |
| Figure 39: Likelihood profiling (change in -log(likelihood)) for unfished recruitment (R ₀) for the |
| sensitivity models where M varied. Top LH model is the reference model |
| Figure 40: Spawning biomass trajectories (depletion %) from the proposed final model options in the |
| grid |
| Figure 41: Spawning biomass trajectories (1000 t) from the proposed final model options in the grid87 |
| Figure 42: KOBE PLOT FROM GRID RUNS |
| Figure 43: Management outputs from the ensemble of models (grid) used in 2024. Bounds around the |
| main darker line represent the highest and lowest values from the grid of models. The grey band on the |
| catch graph represents estimated optimal catch at MSY (80 % confidence interval). The horizontal rec |
| lines indicate limit or reference points for SSB/SSB _{MSY} and F/F _{MSY} |
| Figure A1: Fits to the LL CPUE index Region 1N from the Somalia catch edition sensitivity run99 |
| Figure A2: Fits to the LL CPUE index Region 1S from the Somalia catch edition sensitivity run99 |
| Figure A3: Fits to the length composition data when the Somalia catches are added to the model. Fits are similar to when the catch data are omitted (in the reference /base model) |
| are surmar to when the eaten data are diffitted (in the reference / base induct) |

| Figure A4: Estimated fraction of recruitment by area from the sensitivity run where recruitment is |
|--|
| allowed to vary between areas (as opposed to being fixed in the reference model). Areas 2 and 4 (region |
| 2 and region 1N) have proportionally higher estimated recruitment than area 1 (region 1S) and area 3 |
| (region 3)101 |
| Figure A5: Fits to the longline CPUE index in region 1S (SURVEY 1; LL1S) when recruitment varies |
| between areas101 |
| Figure A6: Fits to the longline CPUE index in region 1N (SURVEY 4; LL1N) when recruitment varies |
| between areas103 |
| Figure A7: Fits to the aggregated length composition data when recruitment varies between areas. Fits |
| to the LL1N, LL2, LL3 and LINE2 fisheries are worse than in the reference model103 |
| Figure A8: Movement rates of different aged fish between areas when recruitment is allowed to vary |
| between areas. Movement rates are lower than in the reference model, presumably due to the |
| confounding of adult movement and recruitment within the model. Most adult movement in this model |
| is estimated to occur between area 1 (region 1S) and area 3 (region 3) with movement of younger fish |
| from area 4 (region 1N) and area 1 (region 1S). A smaller proportion of adults move from area 3 (region |
| 3, east IO) to area 1 (region 1S), while there is almost no adult movement between area 1 to 4 (adjacent |
| regions 1S and 1N) |

LIST OF TABLES

| Table i: STOCK STATUS INDICATORS FROM MODEL ENSEMBLE9 |
|---|
| Figure iv: Annual joint standardised catch rates (CPUE) for the frozen longline fleets of Japan, Korea, |
| and Taiwan, China from 1975-2024 for each model region. The grey line shows the longline CPUE |
| indices that were included in the 2022 model |
| Table 1: Definition of model fleets within the SS3 model for bigeye tuna in the Indian Ocean, including |
| the gear types used, and region that data are assigned to in the model |
| Table 2: Recent bigeye tuna catches (metric tonnes, t) aggregated by model fleet that have been included |
| in the stock assessment model. The annual catches are presented for 2020- 202422 |
| Table 3: Tag recoveries by year of recovery (box), region of release (number released in bracket), and |
| region of recovery. Region of recovery is defined by the definitions of the fisheries included in the |
| model |
| Table 4: Description of the sequence of model runs to update the 2022 base model |
| Table 5: Main structural assumptions of the bigeye tuna base model and details of estimated parameters. |
| Changes to the 2022 reference model are highlighted in red |
| Table 6: Description of various data inputs and biological parameters that were varied to test model |
| sensitivity to them |
| Table 7: Description of the proposed final model options for the 2025 assessment. The final models |
| consist of a full combination of options below, making a total of 36 models. The options adopted within |
| the reference (base) model ('6_update_bias') are highlighted54 |
| Table 6: Estimates of management quantities for the step-wise updates of the 2022 stock assessment |
| reference model ('0 base 2022') to the 2025 reference model ('6 update bias') |
| Table 9: Estimates of management quantities for the sensitivity testing from the base model options. |
| Current catch (2024) in the model is 82,874 t. Base model is the first model. Internal estimation of M |
| or having M fixed at lower values results in higher estimates of SSB ₀ , and SSB ₂₀₂₄ /SSB ₀ and higher |
| estimates of F ₂₀₂₄ /F _{MSY} . All models estimated C _{MSY} at values higher than current catch |
| Table 10: Estimates of management quantities for the sensitivity testing from the base model options |
| for the addition of Somalia catch, and the inclusion of variable recruitment between areas. Current catch |
| (2024) in the model is 82,874 t. Base model is the first model. Allowing variable recruitment among |
| areas of the model results in higher estimates of of SSB_0 , and SSB_{2024}/SSB_0 and lower estimates of |
| F ₂₀₂₄ /F _{MSY} . Addition of the Somalia catch resulted in higher estimate of SSB ₀ and SSB ₂₀₂₄ /SSB ₀ but a |
| similar estimate of F_{2024}/F_{MSY} . All models estimated C_{MSY} at values higher than current catch79 |
| Table 10 Estimates of management quantities for the stock assessment model options. Current yield |
| (mt) represents yield in 2024 corresponding to fishing mortality at the FMSY level |
| Table 11: STOCK STATUS INDICATORS FROM MODEL ENSEMBLE |
| · · · · · · · · · · · · · · · · · · · |

EXECUTIVE SUMMARY

Introduction

Bigeye tuna (*Thunnus obesus*) is a large pelagic predatory fish found mainly in tropical waters throughout the Indian Ocean where they form a single genetic stock. Bigeye tuna can live for up to 15 years, and reach a maximum size of approximately 250 cm, with a maximum weight of over 210 kg. Sexual maturity is reached at between 100 to 125 cm (approximately three to four years of age).

The stock assessment for bigeye tuna in the Indian Ocean is commissioned every three years, according to the schedule set out within the workplan of the Working Party for Tropical Tunas (WPTT) within the Indian Ocean Tuna Commission (IOTC). In 2025, the stock assessment is based on an update of the 2022 stock assessment model and is a spatially structured age-based integrated model that uses catch rate indices, length-compositions, and tagging data to inform estimates of spawning stock biomass (SSB) and fishing mortality (F), relative to estimated maximum sustainable yield (MSY).

The assessment was completed using Stock Synthesis 3.30 and incorporates all newly available data since the previous assessment, including updated catch data, abundance indices, and updated age and length data that informs a newly estimated growth curve for bigeye tuna in the Indian Ocean.

Methods

The Stock Synthesis 3.30 (SS3.30) assessment model covers the period 1975-2024 and assumes that the Indian Ocean bigeye tuna constitute a single genetic stock, modelled as spatially disaggregated four regions, with 24 fleets. Standardised catch per unit effort (CPUE) series from the main longline fleets (1975-2024), and two purse seine fleets (2010-2024) were included in the model as relative abundance indices of exploitable biomass in each region. Tagging data from a regional tagging program were included to inform abundance, movement, and mortality rates.

Several sensitivities were run as outlined in the data preparatory meeting in May 2025 (27th Meeting of the WPTT) to explore the effects of alternative model assumptions (e.g. changes to estimation methods for natural mortality (M), and growth model parameterisation), and the impact of the inclusion or exclusion of specific datasets (e.g. the inclusion or not of the purse seine CPUE). After sensitivity analyses, and running of diagnostics, including running retrospectives, and age-structured production models (ASPM), the catch data were updated, following a late submission of catch data from Indonesia. The model published in the 'preliminary' assessment included a version of the catch data that were based on the best scientific estimates of Indonesian bigeye tuna catch but were not the official records provided to the Secretariat. On the first day of the 27th WPTT(AS), it was agreed to update the model with the submitted catches.

The model was re-run using this data, and several scenarios were run to characterise the uncertainty in the instantaneous rate of natural mortality (M), as the model is most sensitive to changes in this parameter. After discussions, and assessing various diagnostics, the group chose the reference model with which to run the grid ('6 update bias').

To account for uncertainty within specific model parameters, several model options were then run using the base model in a 'grid' of models using a combination of plausible options for these parameters. This included three options for the steepness parameter (h), three options for the instantaneous rate of natural mortality (M), and two options for selectivity in two frozen longline fleets (LL2 and LL3), and two options for gear creep (catchability). This led to a total of 36 model options in the grid runs that cover an appropriate range of uncertainty in the base model parameterisation.

Results

In 2025, the overall stock status for bigeye tuna in the Indian Ocean is that the stock is **not overfished** and **not subject to overfishing** with a likelihood of 45.6 % of being in the green KOBE quadrant (Figure i, Table i) over an ensemble of 36 models that encompass the main uncertainties within the model. The base model in the figure is 'io h80 Gnew MBase2025 sD LL'.

Table i: STOCK STATUS INDICATORS FROM MODEL ENSEMBLE

| Catch in 2024: | 82,874 t |
|---|------------------|
| Average catch 2020–2024: | 87,721 t |
| MSY (1000 t) (plausible range): | 100 (94-106) |
| F _{MSY} | 0.27 (0.21-0.33) |
| SSB ₀ (1000 t) (80% CI): | 985 (623-1346) |
| SSB ₂₀₂₄ (1000 t) (80% CI): | 266 (172-359) |
| SSB_{MSY} | 276 (143-409) |
| SSB ₂₀₂₄ /SSB ₀ (80% CI): | 0.27 (0.23-0.32) |
| SSB ₂₀₂₄ / SSB _{MSY} | 1.02 (0.75-1.29) |
| F ₂₀₂₄ / F _{MSY} | 0.94 (0.69-1.19) |

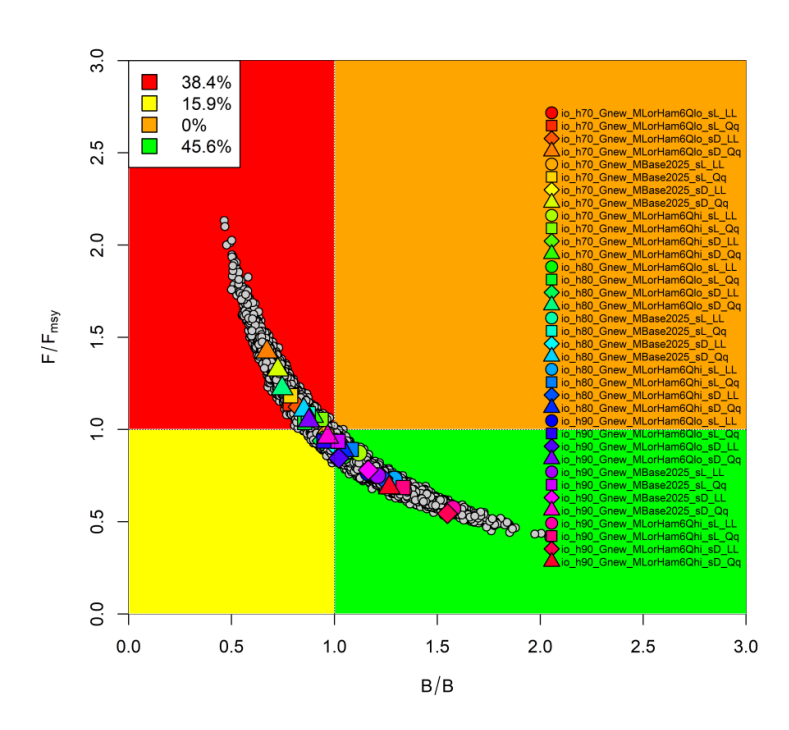


Figure i: Output from the KOBE plots from the ensemble of models in the grid.

In the 2022 assessment (using data up to 2021) the model ensemble estimated that the stock was **overfished** and **subject to overfishing** in 2021, this was a change from the 2019 assessment when the stock was estimated to be **not overfished** but subject to **overfishing**.

The estimated biomass trajectory shows a decline from exploited but equilibrium spawning stock biomass levels in 1975 to 2012 (Figure 43). Biomass levels appear to have stabilised after a decline from 2012 to 2021 and are increasing in the final years of the model, providing a more positive outlook for the stock, presumably as there are now several years of catch at or below that of MSY and fishing mortality is cycling around and above that of F/F_{MSY} . As there is a significant lack of representative biological data (length data, and representative ages), the model is forced to fit closely to the main abundance indices from the longline fleets. As there have been increases in these indices in the three

most recent years (2022-2024 inclusive), alongside decreased catches, the CPUE indices alongside lower catches are driving the increase in estimated biomass in the model.

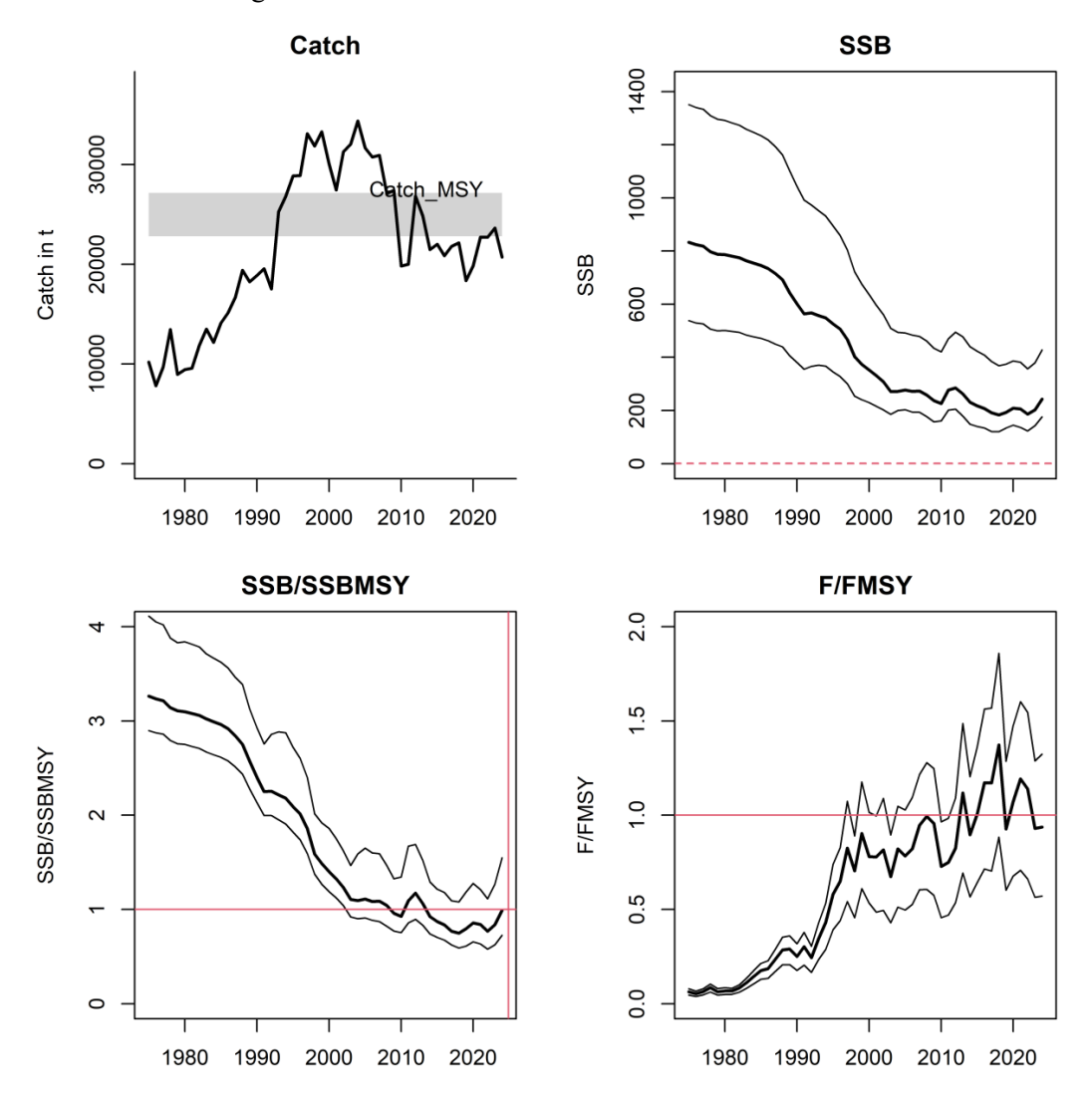


Figure ii: Management outputs from the ensemble of models (grid) used in 2025. Bounds around the main darker line represent the highest and lowest values from the grid of models. The grey band on the catch graph represents estimated optimal catch at MSY (80 % confidence interval). The horizontal red lines indicate limit or reference points for SSB/SSB_{MSY} and F/F_{MSY} . The red vertical line shows the current year (2025).

Catch

In the three years since the previous assessment, total catch has averaged 89,432 tonnes per year from all fleets within the fishery (Figure iii). Approximately 30 % of catch was taken by frozen longliners (LL) and 29 % by PSLS vessels in 2024.

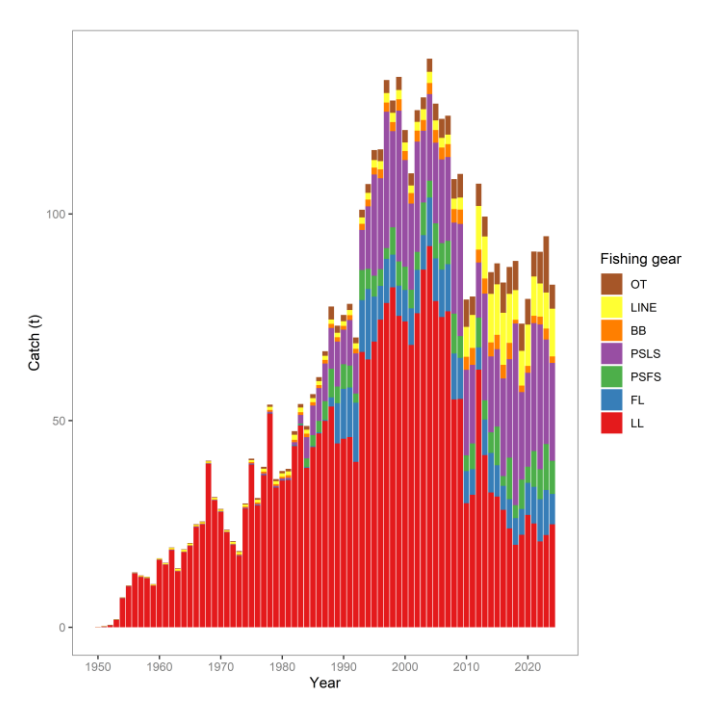


Figure iii: Estimated raised catches for the Indian Ocean bigeye tuna fishery from 1975-2024.

Catch rates

Standardised catch rates included in the base model are a joint-CPUE provided by Japan, Taiwan (China), and Korea, based on catches from frozen longline fleets (Figure iv). Detailed methods for these indices can be found in the documents provided at the 27th Working Group for Tropical Tunas (Data Preparatory) in May 2025.

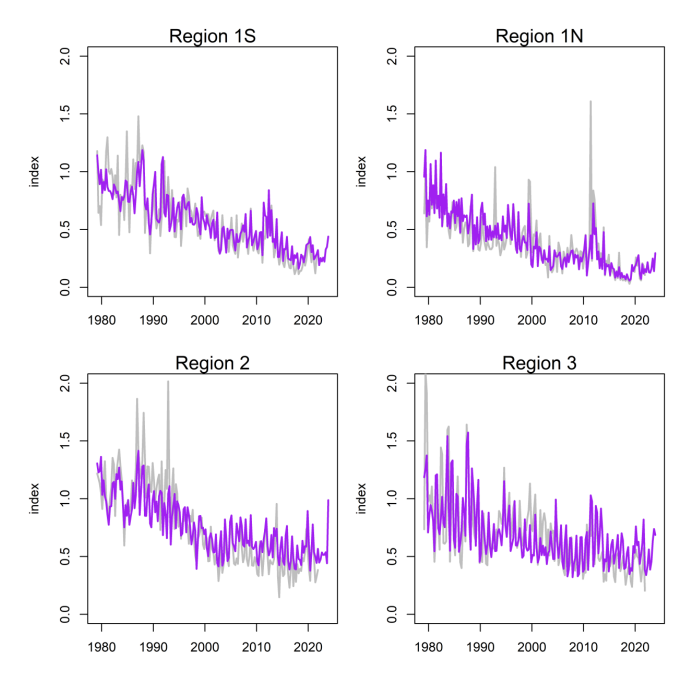


Figure iv: Annual joint standardised catch rates (CPUE) for the frozen longline fleets of Japan, Korea, and Taiwan, China from 1975-2024 for each model region. The grey line shows the longline CPUE indices that were included in the 2022 model.

Key sensitivities

The model was most sensitive to changes to the estimated instantaneous rate of natural mortality (M), and a change in the growth estimation to the newer estimates of age-at-length for bigeye tuna provided in 2025. The addition of the most recent longline CPUE indices also provided a more positive outlook on the stock than the previous indices. The model was relatively insensitive to the addition of the purse seine CPUE indices.

The model was sensitive to different catch scenarios – as shown when moving to the new catches provided by Indonesia, and by an additional post-meeting run of the model that included catches submitted by Somalia for 2024. This raises an important point of ensuring accurate catches are used in the model.

Recommendations for future assessments

A summary of recommendations for future assessments of bigeye tuna in the Indian Ocean are provided below. This can be added to during the assessment meeting.

- Improved quality and quantity of length composition data: It is recommended that improvements in both quantity and quality of length frequency data are provided to the Secretariat prior to the next assessment of bigeye tuna in 2028, and that any length data omitted in this assessment are reassessed for suitability and inclusion in 2028. Results from a recent consultancy with Dr. Paul Medley may inform the next BET assessment, alongside other tropical tuna stock assessments. Additionally, a detailed investigation of current included length frequency data, particularly those in the purse seine fisheries may provide a better understanding of why the model is underfitting to the mean length data in these fisheries.
- Further development of additional abundance indices: as with other tuna assessments in the IOTC, the abundance indices are not representative of the total extent of the tuna fishery and associated catch data used in the assessment. There is additional concern regarding the contracting spatial extent of Korean and Japanese frozen longline fleets. It is recommended that other CPCs develop CPUE series for consideration in stock assessment of bigeye tuna. Standardised CPUE indices can either be included in an integrated modelling platform or contribute to overall knowledge of various components of the stock. Development of appropriate CPUE standardisations can be supported by the Secretariat or completed by the Secretariat (if appropriate operational data are provided).
- Ageing data: Currently there are a total of 253 data points for BET within the assessment model. This represents a minute percentage of the fish being caught. The samples cover only a few years of fishing, all within the last 10 years. It is strongly recommended that more fish are aged, encompassing both male and female fish, from all length-bins across the spatial extent of the fishery, to build a reasonable timeseries of biologically informative data. Age data should be accompanied by detailed information on the source of the fish (e.g. time, date, location, sex, fishing gear, vessel flag etc.) if the data are to be used to either estimate age-at-length within the model (as data need to be allocated to appropriate timesteps, model areas, and model fleets) or to account for changes in age-at-length over time or space (due to population dynamics, environmental factors, such as climate change or high fishing effort).
- Research into recruitment variability: In this iteration of the BET stock assessment model, area-based recruitment was fixed (not estimated by the model), resulting in high estimates of adult movement between the areas. It is unlikely that recruitment is equal in all areas, but further research (and/or analyses of published research) is required to ensure that parameterisation of area-based recruitment is based on biological information, and not on the longline CPUE indices (as in previous models), which are unlikely to be an index of recruitment.
- Characterisation of model fleets: Over time, the gear types and catch composition have changed, possibly resulting in model fleets that contain inconsistent selectivity and/or targeting practices. This was identified in particular for the BB1N fishery during the 27th WPTT(AS), and the 2028 assessment would benefit from investigating model fleet composition.

ACKNOWLEDGEMENTS

This stock assessment was informed by previous assessments of bigeye tuna (*Thunnus obesus*) in the Indian Ocean, and from reading reports of recent assessments undertaken by the International Commission for the Conservation of Atlantic Tunas (ICCAT), the Western and Central Pacific Fisheries Commission (WCPFC), and the Inter-American Tropical Tuna Commission (IATTC) in the Atlantic, Western Pacific, and Eastern Pacific Oceans respectively. The 27th meeting of the Working Group for Tropical Tunas in May 2025 (Data Preparatory meeting) provided the starting input parameters, and various scenarios to test for model sensitivities, alongside possibilities for the final grid of models presented in this report, that will be discussed and finalised at the 27th meeting of the Working Group for Tropical Tunas (Assessment meeting) in October 2025, in Seychelles.

The assessment benefited greatly from updated ageing data provided by Dr. Paige Eveson, Dr. Jessica Farley, and the team at the Commonwealth Scientific and Industrial Research Organisation of Australia (CSIRO), and from updated abundance indices (catch per unit effort (CPUE)) from longline vessels (joint CPUE from Japan, Taiwan(China), and Korea), and purse seine vessels (CPUE lead by European Union (Spain), at AZTI).

The abundance index for the longline fleet was developed as a collaborative effort between three nations, and the presence of observers (Dr. Gorka Merino, Dr. Simon Hoyle, Dr. Genevieve Phillips), and the authors of the assessment would like to acknowledge the efforts of this group in developing, reviewing, and producing three separate species' abundance indices in one year.

The assessment was greatly assisted by active discussions at the 27th meeting of the Working Group for Tropical Tunas in May 2025 (Data Preparatory meeting), and the Assessment meeting in October 2025. We acknowledge and are grateful for the preparation, and on-going active participation of all participants during these meetings.

We thank all the observers who collect and provide biological data for the assessment of tuna stocks in the IOTC Area of Competence, the IOTC Data Team for providing data to allow for a complete assessment of the stock, and previous stock assessment scientists at the IOTC for their code, and previous models which form the basis of this assessment.

1. INTRODUCTION

This paper presents the 2025 stock assessment of bigeye tuna (*Thunnus obesus*; BET) in the Indian Ocean (IO). As in previous assessments, the objectives of the 2025 bigeye tuna assessment are to estimate population level parameters which indicate the stock status and the impacts of fishing, such as time series of recruitment, spawning stock biomass, biomass depletion, and fishing mortality. The stock status is summarised using reference points that are adopted by the Indian Ocean Tuna Commission (IOTC).

The current assessment is carried out using the stock assessment framework Stock Synthesis 3.30 (Methot, 2013, Methot & Werner, 2013) using a length-based, age- and spatially structured population model. Previous stock assessments have also been conducted using Stock Synthesis (Shono et al. 2009; Kolody et al. 2010, Langley et al., 2013a, 2013b, 2016; Fu, 2019, Fu et al, 2022) and ASPM (Age-Structured Production Model) in 2011 (Nishida & Rademeyer, 2011). A summary of previous models from the last four stock assessments follows.

In 2013, there was a thorough examination of the key model assumptions, and the outputs from the assessment provided the basis for the management advice for bigeye tuna during the 15th Working Party for Tropical Tunas (WPTT15). However, the spatial dynamics of these models were not considered to adequately represent the dynamics of the stock, specifically the regional distribution of biomass, and the movement dynamics. Sensitivity runs suggested the model was sensitive to the spatial structure of the model (one or three regions), the tag mixing period (four or eight quarters), and the relative weighting of the length-frequency data. The final assessment models did not incorporate the available tagging data due to these issues.

In 2016, therefore, the stock assessment included a review of the spatial stratification and parameterisation of the models so that the tagging data could be integrated into the model [Langley, 2016; IOTC 2016]. The 2016 assessment model utilised the new composite longline catch per unit effort (CPUE) indices derived from the main distant water longline fleets, replacing the Japanese longline CPUE indices used in the previous assessment. A range of sensitivity runs were conducted, relating to natural mortality (M), selectivity and stock-recruitment (h) steepness. As such, the final assessment captured the uncertainty in the stock recruitment relationship (SRR), and the influence of the tagging data on the outputs. In 2016, the model estimated spawning stock biomass (SSB) to be above the SSB at maximum sustainable yield (MSY; SSB_{MSY}). Fishing mortality (F) was estimated to be below the level that can be sustained at maximum sustainable yield (F_{MSY}).

In 2019, the assessment adopted a new regional weighting scheme for the longline CPUE indices based on comprehensive analyses and also adopted a revised procedure to correct for tag loss and reporting. The assessment model estimated a significant increase in fishing mortality (F) in 2018, driven by an increase in catches from the European Union (EU) purse seine fish aggregating device associated (FAD) fishery in 2018. The Working Party for Tropical Tunas (WPTT) considered this was primarily due to a change in the estimation of species composition for catches reported by the EU purse seine fleet in 2018, rather than an increase in bigeye tuna catch specifically (IOTC 2019a). The magnitude of catch increase was not considered accurate.

To incorporate catch from EU (Spain) purse seine fisheries in 2018 into the model, the catch was revised by attributing the species composition recorded in the EU (Spain) purse seine catches in 2017 to the total catches of bigeye from the EU (Spain) in 2018 see IOTC 2019a for further details.

The final assessment adopted an ensemble of 12 models that covered major components of structural uncertainty to characterise the stock status and predict future scenarios (IOTC 2019a). In 2019, the assessment estimated that the spawning stock biomass in 2018 was above SSB_{MSY} , but the fishing mortality was above F_{MSY} . The stock was determined to be **not overfished** but **experiencing overfishing**.

In 2022, the IOTC adopted a Management Procedure (MP) for recommending the Total Allowable Catch (TAC) for bigeye tuna [Resolution 22/03]. The MP contains a harvest control rule that determines the TAC for the next three years, is based on pre-agreed data inputs, and is required to be run by the Scientific Committee (SC) along a pre-arranged schedule (Williams 2021a; Resolution 22/03). As such,

the stock assessment no longer provides TAC advice, but does provide information on bigeye tuna stock status, which can be used to evaluate the performance of the MP (Williams et al., 2021b). The MP was run in 2025 (Williams et al., 2025), and an evaluation of the exceptional circumstances was presented at the same meeting (Preece et al., 2025).

In the 2025 assessment, there are only a few changes and/or improvements to the analysis in addition to the usual updates to the data. The changes are discussed in detail in the relevant sections of the report and included here briefly for clarity. The model development included testing various methods, including:

- Internal estimation of natural mortality, and application of the Lorenzen form of natural mortality (recommendation in the 2023 CAPAM Tuna Good Practices Workshop). This was carried out by the WCPFC assessment of bigeye tuna in 2023 and the ICCAT assessment of bigeye tuna in 2025.
- An update to growth parameters from a new ageing study (Eveson et al., 2025) that builds on the results presented prior to the 2022 assessment, including changing the model structure from a von Bertalanffy growth model with age-specific *k* parameters to a classical von Bertalanffy growth model.
- Internal estimation of growth parameters was tested to understand the sensitivity of the model to this method (using conditional-age-at-length, CAAL within Stock Synthesis), and to check for any potential model misspecification with relation to growth parameters currently estimated externally.
- Inclusion of both the updated joint CPUE longline indices from Japan, Korea, and Taiwan (China), and European (Spain) purse seine CPUE indices from tuna associated sets in two regions of the model.

Most of these sensitivity runs are included in rev2 of the report, and the initial presentation of the stock assessment at the 27^{th} WPTT(AS). On the first day of the assessment meeting, a new, updated catch dataset were presented to the WP by the IOTC Secretariat. This dataset included revised catches from Indonesia that reduced the catches in 2023 and 2024 by a total of $\sim 20,000$ t. It was agreed by the 27^{th} WPTT(AS) to use this new catch dataset in the 2025 assessment.

The assessment was re-run, including a range of sensitivity runs that focussed on the key biological parameter that the model is sensitive to (M), and these sensitivities runs are outlined in this report. A grid of models was developed around a reference model, and 36 models were run to determine the stock status. On the last morning of the meeting, directly after presenting the final grid run, an error was found in half of the models in the grid, requiring the grid to be re-run. Due to time constraints, this was completed in an intersessional period, alongside two new sensitivity runs that encompassed some additional concerns by the 27th WPTT(AS). The first sensitivity was the inclusion of catch data submitted in 2024 by Somalia (the first such data to be submitted for bigeye tuna, representing 4,100 t in the terminal year (2024) of the assessment. The second sensitivity run was allowing recruitment to vary between the four areas of the model (as opposed to being fixed proportionally between the four areas, as in the reference model). These runs, and results are described in detail in the report and are to be presented at an intersessional meeting of the WPTT on 5th November 2025.

In February 2025, the MP for bigeye tuna was run (Williams et al., 2025), and the TAC was increased and endorsed by a special convening of the Scientific Committee. The TAC increase was capped by the 15 % rule, within the MP, whereby the TAC cannot be increased by more than 15 % of the prior TAC to provide precaution within the harvest control rule.

In summary, this report documents the final iteration of the 2025 stock assessment of the Indian Ocean bigeye tuna stock after consideration of various models during the 27^{th} WPTT(AS) held in Seychelles, in October 2025. The stock assessment is based on the 2022 modelling framework and has incorporated revised and updated data up to the end of 2024, and newly available biological information. The assessment implements a length-based, age-structured and spatially explicit population model fitted to catch per unit effort (CPUE, abundance indices), length composition data, and tagging data. The assessment is implemented in Stock Synthesis (v3.30.24).

2. BACKGROUND

2.1. Stock structure

Bigeye tuna (*Thunnus obesus*, Lowe 1839) is distributed across tropical and subtropical waters across the Atlantic, Indian, and Pacific oceans, while being absent from the Mediterranean. Indian Ocean bigeye tuna are genetically distinct populations from those in the Atlantic, with minimal mixing of adults (Chow et al., 2000, Grewe et al., 2019).

Tagging data from the Regional Tuna Tagging Project-Indian Ocean (RTTP-IO) phase of the Indian Ocean Tuna Tagging Programme (IOTTP) suggest that bigeye tuna migrate quickly and there may be some basin-scale movements, however the limited distribution of tag releases, and small number of returns from vessels external to the European Union (EU) and Seychelles (SEY) purse seine fleets operating in the western equatorial Indian Ocean makes it difficult to quantify large-scale population movements. While there may be some relatively discreet sub-populations, or slow mixing rates among sub-regions, there is no evidence that this is the case in the core area where most of the catch is taken, and presumably where the bulk of the population is located.

Current differences in estimates of growth between oceans supports the hypothesis that there are separate bigeye tuna stocks in the Indian and Pacific Oceans (Farley et al. 2004). Genetic studies indicate that bigeye tuna form a single stock in the Indian Ocean, which is not connected to stocks in the Pacific or Atlantic Oceans (Appleyard et al. 2002; Chiang et al. 2008; Díaz-Arce et al. 2020). Based on tagging data, and current genetic knowledge, the current assessment assumes the Indian Ocean bigeye tuna consists of a single panmitic population and is assessed as a single stock.

In the Pacific Ocean, there have been extensive tagging and genetic studies lead by the Secretariat of the Pacific Community (SPC) and the Inter-American Tropical Tuna Commission (IATTC) (Schaefer et al., 2015; Moore et al., 2020). The tagging studies identify that most tagged fish remained within the general area of release (within 1,500 nautical miles), however some fish move large distances across the Pacific Ocean (> 4,000 nautical miles) presumably mixing with individuals from other regions and thereby reducing the probability of broad-scale genetic structure (Day et al., 2023). There is some evidence of differences in population dynamics across the Pacific Ocean (e.g. growth rates increase from west to east) which would be important to account for in stock assessment structure, however a review of all genetic and non-genetic information on bigeye tuna stock structure in the Pacific found there to be one stock within the Pacific Ocean (Hamer et al., 2023). Similar data are not available for the bigeye tuna in the Indian Ocean as of 2025, however the assessment would benefit from increased information on population structure.

Although there is no population structure within the Indian Ocean bigeye tuna stock assessment (e.g. differential growth, natural mortality), the model partitions the data into regions to account for differences in fishery dynamics (Figure 1).

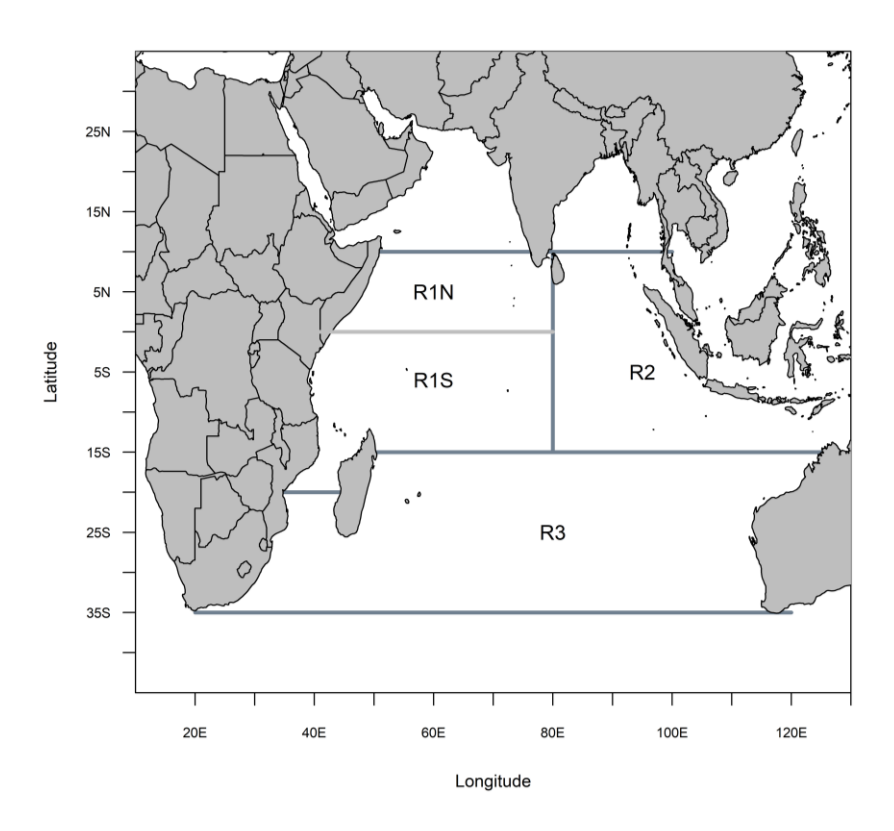


Figure 1: Spatial stratification of the Indian Ocean for the four-region assessment model.

2.2. Biology

Bigeye tuna, *Thunnus obesus* (Lowe, 1839) are large, highly migratory pelagic-oceanic fish within the *Scombaridae* (mackerels, tunas, bonitos). They are relatively fast-growing and have a maximum fork length (FL) of approximately 200 cm (Aires-da Silva et al., 2015; Farley et al., 2017) with an estimated average maximum length of between 169.2 to 172.7 cm in the Indian Ocean (Eveson et al., 2025). There have been two recent studies into growth information for bigeye (Farley et al., 2021; Eveson et al., 2025) which build on initial studies of otoliths (Eveson et al., 2012) and the most recent results presented at the 27^{th} Working Party for Tropical Tunas (Data Preparatory) are incorporated into this assessment, with sensitivity runs to test the impact of changing the form of the growth curve (from a VB log k growth model in 2022 to a von Bertalanffy model in 2025).

The most recent study of age-at-length used ages from 253 tuna, mostly from the north-west Indian Ocean (142 samples) and builds on a study from 2021 where otoliths were collected as part of the 'GERUNDIO' project, using a new method developed to estimate the age of tuna from daily and annual growth zones within otoliths. The new estimates again represent a size-at-age that is slightly larger than the previous assessment, with a slightly longer mean asymptotic length (L^{∞} =169.2-172.7 cm compared to 168 cm FL). There was some evidence of differences between male and female growth curves (Eveson et al., 2025), however more data are required to understand whether this is a true difference, or an artefact of sampling design. This is an area of which requires more research to fully understand the population variation in growth in bigeye tuna.

Bigeye tuna are assumed to attain maturity from 100 cm FL and reach full sexual maturity at 125 cm FL (Shono et al., 2009). Bigeye tuna are hypothesised to be continuous spawners, meaning that when conditions are suitable, they spawn almost daily (Sun et al., 2013). Peaks in spawning have been recorded during the first and fourth quarters of the calendar year (Kume et al., 1971; Sun et al., 2013). Eggs and larvae are pelagic, presumably allowing for genetic mixing throughout the Indian Ocean as tagging studies in both the Indian and Pacific Oceans have showed that adult tuna only really mix with adjacent individuals (Schefer et al., 2015; GERUNDIO Project, IOTC), however Pacific studies suggest that some individuals make very large movements (> 4000 nautical miles; Moore et al., 2020), suggesting long distance movements in adult Indian Ocean bigeye tuna are likely.

Bigeye recruitment remains uncertain as the areas where larvae and early juveniles are concentrated have never been sampled nor studied by scientists (Fonteneau 2004). While the temperate regions are generally believed to be feeding grounds, recruitment is assumed to occur in all regions (hence differentiating between recruitment into the population, vs. spawning).

The instantaneous rate of natural mortality (M) of bigeye tuna is likely to vary with size, as with other tropical tunas (Fonteneau & Pallares, 2004), with a relatively high natural mortality for younger fish, and a lower natural mortality for older fish. From the Regional Tuna Tagging Project (RTTP) data, many tagged fish were captured after 7–8 years at liberty, indicating a considerable proportion of the tagged fish had reached an age of 8–10 years; 8 tags were recovered after 10 years at liberty and a few tags were recovered during the last year (2015), corresponding to an age at recovery of 11–12 years. An aging study of bigeye tuna in the eastern and western Australia waters suggested the longevity of bigeye is more than the 8–10 years which were the maximum age commonly thought (Farley et al. 2004).

There is no additional information on the oldest bigeye tuna since the previous assessment, so this remains at 14.7 years old (Farley et al., 2020).

2.3. Indian Ocean bigeye tuna fishery overview

Bigeye tuna is an important species within tuna fisheries in the Indian Ocean. As with other tuna fisheries, larger individuals are targeted by longliners, while smaller individuals are caught by purse seine vessels utilising Fish Aggregating Devices (FADs) (Fonteneau 2004). The distant-water longline fishery for bigeye tuna started operation in the Indian Ocean during the early 1950s.

The distant-water longline fishery commenced operation in the Indian Ocean during the early 1950s. At the start of the fishery, bigeye tuna represented a significant component of the total catch from the longline fishery and catches increased steadily over the subsequent decades, reaching a peak in the late 1990s-early 2000s. The purse-seine fisheries and fresh-chilled longline fisheries developed from the mid-1980s, and total bigeye tuna catches peaked at about 150,000 t in the late 1990s (Figure 2). During the mid-2000s, the total annual bigeye catch declined considerably, primarily due to a decline in the longline catch in the western equatorial region in response to the threat of piracy off the Somali coast. The total annual catch declined to around 79,000 t in 2010 but recovered somewhat over the following years, reaching around 107,000 t in 2012. The total annual catch has declined since then and was 88,615 t in 2018 (there were exceptionally high catches from the purse seine fisheries during 2018 which were potentially biased by changes in data processing methodologies confirmed by the EU (Spain) for its purse seine fleet for that year, see IOTC 2019 a, b. These catches have been corrected in subsequent assessments). The annual catch decreased in 2019, but increased in 2020, and was around 95 022 t in 2021 before revisions to catch by Indonesia. The revised total catch for 2021 is approximately 90,882 t, and this remained steady in 2022 at 90,836 t. The first two iterations of the bigeye assessment in 2025 (IOTC-2025-WPTT27-15-BET rev1, IOTC-2025-WPTT27-15-BET rev2) used catches of 105,209 t in 2023 and 101,722 t in 2024. The revisions to catches by Indonesia reduced these totals in line with the long-term average, and total bigeve catches in the model are 94,591 t in 2023, and 82,874 t in 2024.

The 2023-2024 catches are in the same range as catches for the previous five years, although the catch is more evenly distributed among different fishing gears compared to the domination of the frozen longline fleets seen in previous decades.

During the mid-1970s, the target species of Japanese longliners rapidly shifted from yellowfin tuna to bigeye tuna, accompanied by the introduction of deep-freezing technology that increased the value of Sashimi-grade bigeye (Okamoto 2005). However, since the 1990s, the bigeye component of tropical tuna catches has decreased, and the catch of yellowfin tuna now exceeds that of bigeye for the Japanese fleet. These changes in catch composition were thought to be caused by fleet dynamics whereby a shift in spatial effort occurred and the fishery moved to the yellowfin-tuna-dominant region of the western Indian Ocean. Most of the bigeye tuna catch from the Indian Ocean line fisheries is caught within the latitudinal range 35° S to 10° N.

3. DATA INPUTS

3.1. General notes

Data used in this stock assessment consist of catch and length composition data, longline, and purse seine CPUE indices, and tag-recapture data. In this iteration of the assessment, conditional age-at-length data from a recent study (Eveson et al., 2025) are also used directly as data in the assessment model, for one of the sensitivity runs as was recommended by the review of the 2024 yellowfin tuna assessment and suggested by the participants of the data preparatory meeting. Data are continually being improved and as such catch and length composition datasets may not be identical to those in previous assessments. Where data inputs have substantially changed, it is noted in the sections below, and links to relevant methods papers are provided for further detail.

Model input files along with reproducible code to run the assessment, and all sensitivities are stored by the Secretariat and are available on request.

3.2. Spatial stratification

Stock assessment models often adopt regional structures to account for differences in biological characteristics of the species, regional exploitation pattern, or the level of mixing amongst subpopulations (Vincent, et al. 2018). In the 2013 bigeye assessment (Langley *et al* 2013a), the assessment model was stratified into three regions: western equatorial region (region 1), eastern equatorial region (region 2) and southern region (region 3), based on fishery dynamics. Most of the longline catch is taken within the two equatorial regions (regions 1 and 2; 15° S to 10° N), while the purse seine catch is predominantly taken within the western equatorial region (region 1).

A seasonal longline fishery operates in the southern region (region 3). The longitudinal partitioning of the equatorial area subdivides the distribution of tagged fish recoveries from releases that occurred in region 1. There are also some differences in the temporal trends in the longline CPUE indices from the three regions. The regional restructure was further refined in the 2016 assessment where the western equatorial region (region 1) was subdivided to account for differences in the distribution of tags within this region (see section 2.5 of Langley 2015). Region 1 was therefore partitioned at the equator into the area south of the equator and the area north of the equator, denoted as Region 1S and Region 1N, respectively (Figure 1). The four-region structure was adopted in the 2019 assessment, was used in the 2022 assessment, and is also used in the current assessment.

Future assessments should update spatial stratification based on any new biological information relating to stock structure, as is recommended as good practice in population dynamics models, to ensure regions are well-defined in the model (e.g. Cadrin et al., 2023).

3.3. Temporal stratification

The model covers the period from 1975 - 2024, and assumes an exploited, equilibrium initial state in 1975. Within the model period, annual data are compiled into quarters (Jan–Mar, Apr–Jun, Jul–Sep, Oct–Dec), and the model is iterated using a quarterly time step (representing a total of 200 time-steps) which as treated as a model year in Stock Synthesis (SS3). The quarterly timesteps were used as a proxy for the continuous recruitment of bigeye.

3.4. Definition of model fleets

In SS3, data are required to be aggregated or defined in "fleets" within the overall Indian Ocean fishery. Individual fleets represent relatively homogenous fishing units, with similar selectivity and catchability characteristics that do not vary significantly over time. Twenty-four (or twenty-two, depending on whether the purse seine CPUE indices were included) fleets were defined in the model (Table 1), of which, there are six "survey" fleets, for which only CPUE indices were assigned. The use of "survey" fleets for the CPUE indices was chosen as these indices are based on aggregated datasets and allow for separate estimation of selectivity and catchability to those of the "catch fleets" within the model framework. Fleets were defined based on the fishing gear type, fishery type (e.g. fresh vs. frozen or free school vs. fish aggregating device (FAD) associated sets for purse seiners), and fleet dynamics (e.g. spatial and temporal extent of the fishery).

The definitions of model fleets were the same as those used in the previous two iterations of the SS3 stock assessment. The main longline fishery was split into two main fleets based on vessel type (fresh vs. frozen). Freezing longline fisheries are defined as vessels using drifting longlines for which one of the following conditions apply: (i) the vessel hull is made of steel; (ii) vessel length is 30 m or longer; (iii) most of the catch of target species are frozen. A composite frozen longline fleet was defined in each region (LL1N, LL1S, LL2, LL3) aggregating the longline catch from all freezing longline vessels.

The fresh tuna longline fishery is comprised of vessels those using drifting longlines for which one of the following conditions apply: (i) the vessel has a fibreglass, Fibre-Reinforced Plastic (FRP), or wooden hull; (ii) vessel length is less than 30 m; (iii) the catch of target species remains fresh or in refrigerated seawater. Most fresh-tuna longline vessels operate in region 2, therefore the fresh-tuna longline fleet is comprised of vessels principally from Indonesia and Taiwan (China) in region 2 (FL 2).

The purse seine catch fisheries are defined into two groupings based on the fishing methods used: catches from sets on FAD-associated schools of tuna (purse seine log school; PSLS) and from sets on free schooling tuna (purse seine free schools; PS FS). Purse seine fisheries operate within region 1N, region 1S, and region 2. Individual purse seine fleets were therefore defined for each region separately.

A single bait boat fleet was defined within region 1N. The fishery included the pole-and-line and small seine fisheries (so-called as they catch smaller fish). Most of the catch associated with this fleet occurs in region 1N, with small amounts of catch from regions 1S and region 2, for the stock assessment, all catch is assigned to the bait boat fleet in region 1N.

An additional line-based fleet was defined within region 2, representing a mixture of fisheries that use handlines, small longlines, and the gillnet and longline combination fishery of Sri Lanka. Although some handline catch is taken from a fishery in region 1, all catch data were assigned to the line fleet in region 2.

For region 1N and region 2, a miscellaneous ("Other") fleet was defined comprising catches from artisanal fisheries other than those specified above (e.g. gillnet, trolling and a range of small gears).

Table 1: Definition of model fleets within the SS3 model for bigeye tuna in the Indian Ocean, including the gear types used, and region that data are assigned to in the model.

| Code | Method | Region | Notes |
|--------|---|--------|--|
| FL2 | Longline, fresh tuna fleets | 2 | |
| LL1N | Longline, frozen tuna | 1N | |
| LL1S | Longline, frozen tuna | 1S | |
| LL2 | Longline, frozen tuna | 2 | |
| LL3 | Longline, frozen tuna | 3 | |
| PSFS1N | Purse seine, free schooling | 1N | |
| PSFS1S | Purse seine, free schooling | 1S | |
| PSFS2 | Purse seine, free schooling | 2 | |
| PSLS1N | Purse seine, FAD associated sets | 1N | |
| PSLS1S | Purse seine, FAD associated sets | 1S | |
| PSLS2 | Purse seine, FAD associated sets | 2 | |
| BB1N | Bait boat and small-scale encircling gears (PSS, RN) | 1N | Previously characterised as mainly bait boat catch from the Maldivian fisheries. Requires better characterisation and possible splitting of gear in 2028 assessment. |
| LINE2 | Mixed line gears (handline, gillnet/longline combination) | 2 | Gears grouped on the basis that they primarily catch large bigeye tuna. |
| OT1N | Other (trolling, gillnet, unclassified) | 1N | |
| OT2 | Other (trolling, gillnet, unclassified) | 2 | |

3.5. Catch data

3.5.1. General notes

Catch data were compiled based on the fleet definitions in Table 1. An update of quarterly catches by fleet was provided by the IOTC Secretariat, including catches since the last assessment (2022–2024 IOTC-WPTT27-AS-BET-CEraised_1950-2024. This dataset was used for the first two iterations of the assessment, however on the first day of the 27th WPTT(AS), a newly revised dataset was provided by the IOTC Secretariat and this dataset was used for this, final assessment (IOTC-WPTT27-AS-BET-CEraised_1950_2024_Rev1).

Somalia also had submitted catch data for the first time in 2024, with a total of 4,100 t in the terminal year of the assessment. It was agreed by the 27th WPTT(AS) to exclude these data from the model, but at the end of the meeting, a request was made to run a sensitivity run with these data included. This is included in the report.

The catch time series was very similar to that of the previous assessment, except for the case of the Indonesia data where revised estimates of data from all fisheries has caused differences in the total catch of bigeye tuna, both historically, and for the terminal two years in the assessment, which were revised downwards. Total annual catches for 2022, 2023 and 2024 included in the updated catch history are 90,832, 94,591, and 82,874 t respectively (Table 2).

Table 2: Recent bigeye tuna catches (metric tonnes, t) aggregated by model fleet that have been included in the stock assessment model. The annual catches are presented for 2020- 2024.

| Fleet | 2020 | 2021 | 2022 | 2023 | 2024 |
|-----------|--------|--------|--------|--------|--------|
| FL2 | 7,772 | 8,885 | 10,205 | 10,885 | 7,338 |
| LL1S | 14,255 | 14,729 | 8,635 | 10,352 | 13,407 |
| LL2 | 4,228 | 5,008 | 4,370 | 4,138 | 4,895 |
| LL3 | 3,102 | 3,144 | 2,641 | 2,904 | 3,071 |
| PSFS1S | 3,176 | 2,257 | 6,190 | 9,659 | 5,753 |
| OT1N | 2,990 | 1,709 | 2,191 | 3,363 | 3,924 |
| OT2 | 3,225 | 4,310 | 5,471 | 10,251 | 1,885 |
| PSLS1S | 10,886 | 10,236 | 13,294 | 12,721 | 10,543 |
| PSLS2 | 2,351 | 3,308 | 6,867 | 1,757 | 4,581 |
| BB1N | 1,664 | 1,771 | 1,901 | 2,649 | 1,571 |
| LINE2 | 9,989 | 9,521 | 8,020 | 8,735 | 11,558 |
| LL1N | 5,568 | 2,208 | 5,114 | 4,917 | 3,530 |
| PSFS1N | 742 | 6,393 | 1,065 | 1,456 | 2,265 |
| PSLS1N | 9,473 | 17,403 | 14,872 | 10,804 | 8,552 |
| Total (t) | 79,421 | 90,884 | 90,832 | 94,591 | 82,874 |

3.5.2. Longline, frozen (LL1N, LL1S, LL2, LL3)

The frozen longline fleets operate throughout the Indian Ocean although catches are concentrated in the equatorial region. Catches were primarily from Japanese, Korean and Taiwanese (China) distant-water longline vessels. Most (62%) of the frozen longline catch has in the past been taken from the western equatorial region and annual catches from the LL1 fishery (LL1S and LL1N) steadily increased from the early 1950s to reach a peak of 63-68,000 t in 2003–2004. Catches of approximately 55,000 t were maintained during 2005–07, before declining rapidly to \sim 15,000 t in 2010–2011. In 2012, catch increased again to \sim 53,000 t, before again declining to \sim 14,000 t in 2018 (Figure 2 & 3). The catch from LL1N and LL1S in 2024 has increased to 16,937 t.

Annual catches from the LL2 fleet fluctuated between $\sim 10-20,\!000$ t from 1975 to 2011. In the subsequent years, catches have declined sharply to $\sim 3-4,\!000$ t between 2012 and 2024 (Figure ,3). The catch in 2024 has increased slightly to 4,875 t.

Annual longline catches from the LL3 fleet were comparatively low, averaging $\sim 3,000$ t from 1960 to 1990 (Figure ,3). Catches then increased to a significant peak of 22,000 t in 1995, before declining steadily to $\sim 4,000$ t in 2010, remaining between $\sim 2,500 - 4,300$ t until 2024.

3.5.3. Longline, fresh (FL2)

The fresh tuna fleets developed in the late 1980s, and annual catches rapidly increased to reach a peak of $\sim 30-35{,}000$ t in the late 1990s to early 2000s. Catches declined sharply in 2003 and then again in 2010, as some vessels moved south to target albacore tuna (*Thunnus alalunga*). Annual catches were $\sim 5{,}800-9{,}500$ t between 2011 and 2021, before increasing in 2022 and 2023 to $> 10{,}000$ t before declining to 7,338 t in 2024.

3.5.4. Purse seine (PSFS1N, PSFS1S, PSFS2, PSLS1N, PSLS1S, PSLS2)

Almost all of the industrial purse-seine catch was taken within the western equatorial region and catches were dominated by the FAD associated schools (PSLS1N and PSLS1S) (Figure 3). Annual catches from the PSLS1 (N and S) fisheries reached a peak of $\sim 30,000$ t in the late 1990s and have fluctuated at 15 -25,000 t over the last decade, except for 2012, when lower catches occurred. Since the late 1990s,

annual catches from the purse-seine free-school fishery (PSFS1N and PSFS1S) have fluctuated between $50-100,\!000$ t. While the activities of purse seiners have also been affected by piracy in the western Indian Ocean, the decline in catches were not as marked as for longline fleets (IOTC 2018a, b). Relatively minor catches were taken intermittently by the purse-seine fisheries in the eastern equatorial region.

There was a marked increase of reported catches on the purse seine FAD-associated schools in 2018. The WPTT21 considered this magnitude of increase of catches is not credible and is likely to have reflected several changes related to the methodologies to produce catch statistics by EU,Spain in 2018. The WPTT21 identified a methodology to revise the bigeye tuna catches reported by EU,Spain in 2018 (limited to their log-associated school component), which applied the species composition recorded for the log-associated component of EU,Spain purse seine catches in 2017 to the total catches (log-associated) reported in 2018 by the same fleet (IOTC 2019a). The method was subsequently developed further during the WPDCS15 (IOTC 2019b), which applied a spatial-temporal re-estimation procedure, based on several proxying scenarios. The WPTT24(DP) in 2022 agreed to use the proxying scenario number four (as recommended by the WPDCS15) to re-estimate Spanish purse seine catch for the 2022 stock assessment model (IOTC 2022). This approach caused marked reductions in catches of bigeye tuna reported by the EU purse seine fleet component in 2018 (~ 12,000 t). The purse seine FAD-associated sets' catch significantly increased in 2021, with catches from region 1N more than doubling those of the previous year (Table 2).

Annual catches for each fleet are outlined in Table 2.

3.5.5. Bait boat (BB1N)

Bigeye tuna catch from the Maldives bait boat fishery are assigned to the BB1N fleet in the model, however the model fleet is mostly made up of Indonesian catches in recent years. Catches of this model fleet have significantly changed since the revision of catch data from Indonesia, and catches are recorded as steadily increasing from $\sim 2,500$ t in 2000 to $\sim 4,000$ t in 2017 before a sharp drop in catches to ~ 900 t in 2018. Catches have steadily increased again until 2023 ($\sim 2,600$ t) before another decline in 2024 (1,571 t).

3.5.6. Line, small-scale (LINE2)

This fleet encompasses small-scale fisheries that use handlines, small longlines, and the gillnet/longline combination fishery of Sri Lanka. Similarly to the BB2 fleet, catches increased from a minimal level in the 1970s to around 2,900 t in 2009 before a sharp increase in catches from 2010 to 2023 (~7-10,000 t). Catches increased to 11,558 t in 2024.

3.5.7. Other (OT1N, OT2)

The fisheries included in the 'other' fleets are gillnet, trolling, and other minor artisanal gears not covered in the other fleets. Data are split into two regions within the equatorial ocean. Within the western Indian Ocean, the OT1 fleet is primarily comprised of the Iranian driftnet fishery that operates on the high seas. Total catches were negligible prior to 2005 but have increased to 10,251 t (OT1N) and 3,362 t (OT2) in 2023 (Figure 3). Catches dropped in the OT1N fleet dramatically in 2024 to 1,884 t, while catches in the OT2 fishery remained steady at 3,924 t. Catch increases are attributed to major changes within the fisheries, including gear creep (increase in boat size, development of fishing techniques) and a change in fishing areas (IOTC 2018). The OT2 fleet is primarily comprised of the Indonesian troll and gillnet fisheries.

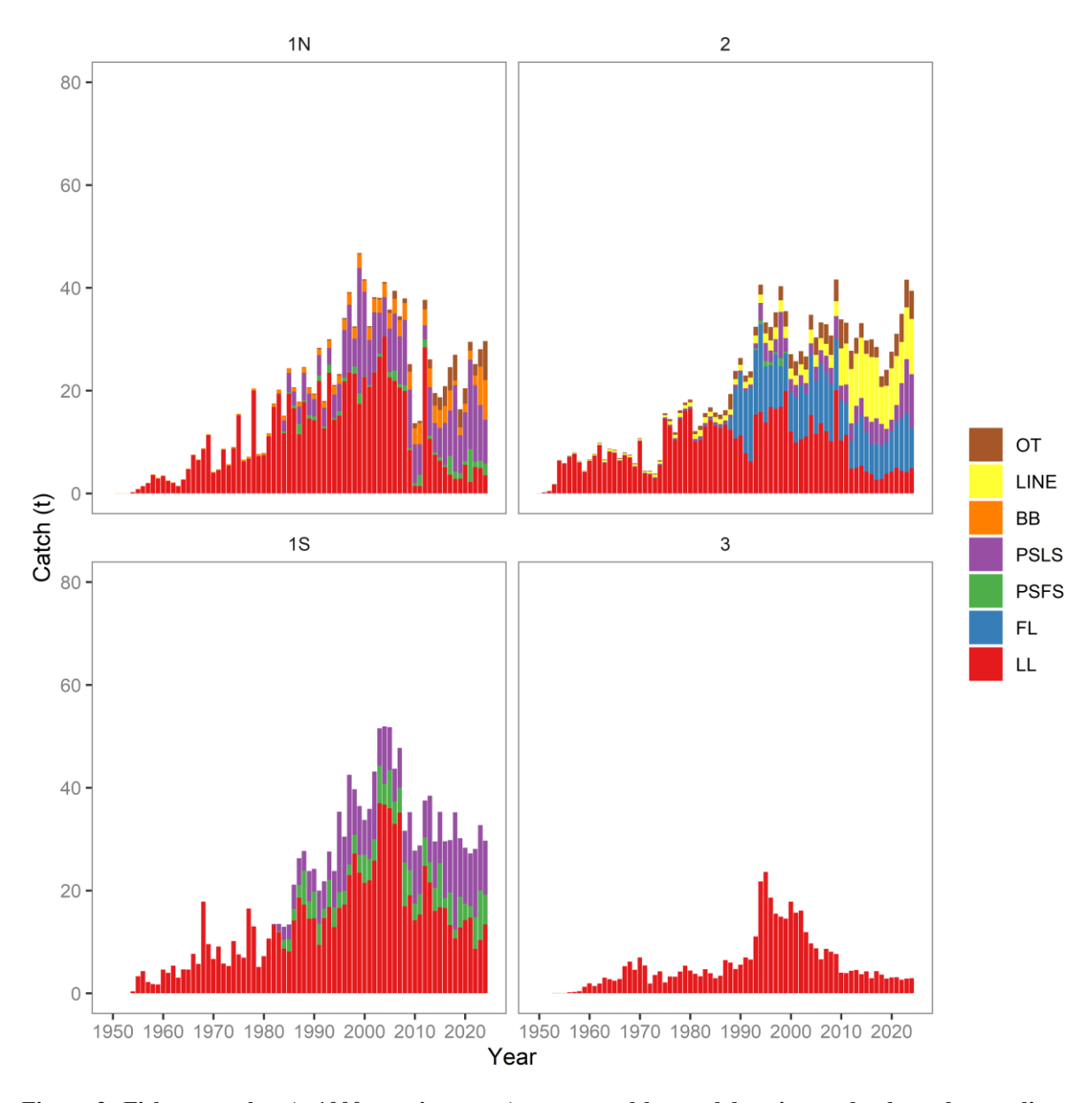


Figure 2: Fishery catches (x 1000 metric tonnes) aggregated by model region and coloured according to fishing fleet in the model.

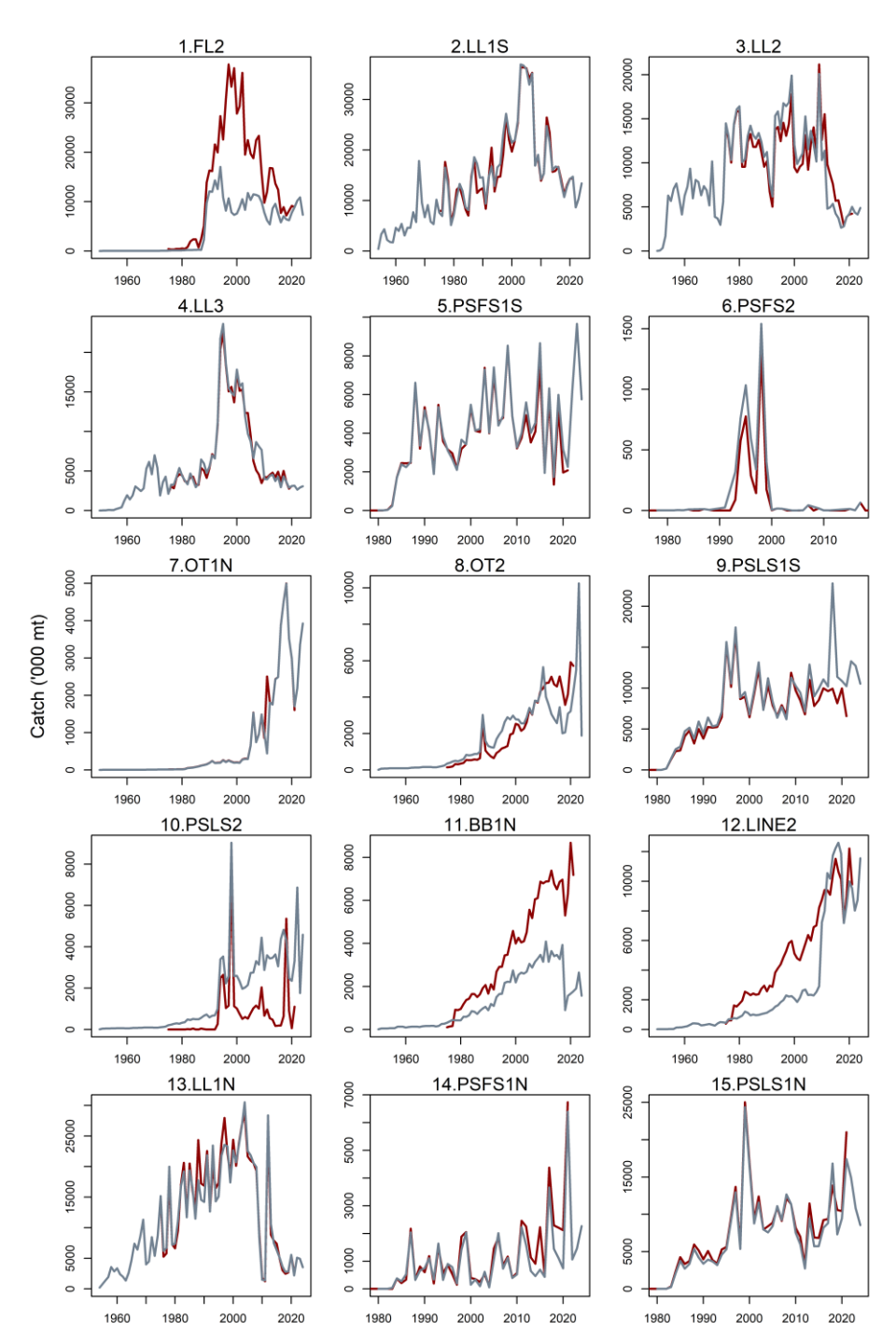


Figure 3: Fishery catches (metric tonnes) aggregated by year. Note the y-axes differ between plots. Red lines are catches used in the 2022 assessment. The differences in catch are mainly due to the revision of catch data by Indonesia, although some changes will be due to general improvements in the data quality over time.

3.6. Abundance indices

3.6.1. Longline CPUE

The 2022 assessment used longline CPUE series provided by Japan, Korea, and Taiwan (China) developed during a joint-CPUE workshop (Kitakado et al., 2022) and the 2025 assessment includes longline CPUE series that have been developed by the same collaborative effort between Japan, Korea, and Taiwan (China). The series were presented at the 27th Working Party for Tropical Tunas (Data Preparatory) (IOTC-2025-WPTT27(DP)-09) alongside a report detailing the methods (Kitakado et al., 2025). The CPUE series were developed at a joint workshop where there were outside observers, but only representatives from the three nations had access to the operational data.

The CPUE standardisation included operational data on catch numbers by species, spatio-temporal data (1 ° latitude and longitude; daily records), vessel identification (vessel ID), number of hooks used, hooks between floats (HBF – for regions 1N, 1S and 2), and clustering outcomes for region 3 to account for changes to target species during fishing operations. Data covers the period 1979 - 2024 (Japan and Korea), and 2005 - 2024 (Taiwan, China). Data screening took place to ensure only relevant data were included – e.g. vessels needed to have \geq 20 data points; with \geq 10 positive (e.g. non-zero) CPUE data; and data were subjected to 20 % sub-sampling in each of the spatio-temporal covariates.

Generalised Linear Models (GLMs) were used to standardise the CPUE using the following covariates: time (quarters); location (5 $^{\circ}$ latitude x longitude grid); vessel ID; cluster category (e.g. target species); HBF as a mean value, allowing for depth stratification (shallow: \leq 7 HBF; medium: 8 – 13 HBF; and deep water: \geq 14 HBF).

The indices produced show broadly the same trends as the analyses in 2019, and 2022, despite differences in the methods used (see Kitakado et al., 2025 for more details; Figure 4). There has been a slight increase in standardised CPUE in 2025 for the final few years, which is especially evident in region 2. It is unclear whether this is due to changes in abundance, or differences in the data available for this region.

The CPUE time series is used as the main abundance index from 1979 to 2024 for each of the four model regions (1N, 1S, 2, and 3).

The earlier assessments used the indices developed from the longer time series (1953–2015) but excluded the years prior to 1979 for several reasons: the decline in the indices during the late 1960s–early 1970s is inconsistent with the relatively low level of catch. The 2–3-fold increase in the indices during 1976–1978 was considered to be related to factors other than abundance (Kolody et al 2010, Langley et al 2013b, Langley 2016, Hoyle et al. 2017a).

_

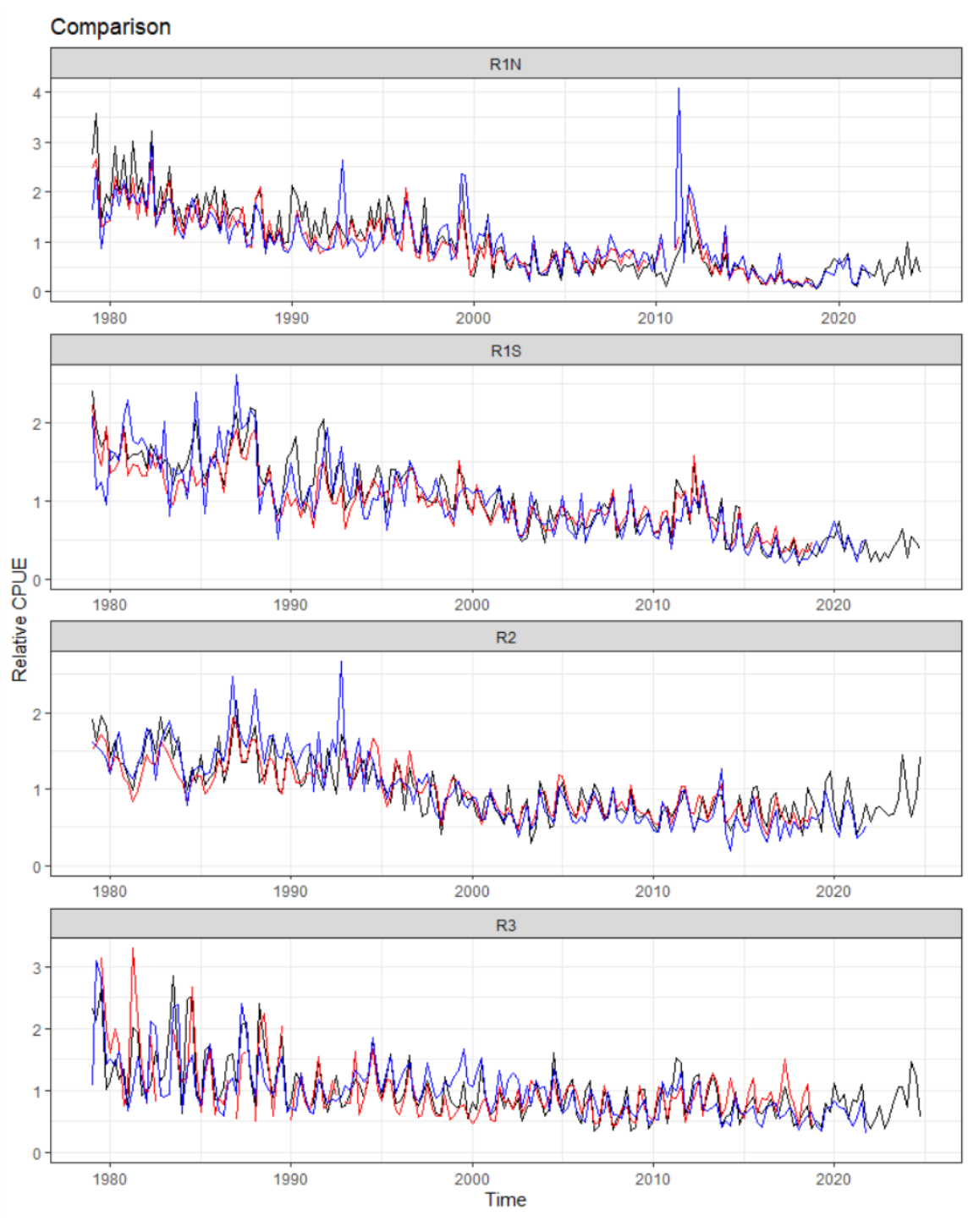


Figure 4: Standardized CPUE series produced in 2019 (red), 2022 (blue), and 2025 (black). Operational-level data were used in the 2019 and 2025 analyses, while aggregated data were used in 2022. Figure taken from Kitakado et al. (2025).

The standardised quarterly CPUE indices used as inputs to the assessment are shown in Figure 4 . The CPUE indices from the four regions exhibit broadly comparable trends, declining by about 65-75% from the early 1980s to 2010s. In the western equatorial regions (regions 1N and 1S), the decline from 1979 to the early 2000s is greater in the northern subregion (region 1N), but this region started from a higher starting CPUE. Both regions have standardised CPUEs that are at the lowest mean point over the entire timeseries of the fishery. The indices in both R1N and R1S peaked in 2011 when the main fleets returned to the main fishing ground but declined rapidly to the lowest level in 2018. Both indices, however increased moderately during 2019 – 2021, and have stabilised around this level up to 2024.

In the eastern tropical region (region 2) there is also a general decline in CPUE since 1980, although the CPUE is relatively stable until the mid-90s when the CPUE remains relatively stable until 2018 when fluctuations in CPUE increase, leading to a relative increase in CPUE from 2021-2024 to levels not seen since the mid-1990s, considering the general reduction in both catch and effort in this area (for Korea and Taiwan, China, for which data are provided), this increase may not be reflective of an increase in abundance, but more an artefact of data availability, and should be treated with caution.

The index in region 3 (temperate region) has remained relatively stable since the start of the timeseries, although again there is an increase in CPUE in the final three years since the last assessment (2022-2024.

In each region, the annual trend in the indices is generally very consistent among all quarters. The CPUE indices from region 3 exhibit considerable seasonal variation, with lower CPUE in the first and fourth quarters (austral summer), and relatively high CPUE in the second and third quarters (austral winter). This seasonality is also somewhat reflected in the longline length composition data, with large fish caught in the third quarter and smaller fish in the first and second quarters. SS3 does not have the flexibility to estimate seasonal catchability or movement dynamics when the model is configured based on a quarterly time step. Consequently, to account for the seasonal variation in the CPUE indices, the Region 3 CPUE indices were incorporated in the model as four separate sets of abundance indices (i.e. one series for each quarter). This follows the same method used in 2022 as there was no evidence to support a different structure within the model.

For the regional longline fleets, a common catchability coefficient was estimated in the assessment model, thereby, linking the respective CPUE indices among regions, as was done in the 2022 model. This significantly increases the power of the model to estimate the relative (and absolute) level of biomass among regions. However, as CPUE indices are essentially density estimates it is necessary to scale the CPUE indices to account for the relative abundance of the stock among regions. The approach used was to determine regional scaling factors that incorporated both the size of the region and the relative catch rate to estimate the relative level of exploitable longline biomass among regions (Hoyle & Langley 2018, Table 3). The relative scaling factors are R1N: 0.799, R1S: 1.000, R2: 0.373+0.486 (0.859), R3: 0.626. These factors are the same as those used in the previous assessment ¹. For each of the principal longline fisheries (LL1N, LL1S, LL2, LL3), the standardised CPUE index was normalised to the mean of the period for which the region scaling factors were derived (i.e. the GLM index from 1979–1994). The normalised GLM index was then scaled by the respective regional scaling factor to account for the regional differences in the relative level of exploitable longline biomass among regions. This follows the same methods as in the 2022 assessment.

Overall, the 2025 CPUE indices show similar trends to the 2022 assessments (Figure 5).

28

¹ The values quoted in the report for the assessment were not the values implemented in the assessment model runs.

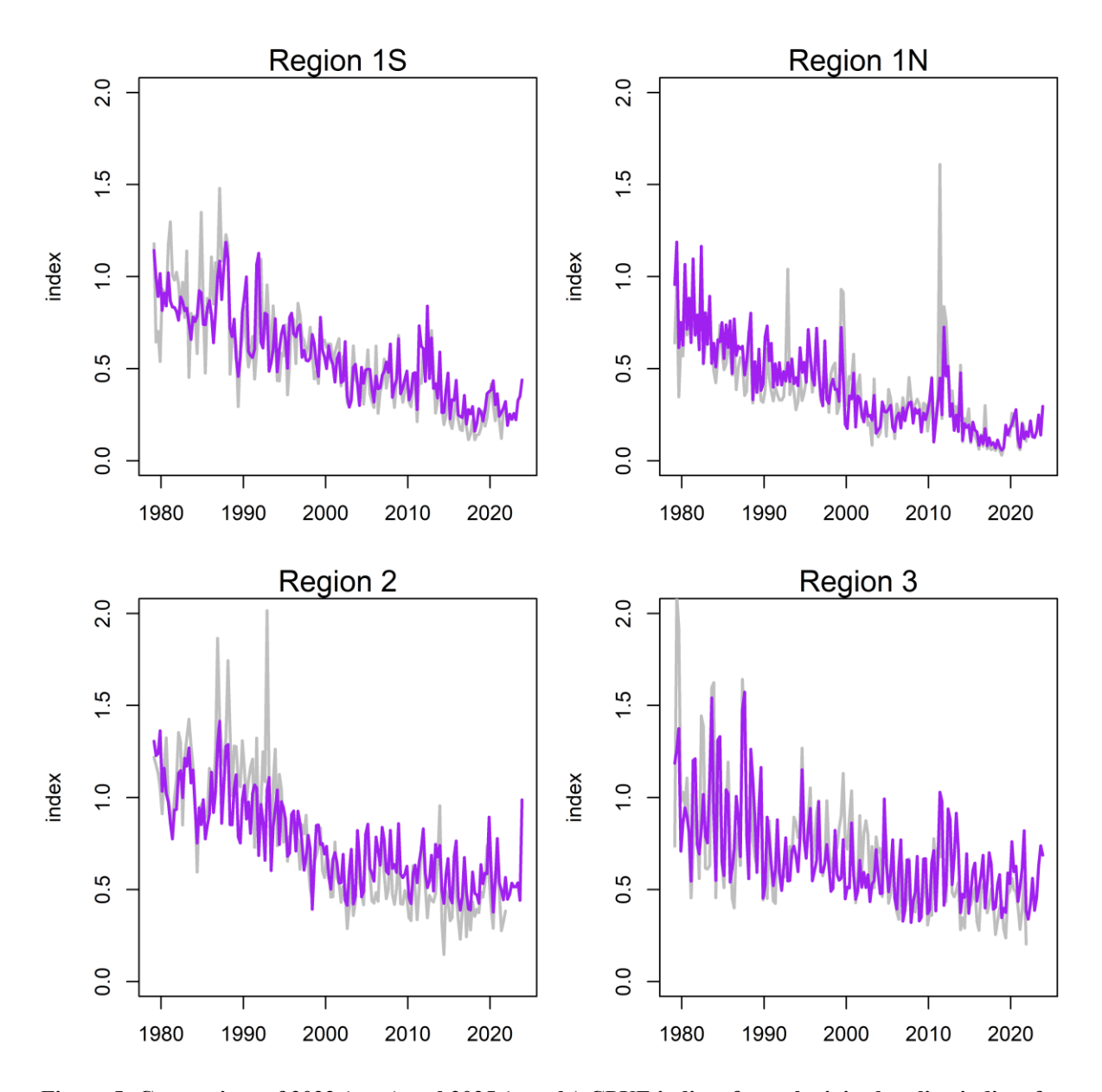


Figure 5: Comparison of 2022 (grey) and 2025 (purple) CPUE indices from the joint longline indices from Taiwan (China), Korea, and Japan.

3.6.2. Purse seine CPUE

The European Union (EU) purse seine fishing vessels in the Indian Ocean have benefitted from observer sampling, and extensive logbook reporting from 1991-2024, and as such there is sufficient data from which to perform CPUE standardisation. As in 2022, standardised indices of bigeye tuna CPUE were developed by the European Union (Spain) (Correa et al., 2025). As purse seine vessels primarily capture smaller individuals, it is hypothesised that CPUE indices from these data can provide abundance indices for juvenile bigeye tuna and therefore likely provide some information on recruitment into the fishery.

Two sets of regional (region 1N and region 1S) indices were developed for two separate timeframes. The 'short' indices were based on data from 2010-2024 using detailed covariates that account for the use of drifting FADs (dFADs) by vessels, and 'long' indices that were based on data from 1991-2024 that do not include these additional covariates. Both indices show similar trends and overlap well over the time period covered by both sets of indices (2010-2024; Figure 6). Although the shorter indices include more covariates that could help with standardisation and explanation of CPUE trends, the authors found that dFAD covariates 'generally had significant impacts on BET (bigeye tuna), but there

[sic] impacts were often contradictory and quite small'. They hypothesise that the bycatch nature of bigeye tuna may go some way to explain the equivocal impact of dFAD covariates on CPUE standardisation.

Sea surface temperature (SST) was found to be the most important environmental explanatory variable, and this was included in both the short and long indices, perhaps confounded with time of day, as juvenile bigeye tuna are known to migrate vertically diurnally (Hino et al., 2019).

For these reasons, although both the long and short indices were tested in the model as sensitivities, the final base model includes the long index as it provides data across a longer time period, and the current scientific estimates show that including dFAD covariates as yet have little impact on the CPUE standardisation, and environmental variables likely have more impact on the abundance and density of juvenile / sub-adult bigeye tuna.

The purse seine CPUE indices were implemented in the SS3 framework as two additional 'survey' fleets, with mirrored selectivity to the PSFS1N and PSFS1S fleets respectively.

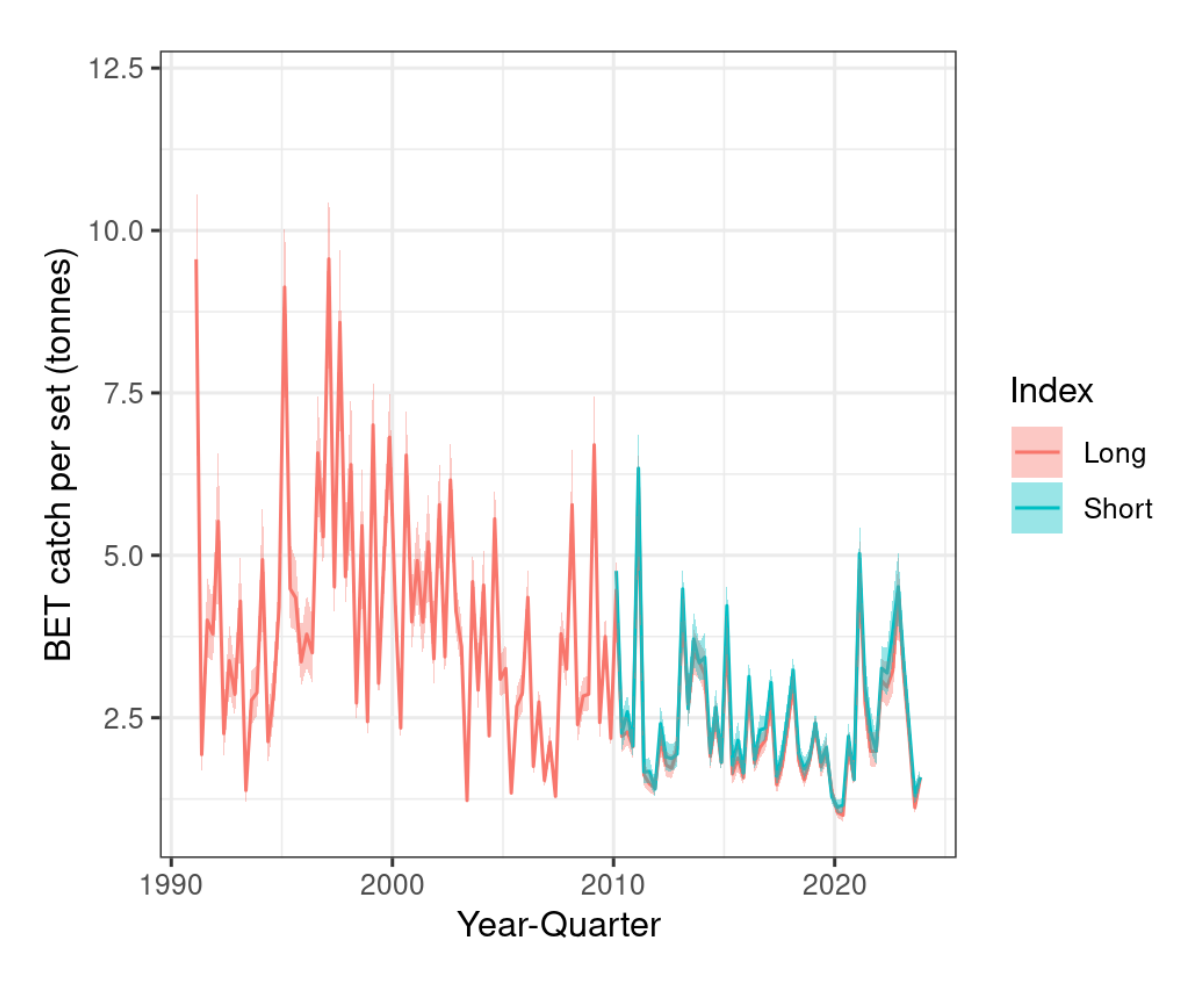


Figure 6: Quarterly standardized CPUE index for the long and short time series superposed (Figure taken from Correa et al., 2025).

To ensure that there was no conflict introduced into the model by including the purse seine CPUE indices, a quantitative comparison between the longline and purse seine CPUE trends was completed using methods developed elsewhere but used within other IOTC Working Parties, and within ICCAT tuna assessments (G. Merino, *pers. comms.*). This analysis confirmed that all CPUE indices showed similar trends and therefore could be included within the base model (Appendix B).

3.7. Length frequency data

Available length-frequency data for each of the defined fisheries were compiled into 95 2-cm size classes (10–12 cm to 198–200 cm) and were aggregated to provide a composite length composition for each year/quarter. Each length frequency observation for purse seine fisheries represents the number of fish sampled raised to the sampling units (sets in the fish compartment) while for fisheries other than purse seine each observation consisted of the actual number of bigeye tuna measured. Each aggregated length sample was assigned an initial sample size. The sample size was determined based on the number of fish included in the aggregated sample, up to a maximum of 1000. The sample size was then divided by 100 resulting in a maximum initial sample size of 10. Purse seine length samples were also assigned an initial sample size of 10. A graphical representation of the availability of length samples is provided in Figure 7. The model structure allocates the data to 4-cm length bins.

3.7.1. Longline, frozen (LL1N, LL1S, LL2, LL3).

Size frequency data are available for the LL1–3 fisheries from 1965 to 2024. Prior to 1995, the length compositions were dominated by sampling from the Japanese longline fleet, while in the subsequent period the size data were increasingly dominated by data collected from the Taiwanese (China) frozen tuna longline fishery. In recent years, length frequency data were also collected from locally based longline fleets (e.g., Seychelles).

Length and weight data were collected from sampling aboard Japanese commercial, research and training vessels. Weight frequency data collected from the fleet have been converted to length frequency data via a processed weight-whole weight conversion factor and a weight-length key (Chassot et al., 2016). While in recent years most of the samples available have come from scientific observers on commercial vessels, in the past, samples came from training and research vessels, and commercial vessels. Matsumoto (2016) suggested that length distribution was similar between sampling sources (commercial and non-commercial vessels) or platform (fishermen, scientists, observers) in the Indian Ocean. Length frequency data from the Taiwanese (China) longline fleet are also available from 1980–2024. Length samples from this component come from commercial vessels and include lengths recorded by fishermen and, to a lesser extent, lengths measured by scientific observers on some of those vessels.

Previous assessments of Indian Ocean bigeye tuna have highlighted the temporal variability in the length composition data from the main longline fisheries. Langley (2016) examined the longline length data to investigate potential sources of variation in fish length. For the LL1 fleet, there were marked differences in the sizes of fish sampled from the various longline vessels during the late 1980s and early 2000s. There were also divergent temporal trends in the lengths of fish sampled amongst the fleets (see Figure A1 of Langley 2016). A similar trend is also apparent in the length composition data from the eastern equatorial region. Langley (2016) restricted the length data to the main area of catch from the bigeye tuna longline fishery for each model region to minimise potential variation in length composition attributable to the collection of length samples from the periphery of the fishery.

The lengths of fish sampled from the Taiwanese (China) fleet increased markedly during the early 2000s and the length compositions of the samples from catches of most fleets were comprised of larger fish during 2005–2015 (see Figure A1 Appendix 1 of Langley 2016). The increase in Taiwanese (China) fish sizes during the period coincided with a large shift in the ratio of the Taiwanese (China) bigeye and yellowfin longline catches in the region during the same period; the ratio of bigeye in the longline catch increased during the late 2000s and remained at a higher level in the subsequent years (Hoyle et al 2015, see Figure 20). A review of the recent Taiwanese length composition data by Geehan & Hoyle (2013) recommended excluding from stock assessments the size data for BET, YFT and ALB from the Taiwanese DWLL fleet after the early-2000s, until the cause of changes in the size frequency data have been determined by the WPTT". A more recent review shows that the sampling behaviour of Taiwanese and Seychelles fleets (mostly reflagged Taiwanese vessels) have changed over time, with patterns in the logbook length data inconsistent with other vessels (Hoyle et al. 2021), and as such the WPTT27 (DP) recommended omitting all Taiwanese and Seychelles logbook length data from the current assessment

(IOTC 2025). However, the length data collected by the scientific observers on Taiwan (China) vessels in the period 2005–2024 were included in the assessment.

In the 2024 dataset, most of the measurements from the SCY length frequency data were incorrectly entered into a database and so ended up being converted into very large fish (all fish were > 400 cm TL). To ensure this was not biasing the model outputs, all 2024 length data from SCY were excluded. Additionally, there were other rows of data (mainly from SCY data) that only included measurements from very large fish (last four length bins), and no other measurements. These were removed from the assessment based on information from the data team (E. Chassot, *pers. comms.*). Future bigeye tuna assessments should undertake a thorough review of the length data and filtering used in the assessment.

For the final data sets used in the model, the length compositions of the LL1N, LL1S, LL2, and LL3 fleets are dominated by fish in the 90–150 cm length range (Figure 8). The average lengths of fish in the sampled catch fluctuated over the study period, with regions 2 and 3 having smaller average sizes than regions 1N and 1S, particularly in the early years (Figure 9).

3.7.2. Longline, fresh tuna fleet (FL2).

Length and weight data were collected during the unloading of catches at several ports, primarily from fresh-tuna longline vessels flagged in Indonesia and Taiwan (China) (IOTC-OFCF sampling). Length data from 2012-2021 were included in the previous assessment, and for the current assessment, an additional three years of data are included (2012–2024).

The composite length composition of the catch is similar to the distant water longline fleet (Figure) and remained relatively stable over the sampling period except in 2012 when there are larger fish in the samples (Figure).

3.7.3. Purse seine (PSFS1N, PSFS1S, PSFS2, PSLS1N, PSLS1S, PSLS2).

Length-frequency samples from purse seiners have been collected from a variety of port sampling programmes since the mid-1980s. The samples are comprised of large numbers of individual fish measurements and represent comprehensive sampling of the main period of the fishery (Figure 8). Limited size data are available from the purse-seine fisheries within region 2.

The FAD-associated purse-seine fishery (PSLS) primarily catches smaller bigeye tuna, while the size composition of the catch from the free-school fishery is bimodal, being comprised of the smaller size range of bigeye and a broad mode of larger fish (Figure). There was a general decline in the average length of fish caught by the PSLS1 fishery from 1990 to 2018 (Figure). The average size of fish sampled from the free-school fishery was variable among quarters, although fish sizes tended to have increased through the 1990s and the early 2000s (Figure). It is unknown whether the trends in the length composition of the purse seine catch are representative of the population or reflect changes in the operation of the fishery.

3.7.4. Bait boat (BB1N)

Limited length samples are available from the fishery (Figure) and the sampled catch was dominated by fish in the smaller length classes (50–70 cm) (Figure and Figure). These samples are not used in the assessment, following previous assessment methods (Fu et al., 2022).

3.7.5. Line, other (LINE2)

Negligible length frequency data are available from the fishery although the available data indicate that the catch was predominantly composed of larger fish (Figure). Fish sampled from this fishery are generally larger than the fish sampled from the other main longline fisheries. In 2020–21 and 2021, the Indonesian line vessels sampled a considerable number of small fish (around 50 cm). It is not known how well these small fish are representative of this fishery therefore these samples are not included in the current assessment.

3.7.6. *Other fleets (OT1N, OT2)*

While catches from the OT1N fleet are dominated by the Iranian driftnet fleet, there are no length samples available from this component of the fishery. Instead, the available OT1N length samples were collected from the 'other' fisheries that operated prior to 2005 (Figure). The aggregate length samples encompass a broad length range (Figure). For the Other 2 (OT2) fleet, limited length samples were collected from the Indonesian small purse seine and troll fisheries. The aggregate length frequency data available include two size modes from the small-scale purse seine samples (Figure). This is probably due to different sizes of fish taken by different modes of fishing (e.g., fishing at night with light, around anchored FADs, etc.). Due to concerns around the representativeness of these samples, they are not included in the assessment, following previous assessments (Fu et al., 2022).

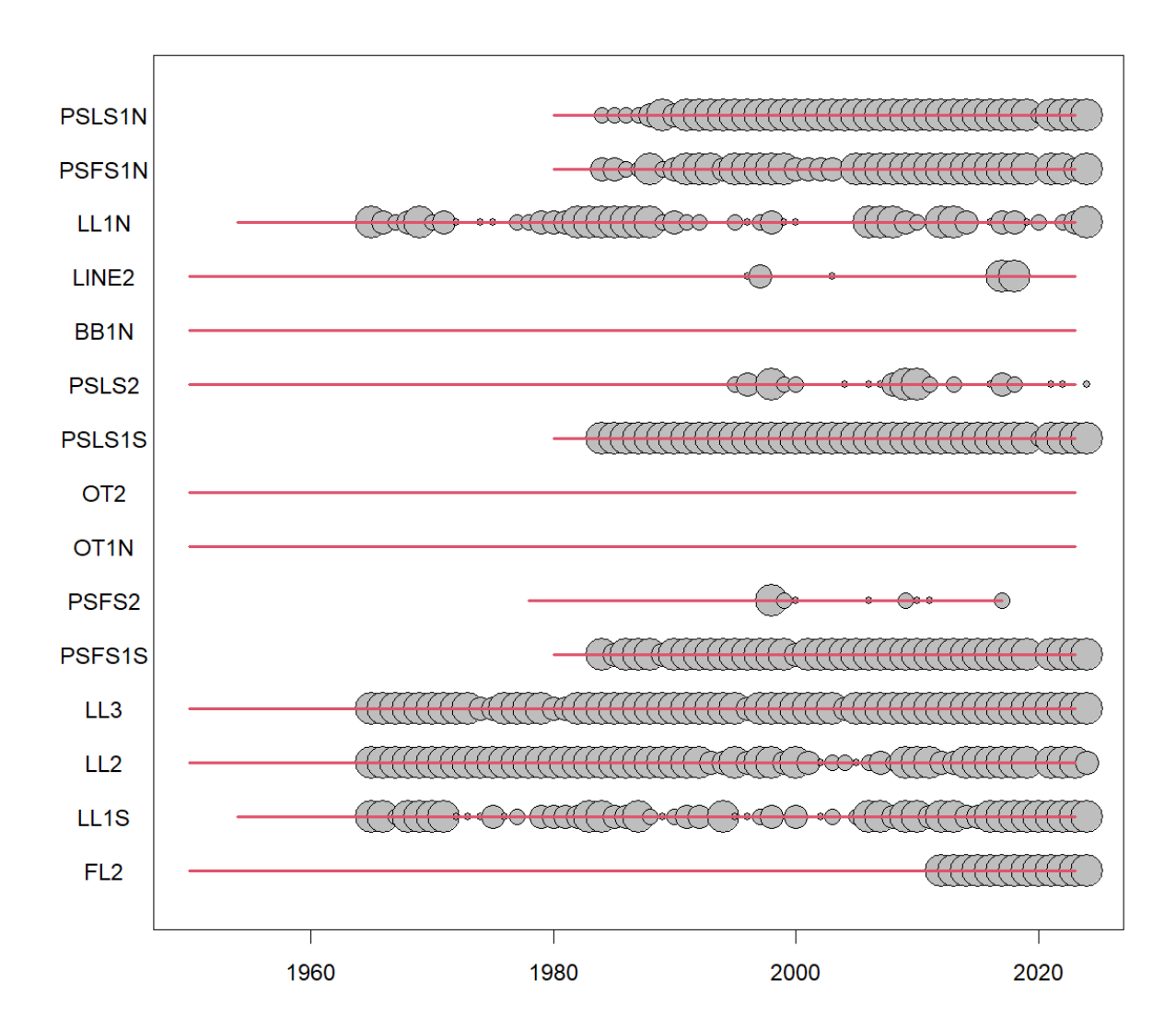
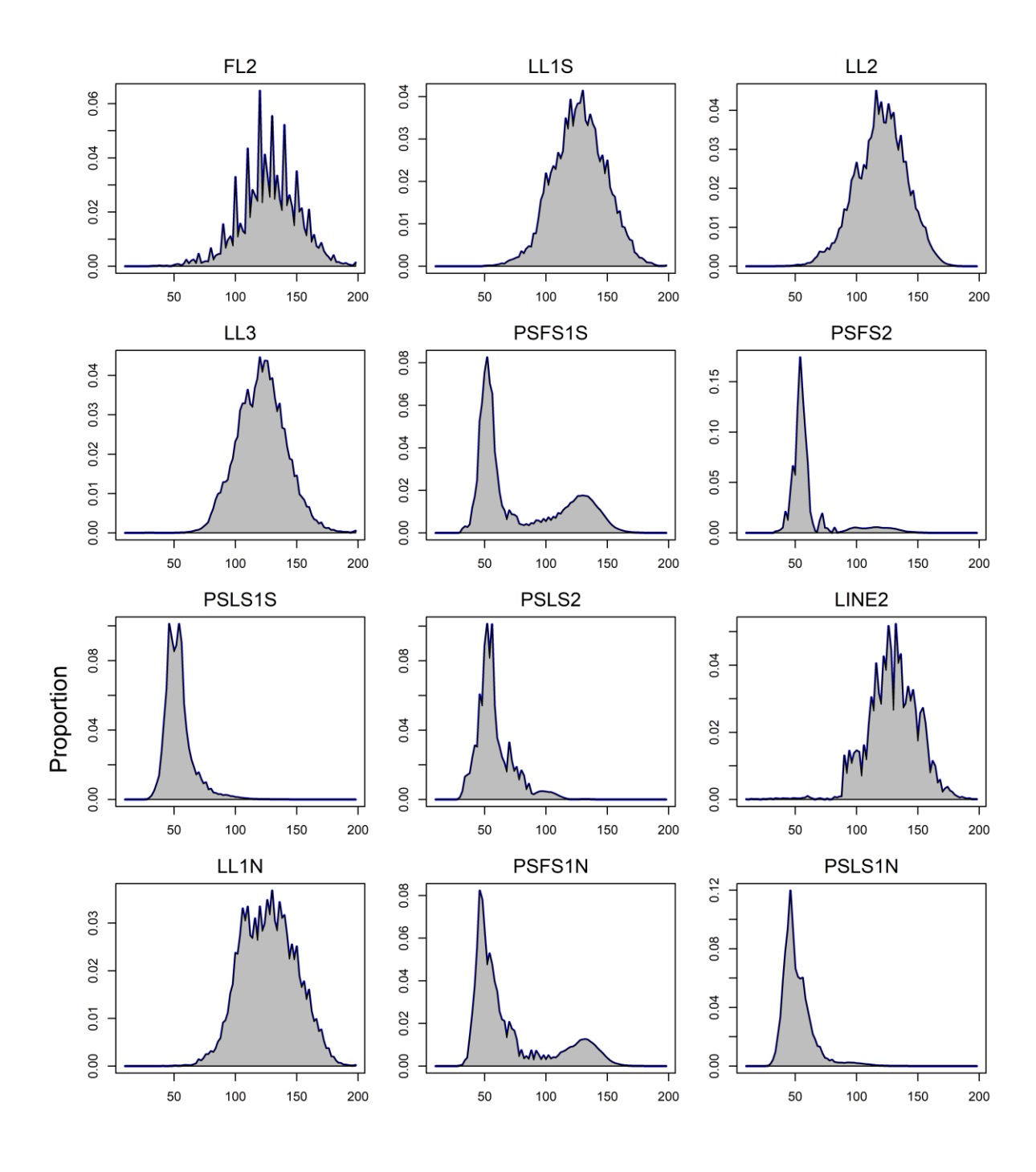
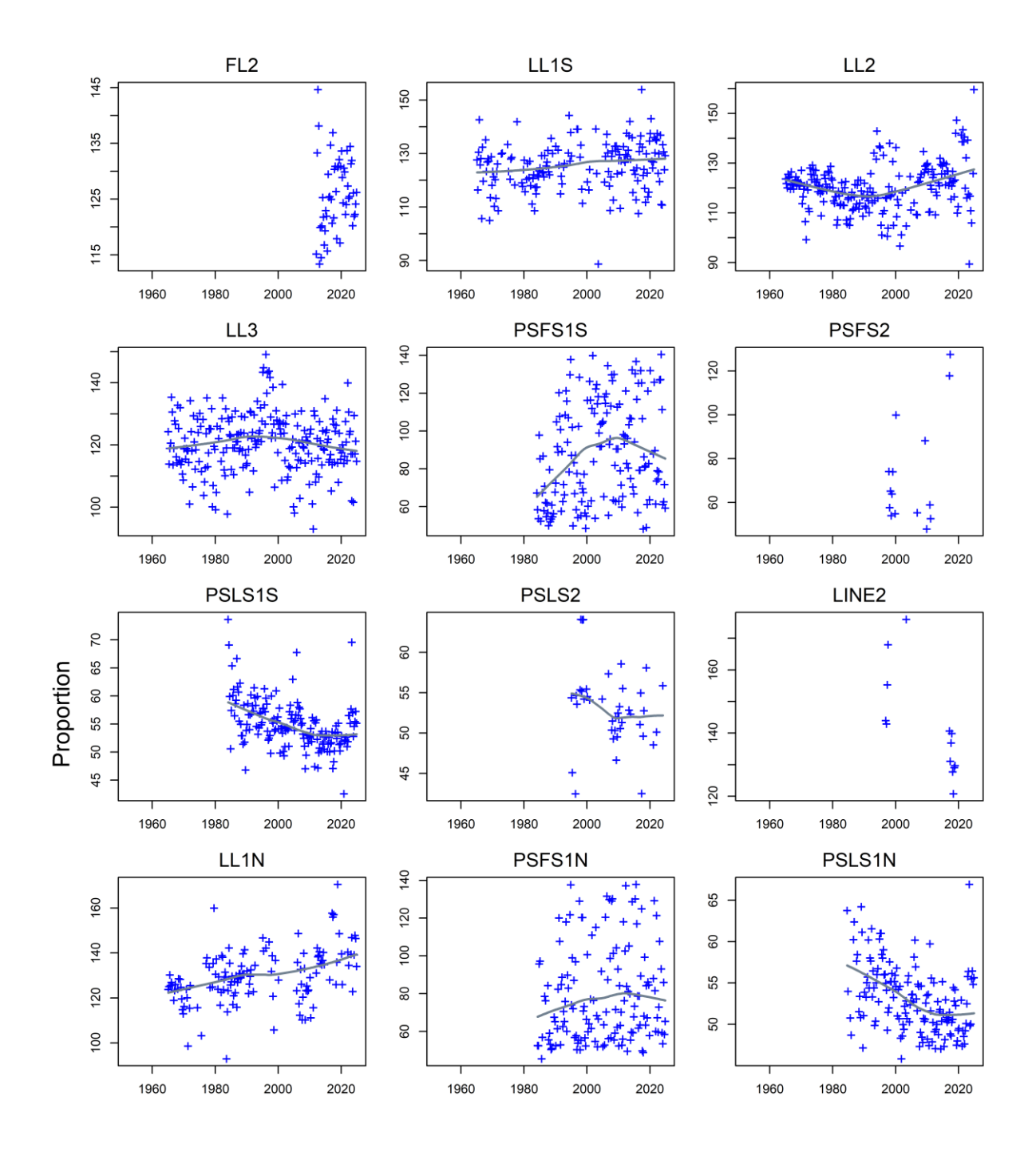


Figure 7: The availability of length sampling data from each fishery by year. The grey circles denote the presence of samples in a specific year (the size indicate number of quarters being sampled). The red horizontal lines indicate the time period over which each fishery operated.



Length (cm)

Figure 8: Length compositions of bigeye tuna samples aggregated by model fishery.



Length (cm)

Figure 9: Mean length (fork length, cm) of bigeye sampled from the principal fisheries by year quarter. The grey line represents the fit of a loess smoother to the dataset.

3.8. Tagging data

Tagging data have not been updated since the 2022 assessment model. The data used consist of bigeye tuna tag releases and returns from the Regional Tuna Tagging Project-Indian Ocean (RTTP-IO) phase of the Indian Ocean Tuna Tagging Programme (IOTTP). Tags were released during 2005–2007 and recoveries were monitored by the IOTTP during 2005–2009 and by the IOTC in the subsequent years.

A total of 34,478 bigeye tuna were released by the RTTP-IO program (removed tagged fish with unknown length). All the bigeye tag releases of the RTTP-IO occurred in a localised area off the Tanzanian coast within the western equatorial region (region 1S) (Figure 10). Most of the releases occurred during the second and third quarters of 2006 and the third quarter of 2007 (Figure 11). In total, 5,674 tag recoveries (removed tags with unknown recovery dates) could be assigned to the fleets included in the model. A relatively high proportion of tag recoveries occurred in the vicinity of the main release location (Table 3). There were also a relatively large number of tags recovered from bigeye tuna catches in the Mozambique Channel. Overall, most of the tags were recovered in the home region, some recoveries occurred in adjacent regions, particularly region 1N. A very small number of tags were recovered in regions 2 and 3 (less than 1%) Figure 10).

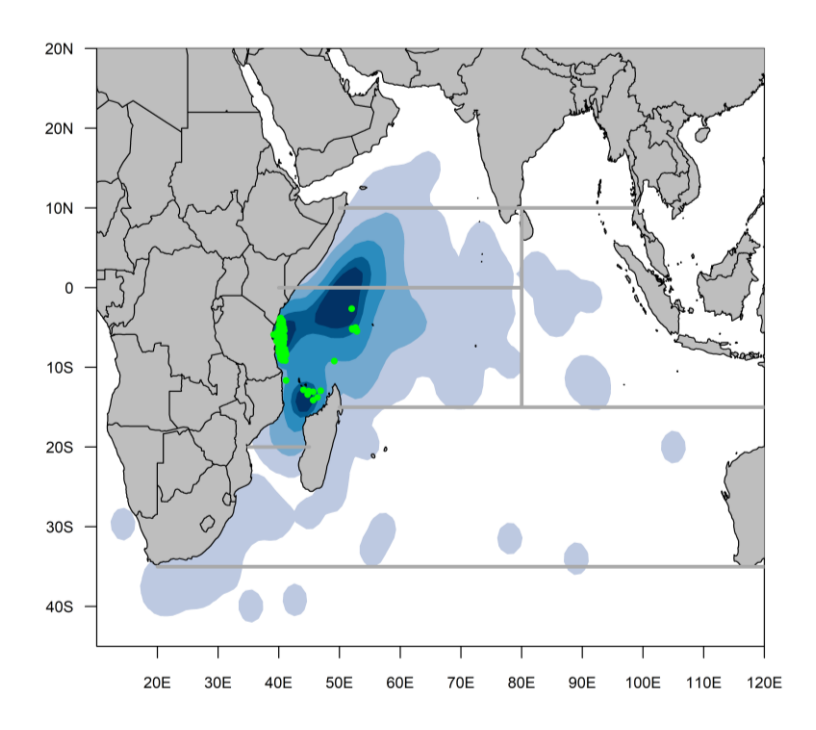


Figure 10: Location of releases (green) and density of recoveries for the bigeye tuna RTTO-IO tag

Program

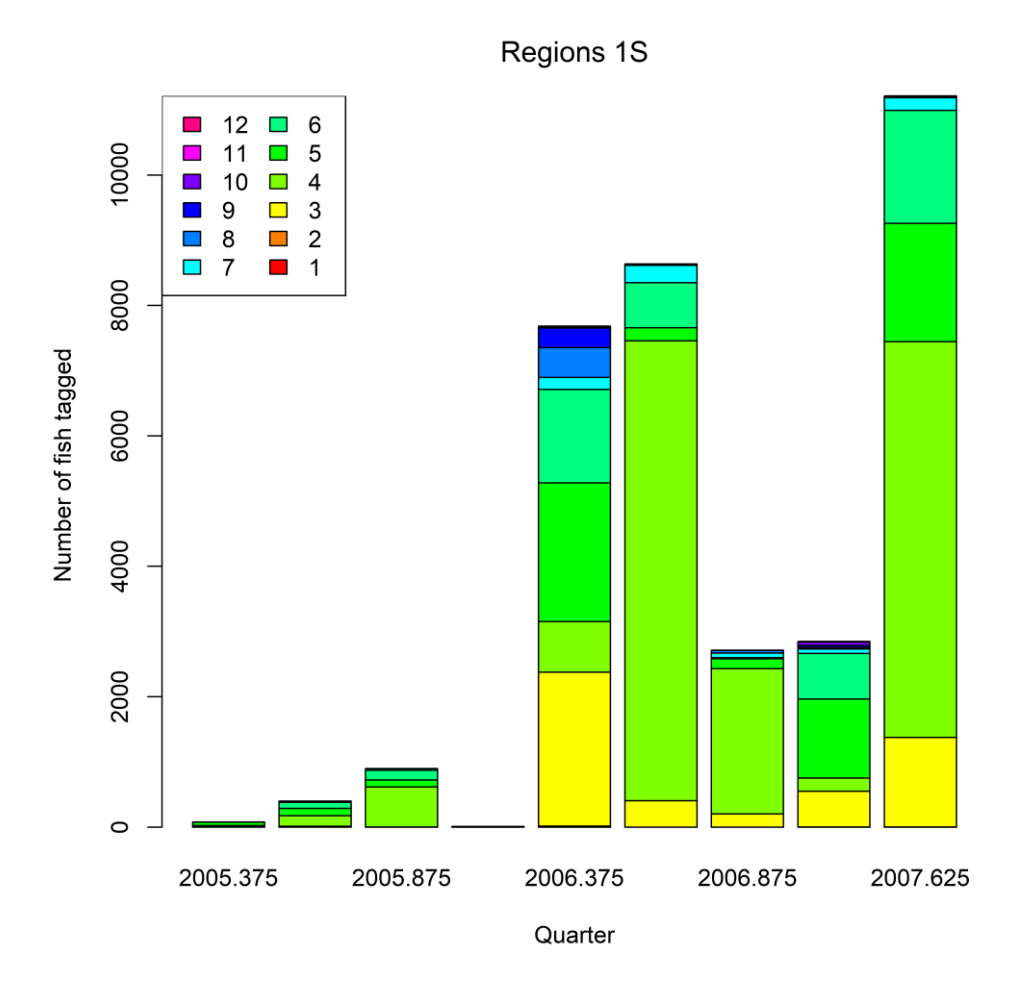


Figure 11: Number of tag releases by quarter and age class (year) included in the assessment data set. All tag releases occurred in region 1S. Ages (year) were assigned based on the length of the fish, and updated growth model from Eveson et al. (2025).

Table 3: Tag recoveries by year of recovery (box), region of release (number released in bracket), and region of recovery. Region of recovery is defined by the definitions of the fisheries included in the model.

| Year | Release region (n releases) | Recoveries by region (n) | | | | |
|------|--------------------------------|--------------------------|-----|---|----|--|
| | | 1S | 1N | 2 | 3 | |
| 2005 | 1S (1,375) | 6 | 5 | | | |
| 2006 | 1S (19,042) | 478 | 256 | 4 | 1 | |
| 2007 | 1S (14,061) | 2,407 | 613 | | 3 | |
| 2008 | | 1,191 | 160 | | 9 | |
| 2009 | | 178 | 18 | 3 | 13 | |
| 2010 | | 107 | 8 | 2 | 15 | |
| 2011 | | 36 | 17 | 2 | 15 | |
| 2012 | | 72 | 14 | | 5 | |
| 2013 | | 13 | | | 1 | |
| 2014 | | 11 | | | | |
| 2015 | | 10 | | | 1 | |

Most of the tag recoveries occurred between mid-2006 and 2008 (Table 3). The number of tag recoveries started to attenuate in 2009 although small numbers of tags were recovered up to the end of 2015. Most of the recaptures near main release locations were from purse seine FAD-associated sets during 2007 and were comprised of tagged fish that had been at liberty for 6–12 months. Recoveries from the purse seine fishery for fish at liberty for at least 12 months were more evenly distributed over the main area fished by the purse seine fleet.

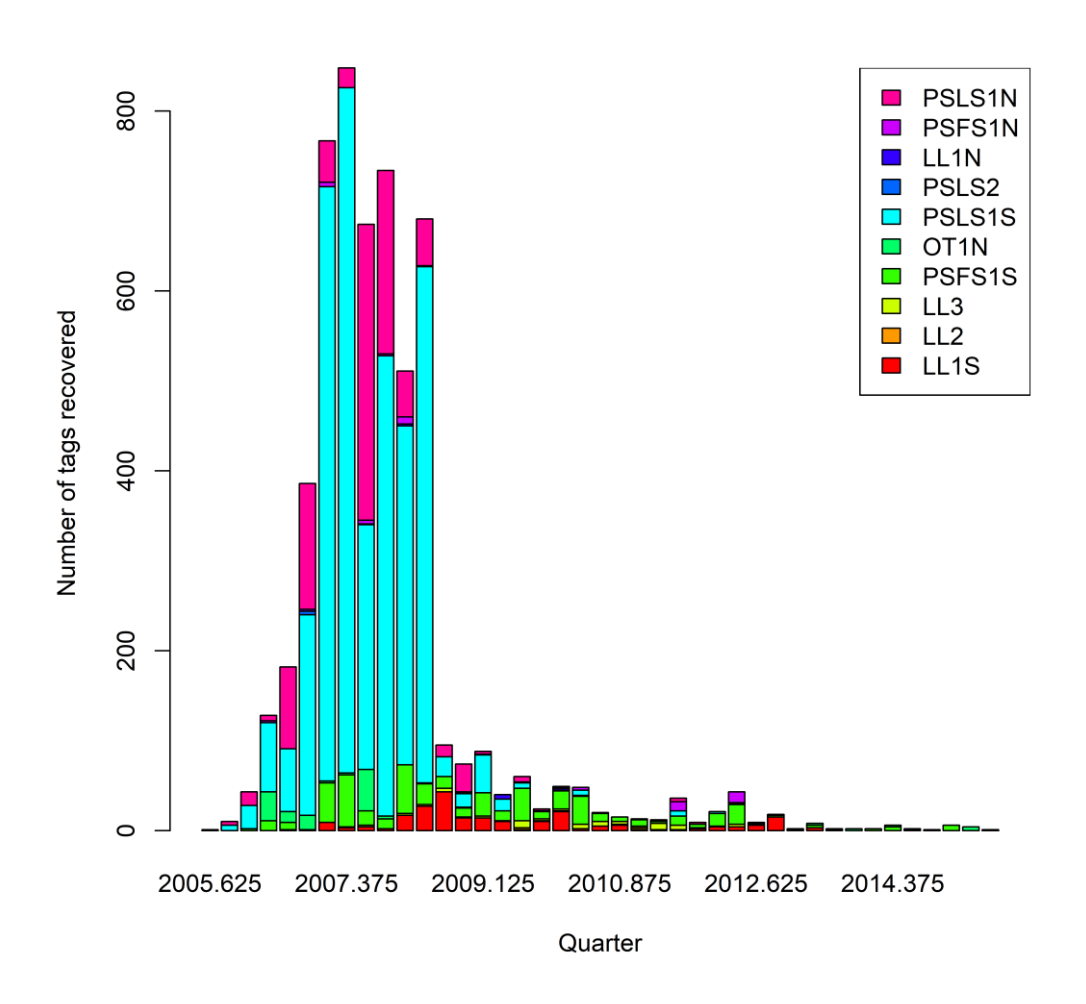


Figure 12: Bigeye tag recoveries by year/quarter and fishery included in the assessment model. Purse seine tag recoveries have not been corrected for reporting rate.

A significant proportion of the tag returns from purse seiners were not accompanied by information concerning the set type. These tag recoveries were assigned to either the free-school or FAD-associated fleets based on the assumed age of the fish at the time of recapture, i.e. based on the age assigned to the release group and the period at liberty. Fish "older" than 12 quarters were assumed to be recaptured by the free-school fleets; "younger" fish were assumed to be recovered by the FAD-associated fleets.

Langley (2016) identified several differences in the recovery rate (number of tags per tonne of catch) from the PSLS fleets between latitudinal zones for tags at liberty for at least 12 months (Tag recovery rates south of 2°S were consistently higher than north of 2°S during the main recovery period). The difference in tag recovery rates between the two main areas of the fishery indicates that the dispersal of tagged bigeye during the 12 month "mixing period" was insufficient to redistribute tagged fish

throughout the bigeye population resident within the western equatorial region (Region 1N and 1S). Consequently, the distribution of PSLS fishery effort (and catch) would have strongly influenced the number of tags recovered from the fishery. Following Langley (2016), the western equatorial region has been partitioned into two regions (Region 1N and Region 1S) in the assessment model account for the potential incomplete mixing of tagged fish.

For incorporation into the assessment model, tag releases were stratified by release region, time period of release (quarter) and age class. The returns from each tag release group were classified by recapture fishery and recapture time period (quarter). The tag data were further adjusted for tag losses and reporting rates to minimize the bias on estimates of fishing mortality and abundance in the assessment model. The procedure is described in below.

3.8.1. Age assignment of tag releases

In the current assessment, the age at release was converted based on the mean growth function. In the previous assessment, the use of an age-length key approach that admits the uncertainty in the size distribution at age had been explored. In the 2025 model, as the growth function has been updated, the tag releases and recaptures have been reassigned to different age groups, based on the new growth function.

3.8.2. Tag mortality

As in the 2022 assessment, the number of tags in each release group was reduced by 30% to account for initial tag mortality. The initial tag mortality estimates of 20.5% was increased by a further 10% to account for an assumed level of tag mortality associated with the best (base) tagger (Hoyle *et al* 2015). The total number of tags released was 34,427 and processing the tags in this way reduced the number to 24,109 tags.

3.8.3. Tag reporting rate

The results of the tag seeding experiments conducted during 2005–2008, have revealed considerable temporal variability in tag reporting rates from the Indian Ocean purse seine fleets (Hillary *et al.* 2008a). Reporting rates were lower in 2005 (57%) compared to 2006 and 2007 (89% and 94%). Quarterly estimates were also available and were similar in magnitude (Hillary *et al.* 2008b). This large increase over time was the result of the development of publicity campaign and tag recovery scheme raising the awareness of the stakeholders (e.g. stevedores and crew). SS3 assumes a constant fishery-specific reporting rate. To account for the temporal change in reporting rate, the number of tag returns from the purse-seine fishery in each stratum (tag group, year/quarter, and length class) were corrected using the respective estimate of the annual reporting rate (Langley 2016).

The approach to correct the number of tag returns for the reporting rate follows Kolody (2011), Fu (2017), and Fu et al. (2018): tags recovered at-sea are assumed to have a 100% reporting rate; tags recovered from landings in Seychelles were corrected for the quarterly estimates of reporting rates from Hillary *et al* (2008b). The tag recoveries were further increased by the proportions of EU PS catches landed outside the Seychelles, to account for purse-seine catches that were not examined for tags. For example, the adjusted number of observed recaptures for a PSLS fleet as input to the model, R_L' was calculated using the following equation:

$$R_L' = R_L^{sea} + \frac{R_L^{sez}}{P^{sez}r^{sez}}$$

where

 R_L^{sea} = the number of observed recaptures recovered at sea for the PSLS fleet.

 R_L^{sez} = the number of observed recaptures recovered in Seychelles for the PSLS fleet.

 r^{sez} = the reporting rates for PS tags removed from the Seychelles

 P^{sez} = the scaling factor to account for the EU PS recaptures not landed in the Seychelles.

The adjusted number of observed recaptures for a PSFS fleet was calculated similarly. A reporting rate of 94% was assumed for the correction of the 2009–2015 tag recoveries. The numbers of tag recoveries were also adjusted for long-term tag loss (tag shedding) based on an analysis by Gaertner and Hallier (2015). Tag shedding rates for bigeye tuna were estimated to be approximately 1.7% per annum.

A total of 24109.4 releases were classified into 50 tag release groups (a reduction from 68 in 2022 using the previous growth model). Most of the tag releases were in the 4–6-year age classes (Figure 6) A total of 5,666 actual tag recoveries were included in the tagging data set. The cumulative effect of processing the tag recovery data increased the number of recoveries to 6,928 tags.

4. MODEL DESCRIPTION

The model was implemented in Stock Synthesis 3.30.24. A detailed description of the model and the general assumptions, alongside detailed technical descriptions of various components can be found in the SS3 User Guide, and associated webpage, and publications. Most of the structure of the model has remained the same since the 2022 model, and as such the sections are the same as in the previous stock assessment report. There have been updates in 2025 to both the growth and natural mortality.

4.1. Population dynamics

The model population structure is comprised of 41 quarterly age classes; the first age class represents fish aged 0–3 months (age 0) and the last age class accumulates all fish age 40 + quarters. The population is aggregated by sex and partitioned by region.

The model commences in 1975 and extends to the end of 2024 in quarterly intervals (192 timesteps).

The initial (1975) age structure of the population was assumed to be in an exploited, equilibrium state. The four main LL fleets were operating prior to 1975, and initial fishing mortality parameters were estimated for each of these fleets, based on early catches and size structure in the commercial catches in the early years. The resulting fishing mortality rates are applied to determine the initial numbers-atage in each model region.

4.1.1. Recruitment

Recruitment of age 0 fish occurs in each quarterly time step of the model. Recruitment was estimated as deviates from the Beverton-Holt (BH) stock recruitment relationship (SRR). The recruitment deviates were estimated for the period that corresponds to the operation of the PSLS fleet which provides catch and length data for the smaller fish and, hence, may be informative regarding the variation in recruitment (1985–2023 (156 deviates; year quarters 232-388)). Recruitment deviates were assumed to have a standard deviation (σ_R) of 0.6. The final model options included three (fixed) values of steepness of the BH SRR (h 0.7, 0.8 and 0.9). These values are considered to encompass the plausible range of steepness values for tuna species such as bigeye tuna and are routinely adopted in tuna assessments conducted by other tuna RFMOs.

The recruitment for bigeye remains uncertain as the areas where larvae and early juveniles are concentrated have never been sampled nor studied by scientists (Fonteneau 2004). While the temperate regions are generally believed to be feeding grounds, recruitment is assumed to occur in all regions (hence differentiating between recruitment into the population vs. spawning.) The overall proportional distribution of recruitment among the four regions was not estimated by the model. Recruitment was estimated across the entire population (e.g. it was fixed among regions but estimated overall). There is little information to indicate that there are significant differences in the pattern of recruitment between the regions, i.e. the CPUE trends are broadly comparable between the equatorial regions and the length composition data from the longline fleets do not appear to be informative regarding recruitment. Length composition data from the fleets targeting smaller fish are available from the western equatorial regions only. The relative distribution of recruitment between the four regions (1N, 1S, 2, 3) was previously assumed to be temporally invariant. However, in 2022 regional recruitment distribution was allowed to vary for 2001–2019 (year quarters 297-372) in the basic model, to account for as the divergent regional CPUE trends in more recent years. As the LL CPUE indices in 2025 are no longer diverging in trends, and all are increasing, the regional recruitment distribution was fixed to revert to being temporally invariant.

A full log-bias adjustment factor $(-\frac{1}{2}\sigma^2)$ is applied to the recruitment deviates (as recruitment variability is assumed to be lognormally distributed, see Methot et al. 2013). Potential underestimation of recruitment variability due to uninformative data implies further bias correction may help ensure that the population scaling parameter R0 represent the long-term average recruitment. The optimal bias correction $(-\frac{1}{2}b\sigma^2, b \le 1)$ can be determined from the relationship between the assumed and estimated recruitment variability (Methot and Taylor 2011). With this approach, bias correction was

applied to the recruitment deviations in the period that is sufficiently informative about the full range of recruitment variability based on the suggested values in the SS3 output.

4.1.2. Growth

In the previous assessment, growth was estimated using data from two studies of bigeye tuna otolith-derived age data, and tag release / recovery data (Eveson *et al* (2012); Farley et al., 2021). This year, additional estimates of age and growth derived from otoliths collected in the Indian Ocean as part of the 'GERUNDIO' project were used to update the previous estimates of Farley et al., (2021) (Eveson et al., 2025). The latest dataset includes estimates of age from both daily and annual growth zones (opaque zones) from 253 bigeye tuna from across the size spectrum found in the Indian Ocean. Preliminary age validation work using otoliths and data from the IOTTP provided evidence that the methods used in the study are accurate. The new estimates represent a length-at-age that is slightly larger than estimated in the 2021 study (L^{∞} =172.7 cm vs 168 cm FL) and, as there was little difference between the different parameterisations of the von-Bertalanffy growth curves, it was agreed by the 27th WPTT to use a traditional VB within SS3 due to the difficulties of establishing accurate ages at which to have age-based k values. (Figure 13 –left).

In this assessment, continuity runs tested the impact of moving away from Eveson (2012) growth (as agreed by 27WPTT(DP)), and sensitivity runs were completed to examine the impact between using Farley (2021) and Eveson (2025) estimates.

Although data were split into two sexes in the analyses presented by Eveson et al. (2025) at the 27th WPTT(DP), there are insufficient data to fully understand whether the differences in growth curves within this dataset are due to differences in biology between males and females, or due to artefacts in the data due to a paucity of representative spatial and temporal variation in the datasets (e.g. to know whether the growth curves are different between male and female fish, sufficient samples from across the range of the species, and from several cohorts (e.g. samples from several years) is necessary to account for other sources of variation).

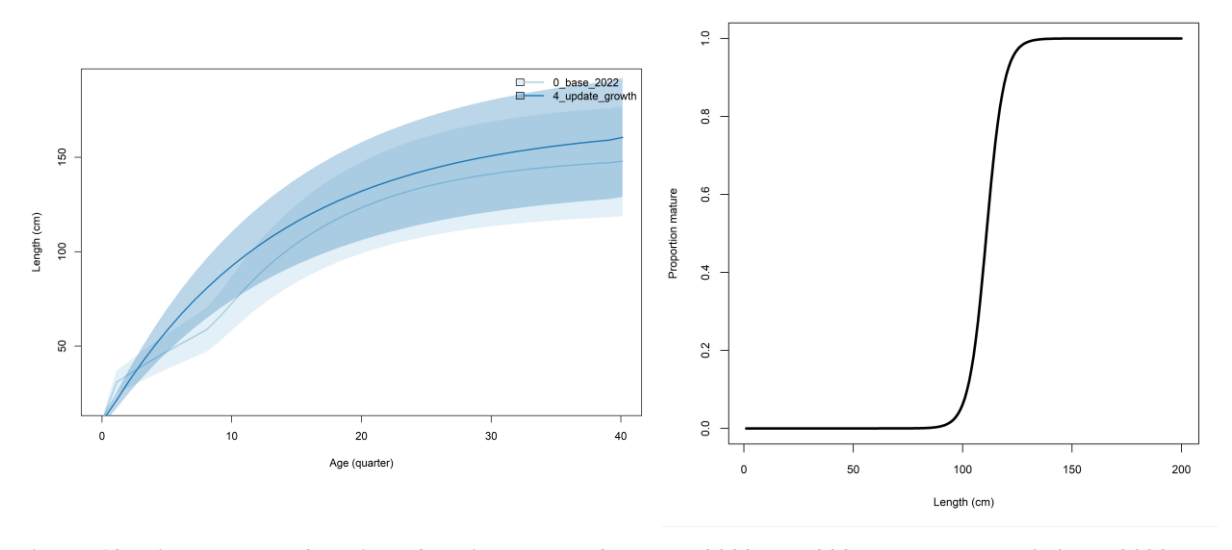


Figure 13: Fixed growth functions for bigeye tuna from the 2022 and 2025 assessments (θ_base_2022 and $\theta_aupdate_growth$ respectively) by Farley et al. 2021 and Eveson et al. 2025 (left), and length-based maturity Ogive following Shono et al (2009) (RHS). For the growth functions, the shaded distributions represent the assumed variability of mean size-at-age in the assessment models.

As has been suggested in reviews of tuna stock assessments, and following other tuna RFMO's testing this feature, it was decided by the 27th WPTT(DP) to test the impact of estimating growth internally within SS3 by using the conditional-age-at-length feature. To implement this in SS3, all age data, with associated length are incorporated into the model, and assigned to relevant fleets, regions, and timesteps within the model. For many of the age samples there was sufficient information to assign data to a fleet, region, and timestep. For all samples information was partially missing (e.g. month of capture, or

specific gear type used to capture the fish), therefore data were assigned to a fleet based on the most likely scenario (e.g. if only gear type was missing, but all other data matched that of a 'purse seine vessel in the NWIO', the data would be assigned to a 'purse seine vessel in the NWIO' and then assigned to a relevant model fleet).

A total of 253 aged fish were included in the dataset: all purse seine related fish were assigned to PSLS fleets (FAD-associated sets), and all line associated fish were assigned to LL fleets (frozen tuna). Allocation of data to fleets, regions, and timesteps was imperfect due to limited data being available for each sample. In the future, it is recommended that all relevant information (date of collection, location of collection, gear type used, vessel flag state) are recorded alongside the otolith data to improve the quality and reliability of data within the assessment model if this method is to be used in final model options.

The length-weight relationship is based on estimates by Chassot et al. (2016) ($a=2.217 \times 10^{-5}$, b=3.01211).

4.1.3. *Maturity*

The size of sexual maturity was equivalent to that applied by Shono et al (2009) and the same as has been used in all subsequent BET assessments as no new information is available for bigeye tuna in the Indian Ocean. Female fish were assumed to attain sexual maturity from 100 cm (F.L.) with full sexual maturity at about 125 cm (Figure –right). Zudaire et. al (2022) estimated reproductive parameters for bigeye tuna in the Indian Ocean as part of the 'GERUNDIO' project. The shape of the preliminary maturity ogive obtained is very different to the ogive currently used in the stock assessment, although the estimates of length at 50% maturity are similar (112.7 cm versus 110.9 cm FL). The proportion mature at length does not reach 100% as expected in the larger length classes and requires further investigation and as such has not been used in this assessment, as in 2022.

At the 27^{th} WPTT(AS), new data were presented on the size at maturity of bigeye tuna in the Indian Ocean, based on a study from Chinese observer data (IOTC-2025-WPTT-27-25) that suggests bigeye tuna reach sexual maturity at ~ 109.3 cm (FL). Prior to the next assessment of bigeye tuna in 2028, these results should be considered to see if the size-at-maturity needs to be updated in the assessment.

4.1.4. Natural mortality

The instantaneous rate of natural mortality (M) varies with age and consists of an average over age classes and age-specific deviations from the overall average M. In many fish stock assessments, M is fixed at a pre-specified value for all ages or sizes and is often not based on data related to the species or fishery being assessed. Incorrectly specifying M within stock assessments (and therefore having a mis-specified model) has been shown to have significant impacts on the relevant estimations of management-relevant indicators (Punt et al., 2021; Maunder et al., 2015).

In previous IO bigeye tuna assessments, age-specific natural mortality has been estimated externally to the model, and input as a fixed M-at-age-function. Natural mortality can also be estimated internally within SS3, a method which allow the data to inform estimates of M within the model. This method requires careful review of the model diagnostics, and plausibility of the final model estimates (Hamel et al., 2023, Punt et al., 2023).

From the RTTP, a considerable number of tagged fish were captured after 7–8 years at liberty, indicating a considerable proportion of the tagged fish had reached an age of 8-10 years; 8 tags were recovered after 10 years at liberty and a few tags were recovered during the most recent year (2015), corresponding to an age at recovery of 11-12 years. The higher level of M estimated in previous stock assessments (e.g. 2019) would result in a very small proportion of the tagged fish reaching 12 years of age, suggesting that a lower level of M is more plausible. The lower level of M is also supported by ageing studies of bigeye tuna in the eastern and western Australia water which suggests the longevity of bigeye is more likely to be 14.7 years, higher than original estimates in the Indian Ocean, but lower than that in the Atlantic Ocean (Farley et al. 2004; Farley et al., 2025).

Hoyle (2022) reviewed approaches for estimating M for bigeye tuna and proposed an approach to provide estimates of age dependent M. The approach involves determining a target level of M based on

the maximum observed age, and the relative M-at-age based on the Lorenzen functional form. The two components are then combined using the approach of Porch (2011) which rescale the Lorenzen curve so that the average mortality rate matches a target value over the relevant life history period. Using this approach, Hoyle (2022) provided four alternative values of target M based two alterative maximum observed ages for bigeye tuna (14.7 years in the Indian Ocean or 17 years in the Atlantic Ocean), and two empirical methods to estimate M (Then et al. (2015)). In the 2022 assessment, three estimates of M were used in the final ensemble of models ("Mbase", "MHamel15", and "MHamel17", Fu et al., 2022)

In the 27^{th} WPTT data preparatory meeting, it was suggested that the "MHamel17" estimate was removed from the 2025 model, as it used an unrealistic estimate for maximum age (17 years) that has not been observed in the Indian Ocean. Additionally, it was suggested that internal estimation of M within SS3 was trialled, alongside "MHamel15". This follows the ICCAT 2025 bigeye tuna stock assessment. To internally estimate M inside SS3, adult tuna ages are specified (4-10 years), so M varies between age 0 to 4, then asymptotes from age 4 to maximum age in the model (40 quarters / 10 years). The curve follows a Lorenzen functional form and has been named "MLorHam6Q" – age in the model is specified in quarters and uses option 6 within the M options in SS3 (see SS3 User Guide). Mean M at Age_{max} estimated outside the model using the same methods and code as used in the ICCAT assessment. Code is available from the Secretariat.

Three starting values for M were used, following methods used in the ICCAT bigeye tuna assessment. The uncertainty grid was built with the values of 50% CI of estimates of M, and the weightings were estimated from the density function assuming lognormal distribution of M with SD=0.31. The three starting values for M were 0.30 (low), 0.37 (medium), 0.45 (high). M was fixed in the model.

A comparison of the various M used in the 2022 base model ("Mbase"), and in the 2025 assessment can be found in Figure 14.

4.1.1. Movement

In Stock Synthesis, movement is implemented as the proportional redistribution of fish amongst regions, including the proportion remaining in the home region. The redistribution of fish occurs instantaneously at the end of each model time step (quarter).

Movement of fish was estimated amongst the four model regions. Movement was parameterised to estimate differential movement from young (8 quarters) to old (≥15 quarters) fish to approximate potential changes in movement dynamics associated with maturation. For each movement transition, two separate movement parameters were estimated (for young and older fish). A linear interpolation between the age specific movement rates was applied to determine movement of the intermediate age classes. Fish younger than age 3 quarters were assumed to remain within the natal region. Movement rates were assumed to be temporally invariant.

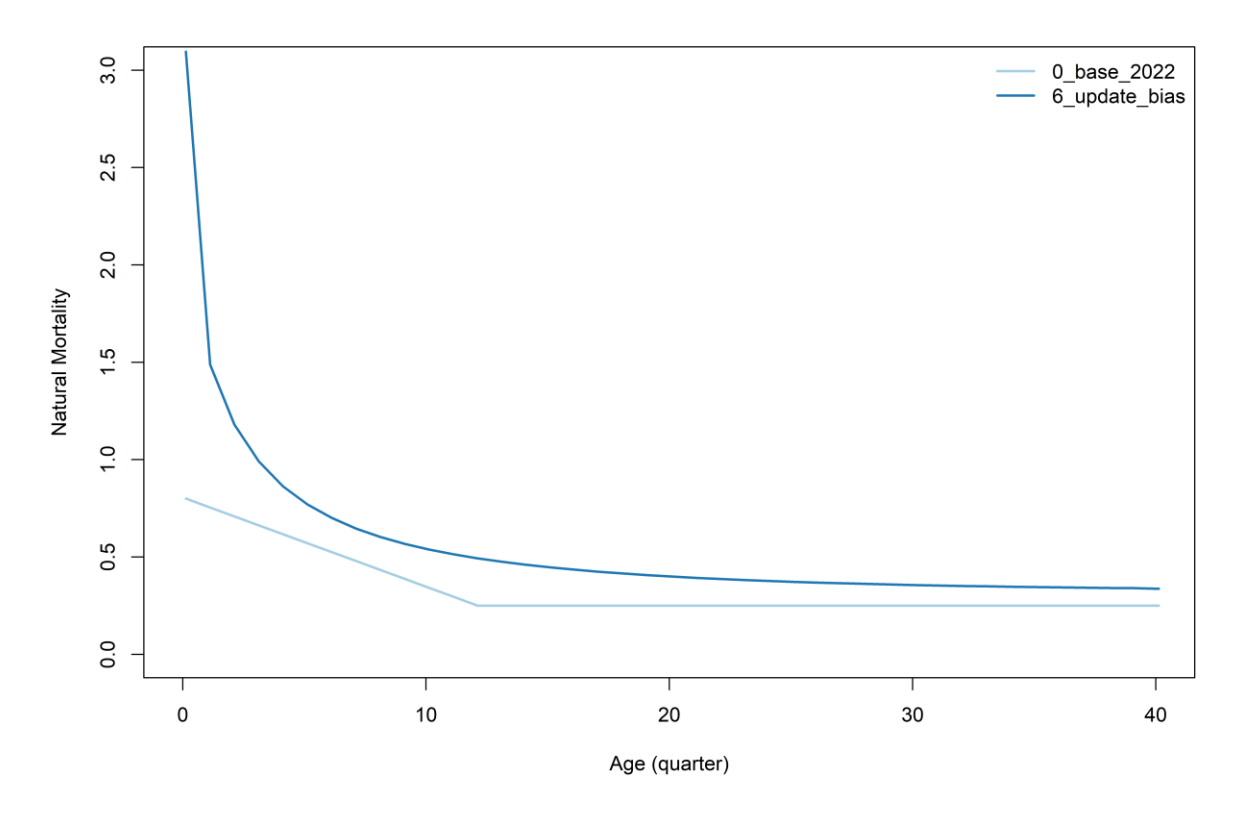


Figure 14: The different instantaneous rates of natural mortality (M) used in the 2022 ("0_base_2022", "6f_Mbase") and 2025 reference model. The 2025 model uses the Hamel & Cope model, using 14.7 years as the Agemax. Age in the graph is in quarters as this is how it is structured in the model.

4.1.2. Fleet dynamics

As in the 2022 model, age-based selectivity was assumed for all fleets. Selectivity is more likely to be a length-based process for most gears. However, as the model has adopted a quarterly resolution, the age-based selectivity is considered adequate in approximating the length-based process. Separate selectivity functions were estimated for each of the four main longline fleets where a logistic function was used for LL1N and LL1S fleets, and a double normal function was used for the LL2 and LL3 fleets. A logistic selectivity was assumed for the FL2 longline fleet.

The selectivity of the PSLS fleets were estimated using a double normal functional form. Separate selectivity functions were estimated for the PSLS1N and PSLS1S fleets. For the PSLS1N and PSLS1S fleets, there was a marked shift in the length composition of the fleet catch in the mid-2000s. The modelling option of accounting for the apparent change in the selectivity of the PSLS1 fleet was explored by incorporating a random walk on the estimation of the selectivity parameters related to the age of the peak selectivity and the width of the ascending limb of the selectivity. The temporal shift in selectivity was not included in the final model options.

To account for the bimodal length composition of the catch from the PSFS fleets, the selectivity was modelled using a cubic spline with six nodes. The selectivity of the PSFS1N and PSFS1S fleets was assumed to be equivalent.

Limited data were available to estimate the selectivity of either the PSLS2 or PSFS2 fleets. The selectivity of these fisheries was constrained (mirrored) to be equivalent to the corresponding fleet selectivity in the western equatorial region 1S.

Limited size data are available from the "Other" fleets. During the previous assessment, attempts to estimate independent selectivity for these fleets were not successful, partly due to the variability in the

length composition between samples. In aggregate, the length compositions are bimodal and similar to the length composition from the PSFS fleets. On that basis, the selectivity for the two "Other" fleets (OT1N and OT2) were assumed to be equivalent to the PSFS fleets. Similarly, limited length data are available for the LINE2 fishery, and the selectivity was assumed to be equivalent to the main longline fleets. Further it has been suggested the length samples from the "bait boat" fleet (mostly from Maldives pole and line fishery) are thought to be of very poor quality; therefore, the selectivity of this fleet was assumed to be equivalent to the PSLS1S fleet.

Fishing mortality was modelled using the hybrid method that estimates the harvest rate using Pope's approximation and then converts it to an approximation of the corresponding F (Methot & Wetzel 2013).

4.2. Dynamics of tagged fish

4.2.1. Tag mixing

In general, the population dynamics of the tagged and untagged populations are governed by the same model structures and parameters. The tagged populations (tag groups) are monitored over time intervals following release. The predicted number of tags in each region and subsequent time intervals are derived based on the movement parameters, natural mortality and fishing mortality. For each time interval, the number of tags recovered by a specific fleet is predicted based the modelled number of tags in each age class in the region, the selectivity of the fleet and the fishing mortality of the specific fleet. The predicted number of tag recoveries is also moderated by the fleet specific reporting rate.

The assessment framework assumes that the probability of capturing a tagged fish is equivalent to the probability of catching an untagged fish. Violation of the assumption of homogeneous mixing of tagged fish at the relevant spatial scale (i.e. region) is likely to introduce a bias in the estimation of fish abundance. In SS3, a mixing period is specified which partitions the tag data sets (by release group); tag recoveries (observed and predicted) from the mixing period are excluded from the tag likelihood and therefore do not influence the estimation procedure.

For bigeye tuna, almost all tags were released from a localised area of region 1S. The tagged bigeye were predominantly aged 4–8 quarters at release, while the selectivity of the PSLS1S is estimated to be 4–11 quarters. Consequently, there is likely to be a limited time (4–8 quarters) during which most of the tagged fish would be available to the PSLS fleets. Thus, a mixing period of four quarters was chosen on the basis that enough tagged fish remained available to the PSLS fleets during the post mixing period, albeit for a relatively limited period.

An analysis of the spatial distribution of the tag recoveries from the purse-seine fleets (see Appendix A of Fu 2019) suggested that the four quarter mixing period may be sufficient to allow for a reasonable degree of mixing of tagged fish within the south-western equatorial region (Region 1S). The dispersal of tags into the north-western equatorial region (Region 1N) will be mediated by the estimated movement rates (from region 1S), however, the distribution of tagged fish in this region is unlikely to be homogeneous and it is likely that tag densities would be higher in the southern area of region 1N (i.e. closer to the release location). Consequently, tag recoveries from the region may be influenced by the spatial distribution of the catch from the fleets.

Specifying a mixing period of 12 months (4 quarters) in the stock assessment model will effectively exclude 76% of all the FAD-associated tag recoveries, while retaining 69% of the free-school recoveries (reducing the total tag recoveries by 66%). This effectively reduces the potential bias introduced by the FAD-associated tag recoveries while maintaining most of the free-school tag recoveries. The remaining FAD-associated tag recoveries are predominantly comprised of fish larger than 80 cm and, arguably, these larger fish are likely to be more evenly distributed that the smaller size category.

4.2.2. Tag reporting

The observed number of tag recoveries for the purse seine fleets were already adjusted to account for the differential tag reporting rates. On that basis, the reporting rates for the purse seine fleets were fixed at 1.0. The model also incorporates the tag recoveries from the other fleets, most notably the LL fleets. There are no external estimates of tag reporting rates available for the longline fishery and, hence, the fishery specific reporting rates were estimated based on uninformative priors and were assumed to be

temporally invariant. Tag recoveries from the longline fleets will be considerably less informative about stock abundance.

The tag mixing process is highly variable in time and space and is likely to vary by release group. Different release groups may experience different levels of tag loss and/or reporting due to tagger effects. Recent development in tag modelling has suggested the modelling of tags conditioned on the number returned, to minimise the bias due to the heterogeneity due to tag losses, reporting, or mixing amongst release groups.

4.3. Modelling methods, parameters, and likelihood

The total likelihood is composed of four main components: catch data, the abundance indices (CPUE), length frequency data and tag release/recovery data. There are also contributions to the total likelihood from the recruitment deviates and priors on the individual model parameters. The model was configured to fit the catch almost exactly so the catch component of the likelihood is very small. There are two components of the tag likelihood: the multinomial likelihood for the distribution of tag recoveries by fleets over time and the negative binomial distribution of expected total recaptures across all regions. Details of the formulation of the individual components of the likelihood are provided in Methot & Wetzel (2013).

The regional CPUE indices are assumed to represent the relative abundance (numbers of fish) of the proportion of the regional population that was vulnerable to the longline fishery. The weighting of the CPUE indices followed the approach of Francis (2011). Following previous assessments, and related analyses, CV of 0.1 was assigned to each set of longline CPUE indices in the base model, to ensure the stock biomass trajectories were broadly consistent with the CPUE indices while allowed for a moderate degree of variability in fitting to the indices. Purse seine indices were given a CV of 0.2 as suggested at the 27th WPTT(DP).

The relative weighting of the tagging data was controlled by the magnitude of the over-dispersion parameters assigned to the individual tag release groups. Following Langley (2016), the over-dispersion parameters for all tag release groups were estimated within the assessment model assuming a relatively uninformative beta prior (mean 10, sd 3). This prior reflected the variability in the tag-recapture data (variance of the standardised residuals) as determined from preliminary model runs (Langley 2016).

For all fleets, except for the PSLS fleets, the individual length frequency observations were assigned an effective sample size (ESS) of 1. For the PSLS fleets an ESS of 10 was assigned to all length observations. The higher weighting of the purse seine PSLS length frequency data reflects the comprehensive nature of the port sampling programme monitoring the catch. There is a high degree of variation in the length composition data from the PSFS fleets which appears related to the bimodal structure in the fishery length compositions; variation in the individual length samples may be attributable to sampling different proportions of the catch from each length mode. Based on the apparent level of sampling error an ESS of 1 was assigned to the length samples from the PSFS fleets.

5. ASSESSMENT MODEL RUNS

A base model was configured that represents a continuity run from the 2022 assessment with updated data and several revisions of the model. A range of sensitivity or exploratory models were later conducted explore alternative assumptions and parameter configurations. On basis of the analyses, final model options were tentatively proposed that include an ensemble of models running over permutations of plausible parameters and/or model settings, from which the stock status was estimated, and uncertainty was quantified (the Grid). The assessment was conducted using the 3.30.24 version of the Stock Synthesis software using R. Most diagnostic plots, and model updates were coded in R and generated using the *r4ss* and *ss3diags* packages. Stock status is reported for the terminal year of the model (2024).

After presentation of this model to the 27th WPTT(AS), the new catch data were incorporated into the model, and the entire run of update models re-run. Some sensitivity analyses were conducted for the parameter 'M', as initially, all models had included M that was estimated internally in the model (which does not follow the methods used in ICCAT and had not been the intention of the 27th WPTT(DP)). One model that included M estimated internally was included in the sensitivities with the updated catch data.

The preliminary assessment in 2025 included two reference models, one model that included a 0.5 % discount on the LL CPUE indices to account for 'gear creep'. After discussions at the 27th WPTT(AS), it was agreed that this model would be included in the 'grid' or model ensemble used to determine stock status but was not included in the model updates to produce the reference model. Therefore this version of the report only includes the one base model for 2025 (0 % discount on the LL CPUE indices).

The below text refers to the final base model that includes revised catch data from Indonesia. However, sensitivity runs that included PS indices were not re-run with the updated catch data. Instead, it was decided, based on the sensitivity runs from the rev1 and rev2 base models, and discussion between working party members, that the PS 'short' CPUE index would be included in the base model.

5.1. Base model

In the 2022 assessment, final model options selected to quantify stock status by the WPTT25(AS) included 24 models with alternative assumptions on selectivity (2 options), steepness (3 values), natural mortality

The 2022 reference model was re-run to ensure continuity, and some revisions were incorporated based on preliminary analyses. These revisions are to improve the assessment model, but they do not represent any major structural changes to the model. The revisions included:

- Updating growth parameters to those from Eveson et al. (2025)
- Updating the instantaneous rate of natural mortality (M) to 'MHamel15' as the reference M
- Updating the recruitment deviations to the appropriate timeframe
- Updating the bias adjustment to recommended values in SS3
- Inclusion of the PS 'short' indices in the update of the CPUE indices

A sequential, stepwise approach was taken for the model updates (Table 4). The configuration of the resulting base model is summarised in Table 5.

Table 4: Description of the sequence of model runs to update the 2022 base model.

| Model | Description |
|----------------------------|--|
| Base_2022 | 2022 reference model with steepness = 0.8, tag lambda =0.1 |
| 0_base_2022 | Updated R and SS3 executable (same version – 3.30) |
| 1-update-catch | Updated and revised catch series, extended the model to 2024 |
| 2-update-CPUE | Updated and revised longline and PS short CPUE indices |
| 3-update-LF | Updated and revised length-frequency data |
| 4-update-growth | Updated growth to Eveson et al. (2025). |
| 5-update-M | Update from 'baseM' to 'MHamel15' – maximum age of 14.7 yrs. |
| 6-update-bias (base_2025a) | Update bias adjustment values to those recommended by SS3. |

Table 5: Main structural assumptions of the bigeye tuna *base* model and details of estimated parameters. Changes to the 2022 reference model are highlighted in red.

| Parameter | Assumptions | Values | | |
|-------------------------------|--|--|--|--|
| | Occurs at the start of each quarter as 0 age fish. | | | |
| Recruitment | Recruitment is a function of Beverton-Holt stock-recruitment relationship (SRR). | $R_0 \text{ Norm}(10,10); h = 0.80$ | | |
| | Regional apportionment of recruitment to R1N, R1S, R2, and R3. | PropR ² Norm(0,1.0) | | |
| | Temporal recruitment deviates from SRR, 1985–2023. | Sigma (σ) $r = 0.6$. 156 deviates. | | |
| | Proportion of recruitment allocated to regions is temporally invariant. | | | |
| Initial population | A function of the equilibrium recruitment in each region assuming population in an initial, exploited state in 1975. | | | |
| | Initial fishing mortality estimated for LL1N,1S,2,3 fisheries. | Norm(0.10,99) | | |
| Age and growth | 41 quarterly age-classes, with the last representing a plus group. | 0 – 40+ | | |
| | Growth based on von Bertalanffy growth model | $L^{\infty} = 167.54288 \text{ cm}, k = 0.300; L_{\min} = 0.200$ | | |
| | SD of length-at-age based on a constant coefficient of variation of average length-at-age. | CV =0.10 | | |
| | Mean weights (W_j) from the weight-length relationship $W = aL^b$. | a = 2.217e-05, $b = 3.01211$ | | |
| Instantaneous | Age-specific, fixed, estimated externally to model using Hamel & Cope (2022); and Age _{max} of 14.7. | 'MHamel15' | | |
| rate of natural mortality (M) | Estimated internally within the model – using age as quarters, option 6 in SS3, and age_{max} of 14.7. | 'MLorHam6Q' | | |
| Maturity | Length specific logistic function from Shono et al (2009). | Maturity of 50% females = 110.888 cm | | |
| Maturity | Mature population includes both male and female fish (single sex model). | Maturity slope = -0.25 | | |
| | Age-dependent with two blocks; age classes 3-8 and 15-40+ (quarters). | 12 movement coefs. Norm(0,4). | | |
| Movement | Ramp function age 8-15 (quarters) | 12 movement cools. (voim(0,1). | | |
| | No movement prior to age class 3 (quarters). | | | |
| | Constant among quarters. | | | |

| | Age specific, constant over time. | | | | |
|-----------------------|--|--|--|--|--|
| Selectivity | Longline – frozen: Separate logistic selectivity parameters for LL1N, LL1S, LL2 and LL3 | Logistic <i>p1</i> Norm(20,10), <i>p2</i> Norm(1,10) | | | |
| | Purse seine: Separate selectivity for PSLS1N, common selectivity PSLS1S and PSLS2. Common selectivity for all PSFS fleets. | | | | |
| | Longline – fresh: LF2 fleet logistic selectivity. | Double Normal | | | |
| | Line: LINE2 share principal longline (frozen) LL selectivity. | Five node cubic spline | | | |
| | Bait boat: BB1N fleet: double normal selectivity. | | | | |
| | Other: OT 1N & 2 share PSFS selectivity. | | | | |
| | CPUE: Longline CPUE indices share principal LL selectivity; purse seine CPUE indices share principle PSLS selectivity. | | | | |
| | Temporally invariant. Shared regional catchability coefficient. | | | | |
| Catchability | No seasonal variation in catchability for LL or PS CPUE. | Unconstrained parameter LLq | | | |
| Cutchabinty | LL2,3 CPUE indices have CV of 0.2; LL1N,1S CV 0.25. | | | | |
| Fishing mortality | Hybrid approach (method 3, see SS3 User Guide (Methot & Wetzel 2013). | | | | |
| Tag mixing | Tags assumed to be randomly mixed at the model region level four quarters following the quarter of release. Accumulation after 28 quarters | | | | |
| | All (adjusted) reporting rates constant over time. | | | | |
| Tag reporting | Common tag reporting rate fixed for all purse seine fleets. | PS RR 1.0 | | | |
| | Non-purse seine tag reporting rates have uninformative priors. | Other fisheries Norm(-0.7,5) | | | |
| Tag variation | Over dispersion parameters estimated for each tag release groups. | Beta prior (mean 10, sd 3) | | | |
| | Multinomial error structure. | | | | |
| Length composition | PSLS length samples assigned maximum effective sample size (ESS) of 10. | | | | |
| | PSFS length samples assigned maximum ESS of 1.0. | | | | |
| | LL and Other fisheries length samples assigned a maximum ESS of 1.0. | | | | |

5.2. Model sensitivity testing

The base models (6_update_bias and 7_update_cpue_LLq) were the starting points for further analyses and exploration of potential sensitivities within the model. Within this phase, variations of key data inputs, biological parameters, and model structures were explored. In 2022, several structural components of the model were explored. In this year's assessment, no major structural changes were tested, and instead the model sensitivity to data inputs, and biological parameters was tested. The aim of doing these runs was to identify any major sources of uncertainty that would impact assessment outputs. If specific data inputs or biological parameters were found to impact the assessment output, the plausible variations in these values were kept in the final ensemble of models used in the 'grid' from which stock status is derived.

Initial sensitivity testing was discussed at the 27th WPTT data preparatory meeting, and some initial explorations agreed on. Further runs were included as model development continued. Table 6 below provides a brief description of the range of alternative model options explored in sensitivity testing.

As the 27th WPTT(DP) agreed that two sets of 'base' models should be used for sensitivity testing (one with a 5% discount on the longline CPUE indices, and one without), there is a suite of models with the longline CPUE indices as they were provided to the Secretariat (**6_update_bias**), and another suite of models that have a 0.5% discount on the longline CPUE indices (**7_update_cpue_LLq**). These sensitivity runs, and their results are detailed in rev2 of the assessment report.

After the presentation of these sensitivity runs to the WPTT(AS), and the subsequent update of new catch data, it was decided that due to the limited time available, only sensitivity runs on the major sensitivity in the model (natural mortality) would be carried out. As the PS CPUE indices had little effect on the overall model, and to ensure the major influences on the PS CPUE index were included, it was decided to include the 'short' PS index in the reference model, and all sensitivity runs. Results using conditional-age-at-length were encouraging, but due to lack of critical data allowing accurate attribution of otoliths (age data) to specific time periods and fleets in the model, it was agreed to drop this sensitivity. Future research and new age-at-length data could allow for this method to be trialled again in the future.

Therefore, four values of fixed M were used, with the Lorenzen-age-based model (option 6 in SS3). Values were chosen based on the log-normal distribution of potential values of M, following the methods of Hamel and Cope (2022), and were M = 0.30, M = 0.37, M = 0.38, and M = 0.45. As initial sensitivity runs had estimated M internally in the model, and the WP wanted to understand the implications of this method, two sensitivity runs were completed where M was estimated internally using the same Lorenzen-age-based model (option 6 in SS3), with starting values of M = 0.37. One version was run using the prior as specified in Hamel and Cope (2022), and another version was run with no prior (following methods in ICCAT).

A range of diagnostic outputs were run for the sensitivity analyses, including likelihood profiling on M, and R0.

At the end of the 27th WPTT(AS), two further sensitivity runs were requested prior to the Scientific Committee:

- 1) Addition of Somalia catch for 2024 (6 update som)
- 2) Estimation of variable recruitment between areas (6 update rec)

These models have been run, and a description of the outputs and fits to data are provided.

Table 6: Description of various data inputs and biological parameters that were varied to test model sensitivity to them.

| Sensitivity | Description of test | | | |
|---|---|--|--|--|
| Instantaneous rate of natural mortality (M) | | | | |
| 6d_PSshort_MLorHam6Qest 6d_PSshort_MLorHam6Qestprior | Internal estimation of age-based M , based on the Lorenzen functional form, and estimation of the rate of M at $age_{max} = 14.7$ yr using methods from (Hamel & Cope 2022), as used in the ICCAT bigeye tuna assessment in 2025. All models include <i>PS_short</i> . One model uses a prior ('estprior'), and the other does not. | | | |
| 6d_PSshort_MLorHam6Qhi 6d_PSshort_MLorHam6Qlo 6d_PSshort_MLorHam6Qshelt | External estimation of age-based M , based on the Lorenzen functional form, and estimation of the rate of M at age _{max} = 14.7 yr using methods from (Hamel & Cope 2022). All models include PS _short. MLorHam6Qhi: $M = 0.45$ MLorHam6Qlo: $M = 0.30$ MLorHam6Qshelt: $M = 0.38$ | | | |
| Addition of new Somalia catch for 2024 | | | | |
| 6_update_som | Addition of new catch data submitted by Somalia in 2024 | | | |
| Estimate differential recruitment between areas | | | | |
| 6 update rec | b update rec Differential recruitment between areas. No time-varying recruitment. | | | |

5.3. Proposed ensemble models (Grid)

On basis of the sensitivity analyses, and discussions at the 27^{th} WPTT(DP) and (AS) meetings, further model options were configured to capture the main uncertainties in the model. From the results of the sensitivity analyses, the model was most sensitive to the instantaneous rate of natural mortality (M), and to include uncertainty in the steepness (h) parameter associated with the stock recruitment relationship (SRR) in tropical tunas, different values of h are proposed for inclusion in the ensemble models. Two options were included for selectivity in the LL2 and LL3 fleets (double normal or logistic selectivity), and two options for gear creep in the LL CPUE indices (0% and 0.5% discount). Therefore, the final models included in the ensemble of models are:

- one option for growth;
- three options for M;
- two options for selectivity
- three options for *h*
- two options for gear creep.

Table 7: Description of the proposed final model options for the 2025 assessment. The final models consist of a full combination of options below, making a total of 36 models. The options adopted within the reference (base) model ('6_update_bias') are highlighted.

| Model options | Description | | | | | |
|--------------------------|---|--|--|--|--|--|
| | | | | | | |
| Steepness (h) in SRR | • $h70: h = 0.70$ | | | | | |
| | • $h80$: $h = 0.80$ | | | | | |
| | • h90: $h = 0.90$ | | | | | |
| | | | | | | |
| Growth | • Gnew: VB growth parameters estimated by Eveson et al. (2025) | | | | | |
| | | | | | | |
| Natural Mortality | Mhamel15 – Lorenzen functional form M with adult M estimated | | | | | |
| · | from the Hamel & Cope (2022) estimator assuming a maximum age | | | | | |
| | of 14.7, see Hoyle 2021- | | | | | |
| | • MLorHam6Qlo – Internally estimated M using 'option 6' within SS3 | | | | | |
| | (see SS3 User Guide), with adult (4-10 quarters) M estimated using | | | | | |
| | Hamel & Cope (2022), assuming a maximum age of 14.7 yr. | | | | | |
| | • MLorHam6Qme – Internally estimated M using 'option 6' within SS3 | | | | | |
| | (see SS3 User Guide), with adult (4-10 quarters) M estimated using | | | | | |
| | Hamel & Cope (2022), assuming a maximum age of 14.7 yr. • Mhamel 17 – Lorenzen functional form M with adult M estimated from | | | | | |
| | | | | | | |
| | the Hamel & Cope (2022) estimator assuming a maximum age of 17, see Hoyle 2021. | | | | | |
| | 500 110 310 2021. | | | | | |
| Salaativity in II2 ± II2 | a Librarita adaptivity for LL2 and LL2 (some as at the first line) | | | | | |
| Selectivity in LL2 + LL3 | • sL: logistic selectivity for LL2 and LL3 (same as other frozen longline fleets) | | | | | |
| | sD: double normal selectivity for LL2 and LL3 | | | | | |
| | 5D. GOUDIC HOLIHAI SCIECTIVITY TOT ELEZ ANG ELES | | | | | |

6. MODELLING RESULTS

6.1. Continuity runs from 2022 model

Updating R had no impact on the model estimates. The previous assessment was also run using SS3.30, but the SS3 executable was updated to version SS3.30.24, which had no effect on the output. Updating the 2022 base model with catch had some impact to historical estimates of spawning stock biomass (hereafter referred to as biomass), between the years 1990 to present, presumably due to re-estimation of catches by Indonesia. Biomass estimates in recent years (2010-2021) were very similar, noting that the recent catches (2022, 2023, 2024) continued to drive the biomass in a downward trajectory.

Updating the CPUE indices (joint frozen longline indices) increased the historical biomass estimates, with a steeper decline in spawning stock biomass between 1999 and 2012 than previously seen. Current biomass estimates (~2012 onwards) show a divergence from the previous model, with biomass estimates plateauing until 2020, but then increasing to 2024, in a more optimistic outlook than before (Figure 15).

Updating the length frequency composition had a slight impact on the biomass estimates, with a slightly higher overall biomass estimate. Similarly, updating the growth parameters had a minor impact on the model SSB estimates – this is quite different to the previous iteration of the reference model, when the previous catch estimates were used. The model was most sensitive to the update of the natural mortality parameter (M), driving overall SSB estimates significantly lower over the whole model time period. The reduction in biomass is overall lower though. The overall trends were similar between models, but overall scale of biomass was significantly decreased by changing the natural mortality (Figure 15). Additionally, the increase in SSB estimated by the model in the final years (2022-2024) is reduced in scale when the M is updated. The model is particularly sensitive to the estimate of natural mortality, as was demonstrated in the previous sensitivity runs (rev1 and rev2 of the assessment), hence the additional sensitivity runs here.

The recruitment bias correction again reduced the initial scale of biomass slightly, but this was countered by a slightly higher estimate of SSB in the final years.

One base model was used to run additional sensitivity runs (6 update bias).

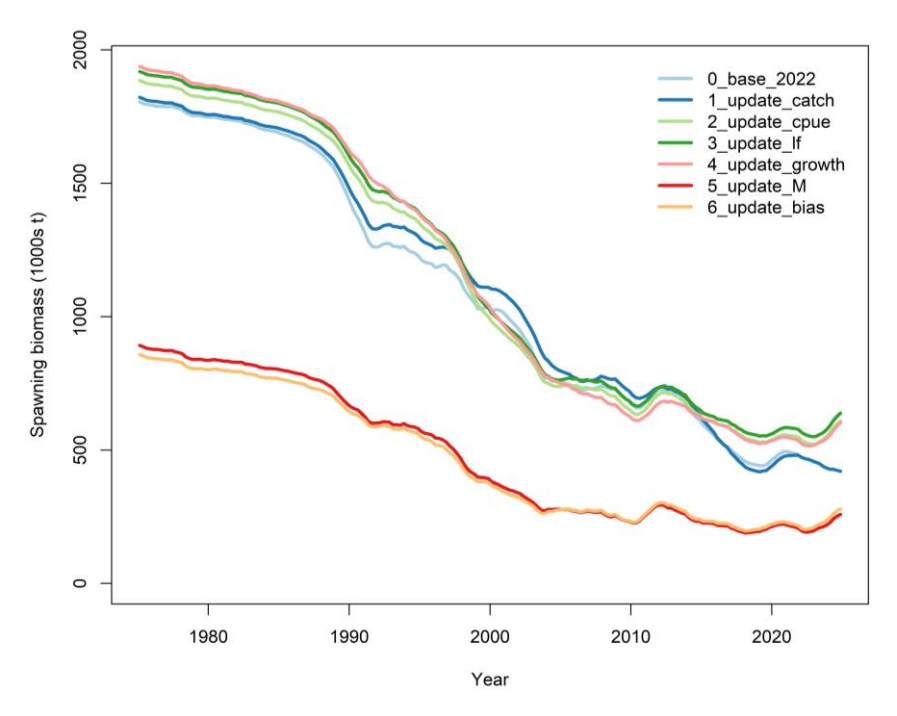


Figure 15: Spawning biomass trajectories for IO bigeye tuna from the stepwise model updates. (from the 2022 assessment reference model '0_base_2022').

Table 6: Estimates of management quantities for the step-wise updates of the 2022 stock assessment reference model ('0_base_2022') to the 2025 reference model ('6_update_bias')

| | SSB ₁₉₇₅ (t) | SSB _{MSY} (t) | SSB ₂₀₂₄ (t) | SSB ₂₀₂₄ SSB ₁₉₇₅ | SSB ₁₉₇₅ SSB _{MSY} | F _{MSY} | F ₂₀₂₄ | $F_{1975}F_{MSY}$ | C _{MSY} (t) |
|-----------------|-------------------------|------------------------|-------------------------|---|--|------------------|-------------------|-------------------|----------------------|
| 0_base_2022 | 1,925,270 | 580,627 | 488,754 | 0.2538624 | 0.8417689 | 0.1868984 | 0.3265353 | 1.7471275 | 91,646 |
| 1_update_catch | 1,942,370 | 551,777 | 425,045 | 0.2188282 | 0.7703207 | 0.1968640 | 0.2114541 | 1.0741128 | 91,944 |
| 2_update_cpue | 2,006,270 | 564,247 | 588,313 | 0.2932373 | 1.0426520 | 0.2085220 | 0.1714211 | 0.8220770 | 89,536 |
| 3_update_lf | 2,039,740 | 555,358 | 616,479 | 0.3022341 | 1.1100569 | 0.2216220 | 0.1806902 | 0.8153080 | 90,160 |
| 4_update_growth | 2,078,410 | 636,998 | 580,408 | 0.2792557 | 0.9111610 | 0.2558120 | 0.2204019 | 0.8615778 | 100,841 |
| 5_update_M | 979,792 | 257,668 | 245,027 | 0.2500801 | 0.9509388 | 0.2879080 | 0.2450979 | 0.8513063 | 102,778 |
| 6_update_bias | 945,276 | 257,728 | 264,356 | 0.2796596 | 1.0257151 | 0.2785296 | 0.2425415 | 0.8707925 | 98,594 |

6.2. Model fits

6.2.1. Base model (6 update bias)

The base models fit the new CPUE indices for the three main fisheries (LL1N, LL1S & LL2), the seasonal CPUE indices from LL3, and the PS short indices well enough (Figure 16 & 17). The residuals did not reveal any obvious patterns in region 1N and region 3, however there is a significant downward trend in region 1S and a significant upward trend in the residuals in region 2 for the LL CPUE indices (Figures 18 & 19). Overall, the variation in the residuals was broadly comparable to the S.E. initially assigned to the CPUE indices.

Appendix B outlines an analyses of the CPUE indices where the trends were compared between the LL and PS CPUE indices, indicating there would be no conflicts introduced by including the PS CPUE indices in the reference model.

Overall, there was a good fit to the aggregated length frequency data for most of the main fisheries with comprehensive sampling (Figure a & b). For the purse seine free school fisheries (PSFS), the relative proportion of fish in the small (≤ 80 cm) and large (> 80cm) length mode is variable over time, probably due to size related schooling behaviour of adult bigeye tuna, resulting in less adequate fits to the length composition distributions, particularly in region 2 for small fish, and region 1S and 1N for larger fish. For the PSFS2 fishery this may also be due to the paucity of data available (Figure 19).

The recent trends in the predicted average fish size for the main longline and purse seine fisheries are broadly consistent with the sampling data. The average length of fish from LL2 is still over-estimated by the model throughout the 1980s and 1990s despite the use of a more flexible, double normal selectivity function (Figure 20). There is a marked decline in the average size of fish sampled from the purse seine FAD fisheries in both region 1S and region 1N (Figure 0), particularly between 2010 to 2020. This trend is not as evident in the predicted average fish size derived from the model for region 2, however there are far fewer samples in this region.

The average length of fish sampled from the PSFS is highly variable (Figure 0) probably reflecting the proportion of the catch sampled from the smaller and larger modes of the combined length composition. The model prediction of average length represents the length of fish in the intermediate length range (80–100 cm).

There is an improvement in the fits to the length data from the fresh tuna longline fisheries in region 2 as in the previous assessment. Although the selectivity in the LINE fishery was assumed to be the same as the frozen longline fisheries (Figures 20), the model fitted the catch samples relatively well, despite the small number of samples. However, there are still insufficient samples to estimate a separate selectivity in this fishery.

The fit to the observed number of tag recoveries was examined for those fisheries which accounted for most of the tag returns (e.g., PSLS1S). The fit to the number of tag recoveries was examined by recombining the tags into individual release periods (i.e., aggregating the releases by age class) and excluding those recoveries that occurred during the mixing period. The fit to the tag recoveries was examined by time period (quarters) and by age at recovery, and by time at liberty (quarters) for the individual release periods and the aggregated data set (all releases combined).

The number of tag recoveries varied considerably amongst the release periods (Figure 21). The tags released in 2005 and the first quarter of 2006 had very low recoveries, probably due to the small number of releases and high tag mortality in the initial phase of the program.

Most of the observed tag recoveries in the post mix period were from the PSLS1S fishery and a high proportion of the total recoveries occurred during the first four quarters following the mixing period Figure 22). Longer-term recoveries were less vulnerable to the PSLS1S fishery (due to the age specific selectivity) and, hence, numbers of recoveries declined considerably (Figure 22).

The fit to the tag recoveries from the PSLS1S fishery by age class (at recovery) suggested that the model under-estimated the overall number of tags recovered from the fishery in younger and older age classes, to varying degrees. Fits were better to all fisheries other than the PSLS fleets (Figures 23). This result

indicates that the age-specific recoveries are inconsistent with the fishery selectivity functions. The tag recoveries from the PSLS fishery included a significant proportion of fish above 80 cm which generally were not vulnerable to the commercial fishery. Limited numbers of tags were also recovered by the PSFS1S and LL1S fisheries after longer periods at liberty (compared to PSLS1S). The model tends to underestimate the number of tag recoveries throughout the age classes from the PSFS1S fishery as in 2022. This may be indicating inadequate mixing of the tags with the fish population vulnerable to the PSFS fishery.

Overall, there was a reasonable fit to the tag recoveries from the PSLS 1S fishery during the main tag recovery period (to 2011), as in 2022, but the model no longer over-estimates the number of longer term tag recoveries from the older age classes (at recovery), i.e. those fish at liberty for a longer period, which could reflect the better specification of natural mortality within the base models in 2025, or could still be a reflection of mis-reporting in tag recoveries. A small number of tags were recovered in region 1N and the model predicts a correspondingly low number of tag recoveries from the region, as in 2022.

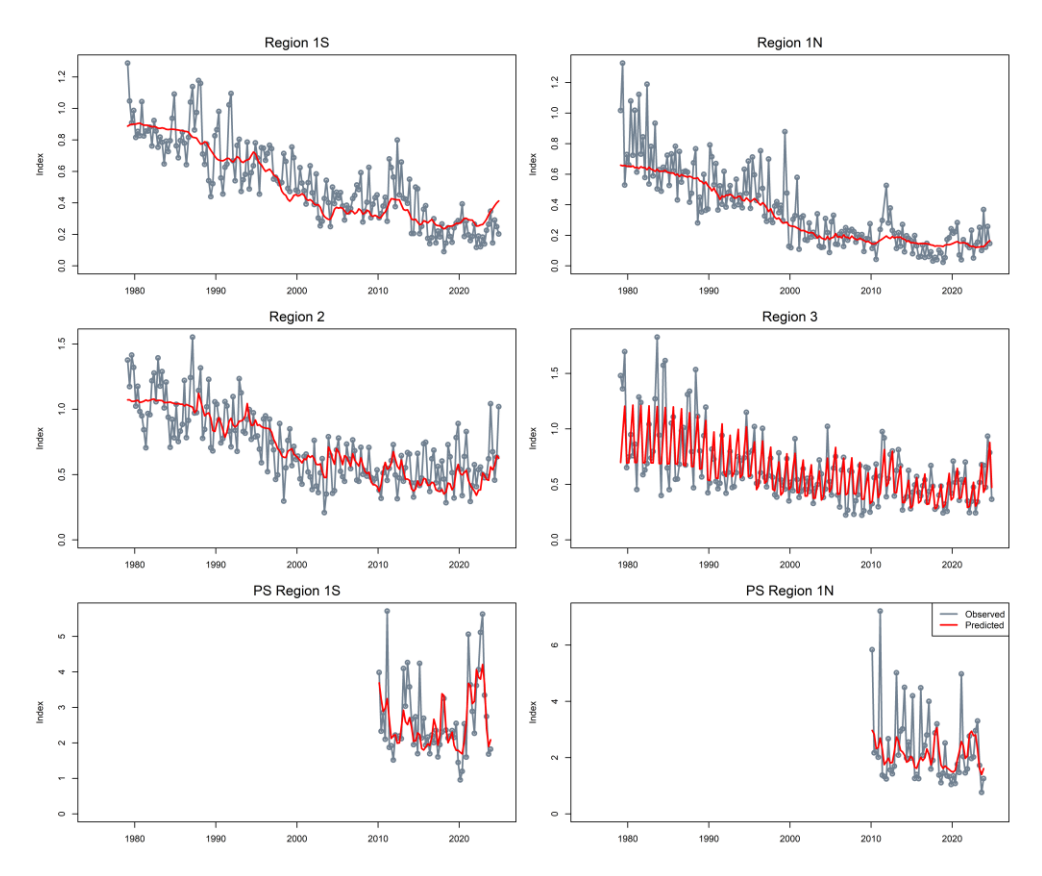


Figure 16: Fits to the joint regional frozen longline CPUE indices (1979-2024) and PS'short' (2010-2024) in the base model '6_update_bias'.

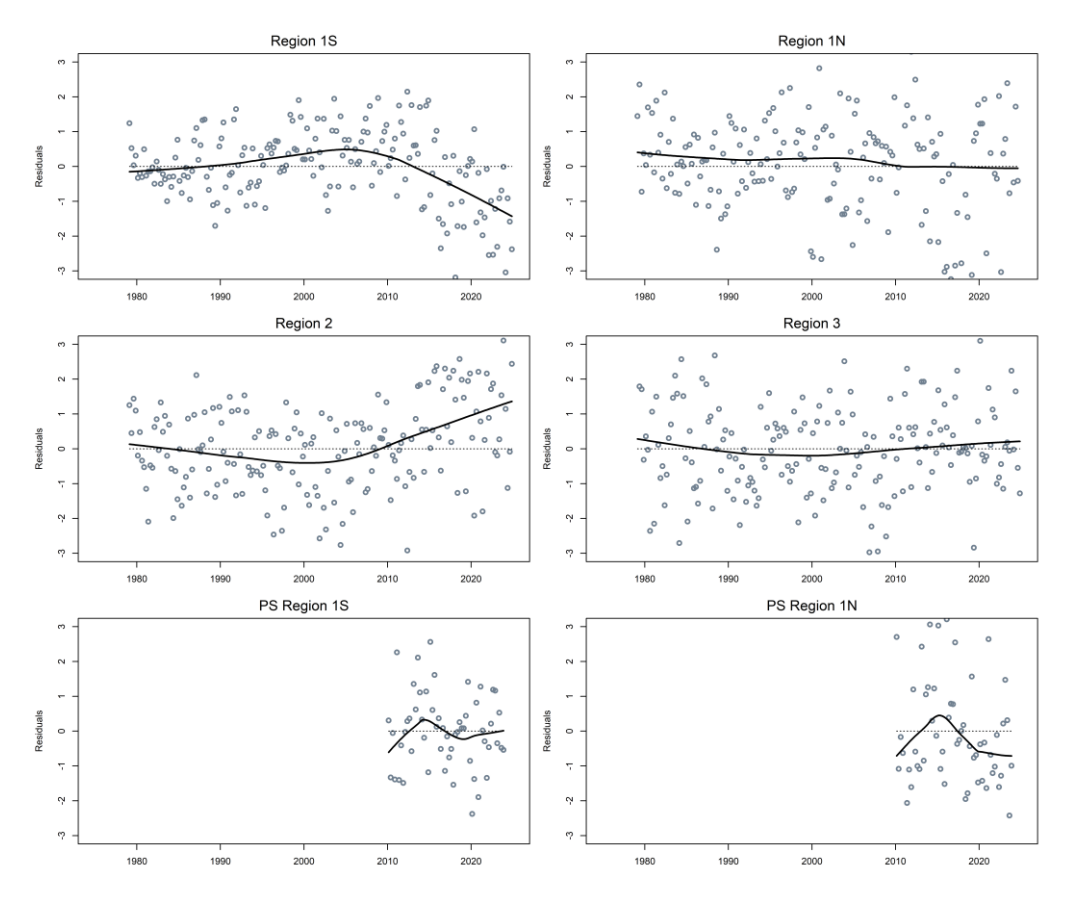


Figure 17: Standardised residuals from the fits to the CPUE indices from the base model '6_update_bias'.

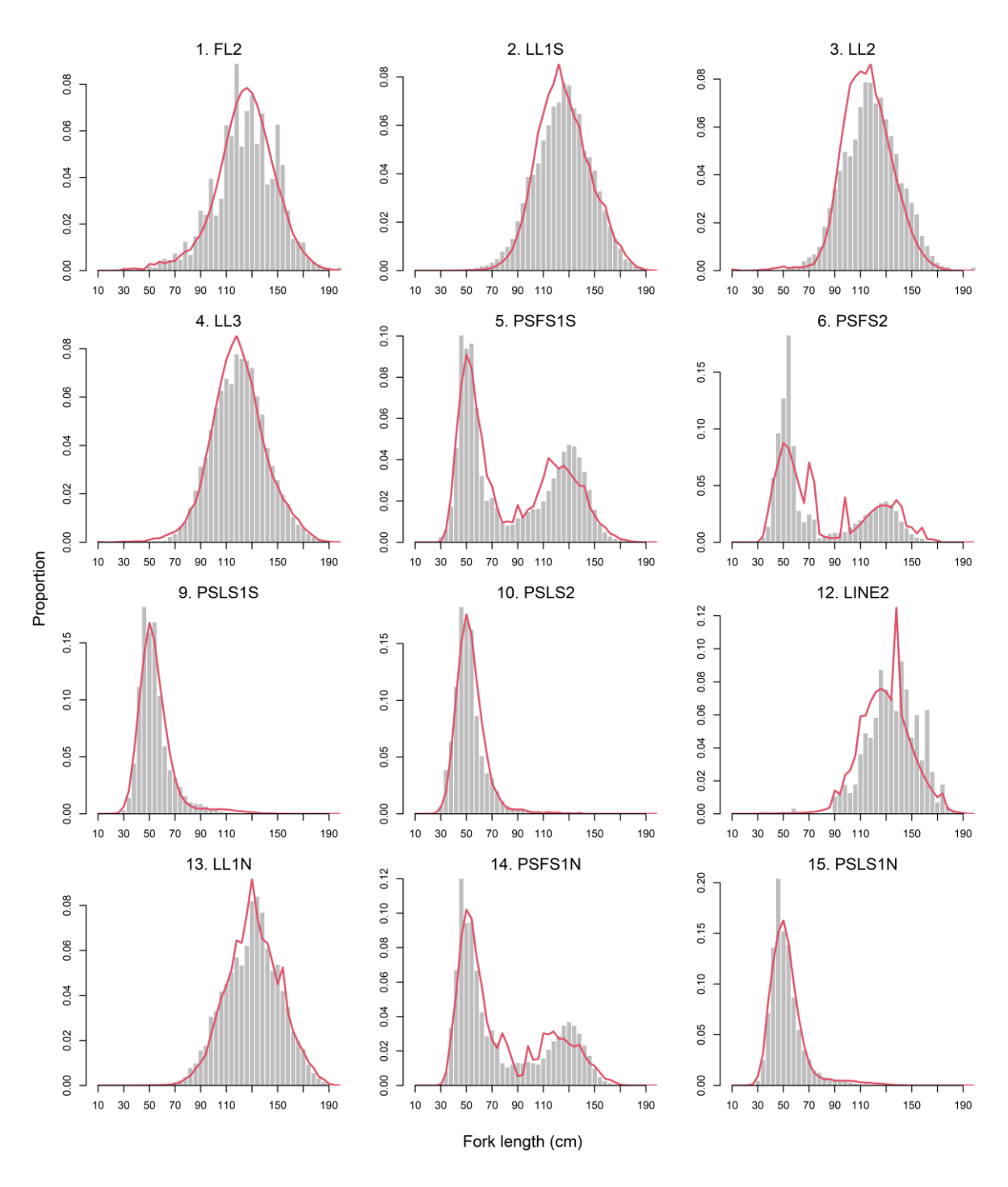


Figure 18: Observed (grey bars) and predicted (red line) length compositions (in 4 cm intervals) for each fishery of bigeye tuna aggregated over time for the base model '6_update_bias'.

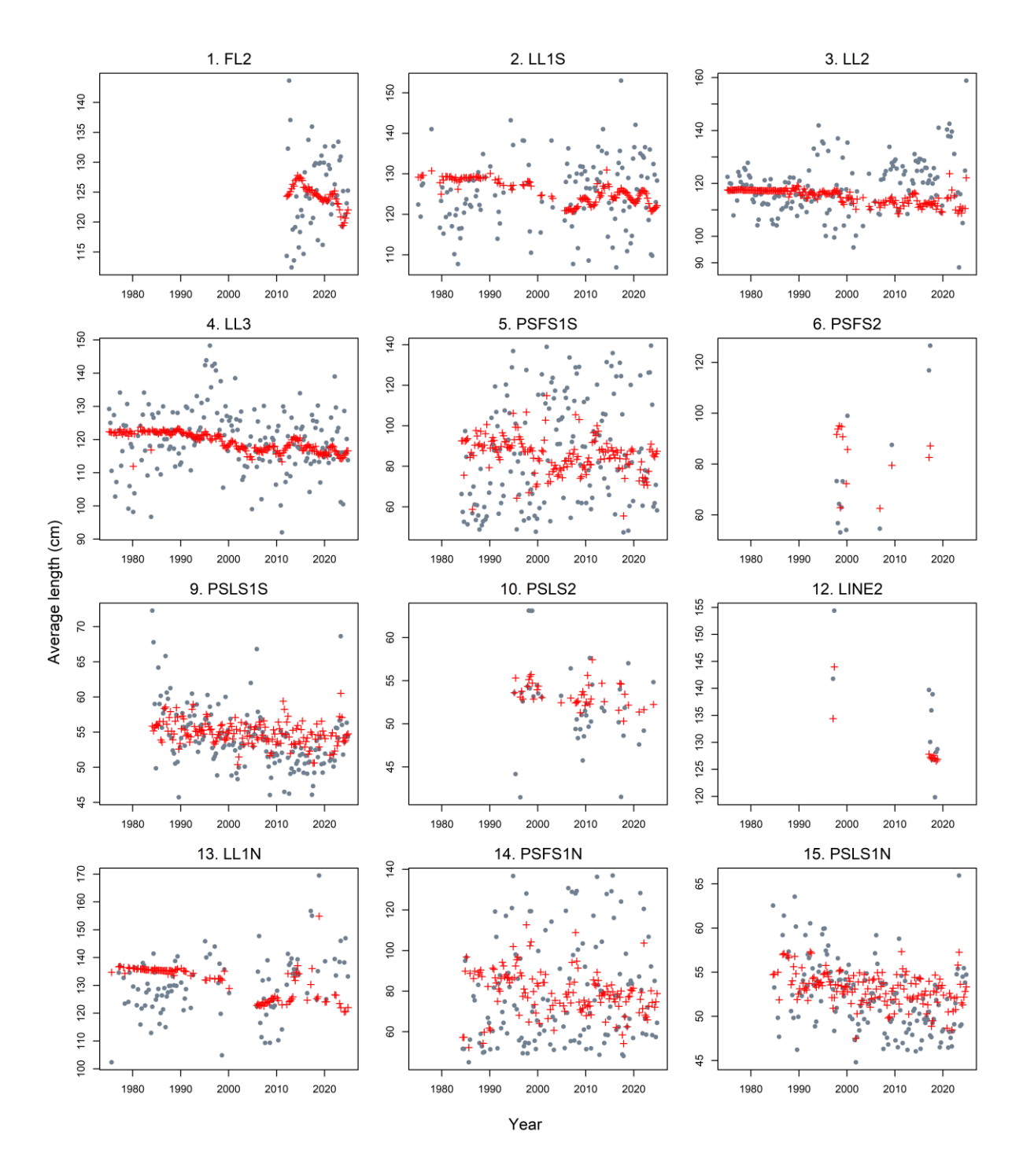


Figure 19: A comparison of the observed (grey points) and predicted (red points and line) average fish length (FL, cm) of bigeye tuna by fishery for the main fisheries with length data for the base model '6_update_bias'.

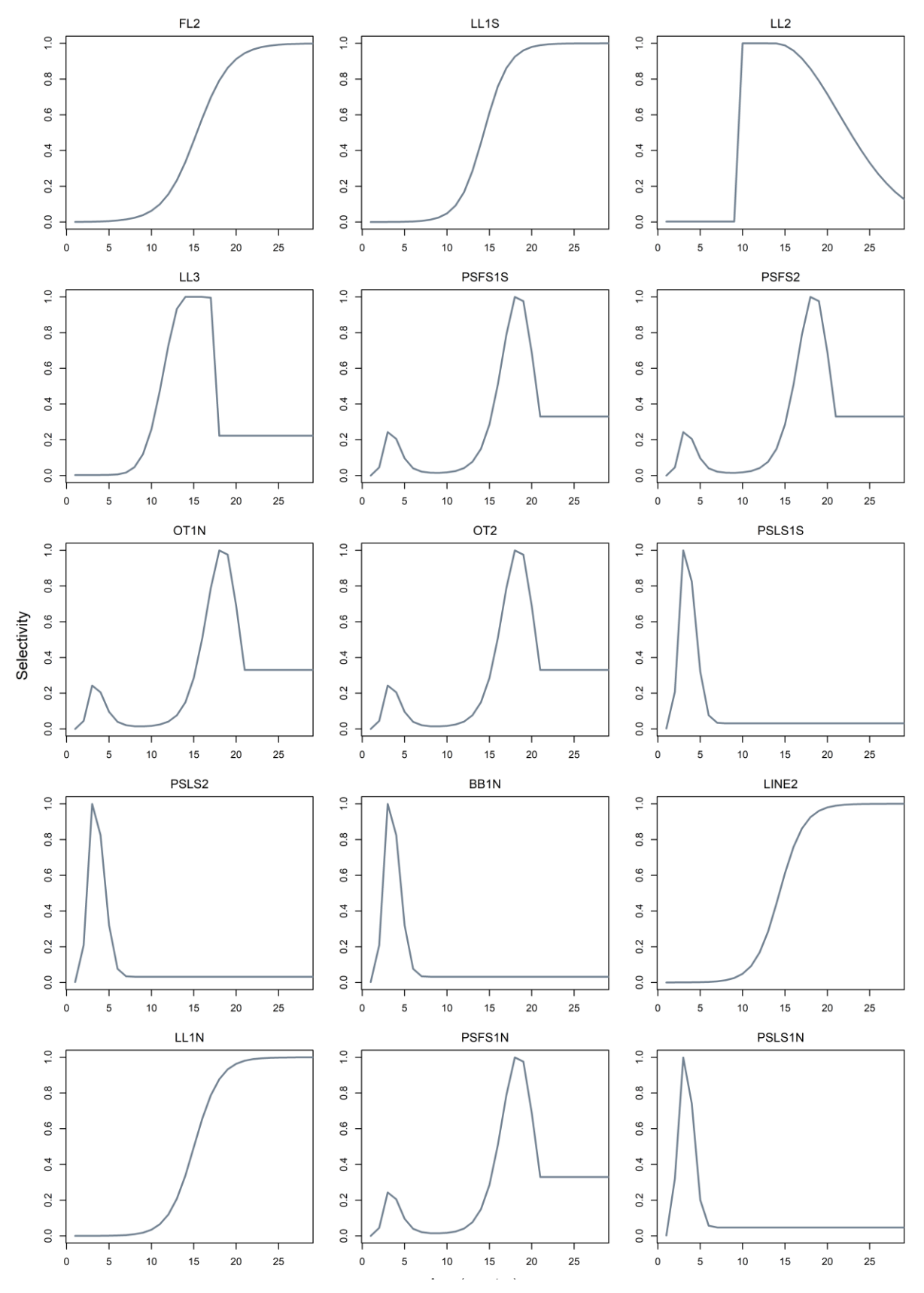


Figure 20: Estimated age-based (quarters) selectivity for model fleets within the base model '6_update_bias'.

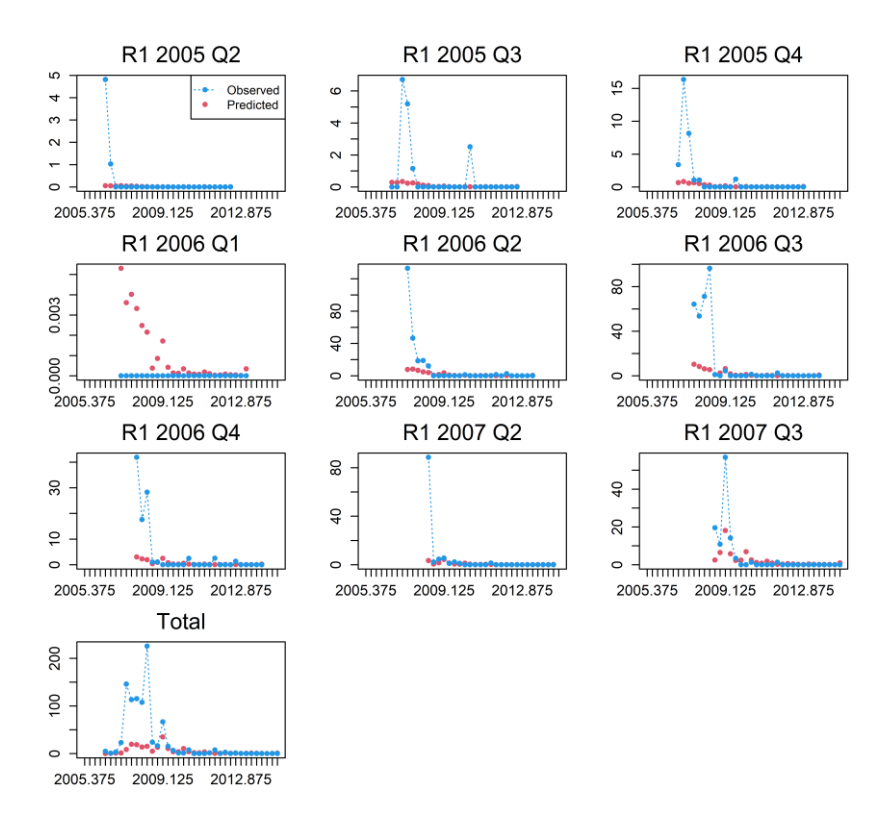


Figure 21: Observed and predicted number of tags recovered by quarter for the PSLS fishery in region 1S (PSLS 1S). Only tags at liberty after the four quarter mixing period are included. Tag recoveries are aggregated for each release group. Base model '6_update_bias'.

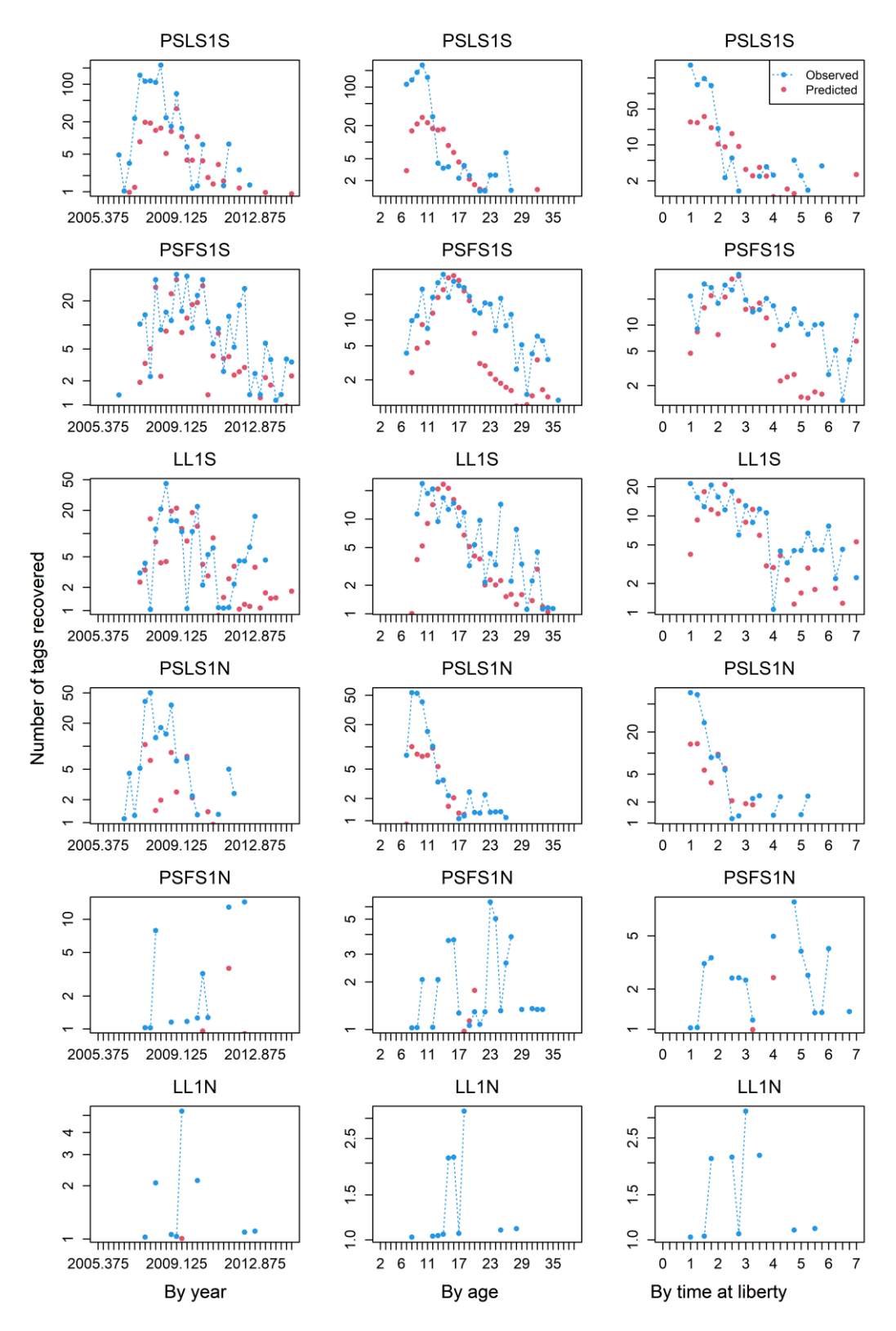


Figure 22: Observed and predicted number of tags recovered by year/quarter time-period (left), by age (mid), and by time at liberty (in quarters, right) for main Purse seine and longline fisheries in region 1N and 1S (PSLS 1S, 1N, PSFS 1S, 1N, and LL 1S, 1N) from '6_update_bias'. Only tags at liberty after the four-quarter mixing period are included. Tag recoveries are aggregated for each of the regional fisheries.

6.3. Model estimates

6.3.1. Selectivity

As in the 2022 model, the estimated parameters in the basic model include: the overall population scale parameter R0, the time series of recruitment deviates, the distribution of recruitment among regions, age specific movement parameters, the fishery selectivity parameters, fishery tag reporting rates and the catchability parameters for the CPUE indices.

The age-specific selectivity functions are presented in Figure 20. Full selectivity is reached for the R1N and 1S longline fisheries at around age 18 (quarters), which the same age as in the 2022 model, despite the updates in the growth function in 2025.

Selectivity for the longline fishery in R2 was predicted to be asymptotic with a steep transition. The selectivity for the longline fishery in R3 was estimated to be pseudo-dome-shaped, with a diminishing right limb from roughly 17-18 quarters, earlier than in 2022. Peak selectivity for the PSLS1N and PSLS1S fisheries is estimated to be a much tighter peak, occurs at ages 3-5 quarters, compared to ages 5-8 in 2022. (Figure 20). For the PSFS fisheries, selectivity was estimated to be bimodal with lower levels of selectivity for younger fish compared to older fish. This represents a departure from 2022 when the modes showed similar levels of selectivity.

6.3.2. Recruitment

As in 2022, recruitment deviates were estimated for the quarterly time steps from 1984–2023. Estimating the recruitment prior to 1984 was quite uncertain. There are longer-term trends visible in the recruitment deviates, with higher-than-average recruitment estimated from 2000 to 2005 (as opposed to 1990-2000 in the 2022 model), and reduced recruitment between 2010 and 2015 (Figure 24), similar to 2022. These trends correspond to periods of higher and lower catches from the PSLS fishery, after revised catches. Recruitment for 2020 to 2022 was estimated to be higher than the long-term mean, presumably to account for the recent increase in CPUE in the longline indices.

Recruitment was assumed to occur in all regions equally as there were no significant differences in CPUE indices between the regions, unlike in the previous model. A sensitivity run was completed to show the difference between models where recruitment was not assumed to occur in all regions equally (as in the 2022 model). The results are detailed in the sensitivity section.

6.3.3. Movement rates

Movement rates were estimated amongst the model regions. The model estimates high movement rates of mature fish amongst regions 1N and 2 (reciprocal movement) (Figure 25). Very low mixing was estimated to occur between regions 1S and any other region (as supported by the tag-return data). Some reciprocal movement of younger fish between regions 1S and region 2 is estimated to occur. These higher rates of movement are a departure from the low rates estimated by the 2022 model, presumably to account for the lack of recruitment variability between regions. This represents an uncertainty in the model structure and / or biological information available for bigeye tuna in the Indian Ocean. Increased information on adult movement would improve the model, especially as the CPUE indices appear to influence the estimated movement rates (Figure 25).

6.3.4. Tag reporting rates

Tag reporting rates were estimated for the non-purse seine fisheries (Figure 25). For some of these fisheries, the estimated reporting rates are unlikely to be influential in the overall assessment as the reported tags were predominately recovered during the tag mix period. However, a considerable proportion of the tag recoveries from the LL1S and LL3 fisheries occurred during the post mixing phase and, hence, the tag reporting rates will have some influence in the model likelihood. For these fisheries, tag reporting rates were estimated at 0.21 and 0.52, respectively. while the reporting rate for the LL1N fishery was estimated to be considerably lower (0.1). The estimates for the LL2 and LL3 fisheries are associated with high uncertainty and probably have reflected the large inter-annual variabilities in the tag recoveries (and reporting) from these fisheries.

6.3.5. Spawning stock biomass

In the base model (6_update_bias), Region 3 accounts for the greater proportion of spawning stock biomass (hereafter biomass), followed by Region 2 (area 2), Region 1S (area 1) and Region 1N (area 4), however by the terminal years, Region 1S accounts for more biomass than Region 2. (Figure 26). These estimates are similar to the previous assessment. There is a double normal selectivity function for the longline fisheries in areas 2 and 3, and the additional biomass in region 3 is potentially a reflection of cryptic biomass in this area (biomass associated with large fish that are unavailable to the LL3 fishing fleet).

Spawning biomass (overall) decreases across all regions until the beginning of the 2000s (year quarter 300; Figure 27) and the beginning of the 2000s. Between 2009 and 2014, biomass somewhat increased before declining quickly to historical low levels in 2020. The spawning biomass increased in all regions over the last three years, particularly in area 1 (Region 1S) (Figure 26), mirroring the increases in frozen longline CPUE indices.

6.3.6. Trends in fishing mortality

The estimates of fishing mortality for the fisheries in regions 2 and 3 were lower than regions 1 and 4 (Figure 28), with the revisions in catch data reducing the previously high fishing mortality rates of the PSLS2 fleet in region 2. The relative mortality rates between fleets have changed since the last assessment, with rates for the longline fleets being much lower than that of the purse seine fleets in regions 1 and 4 (1S and 1N), with a notable increase in the PSLS fleet in region 1 (PSLS1N).

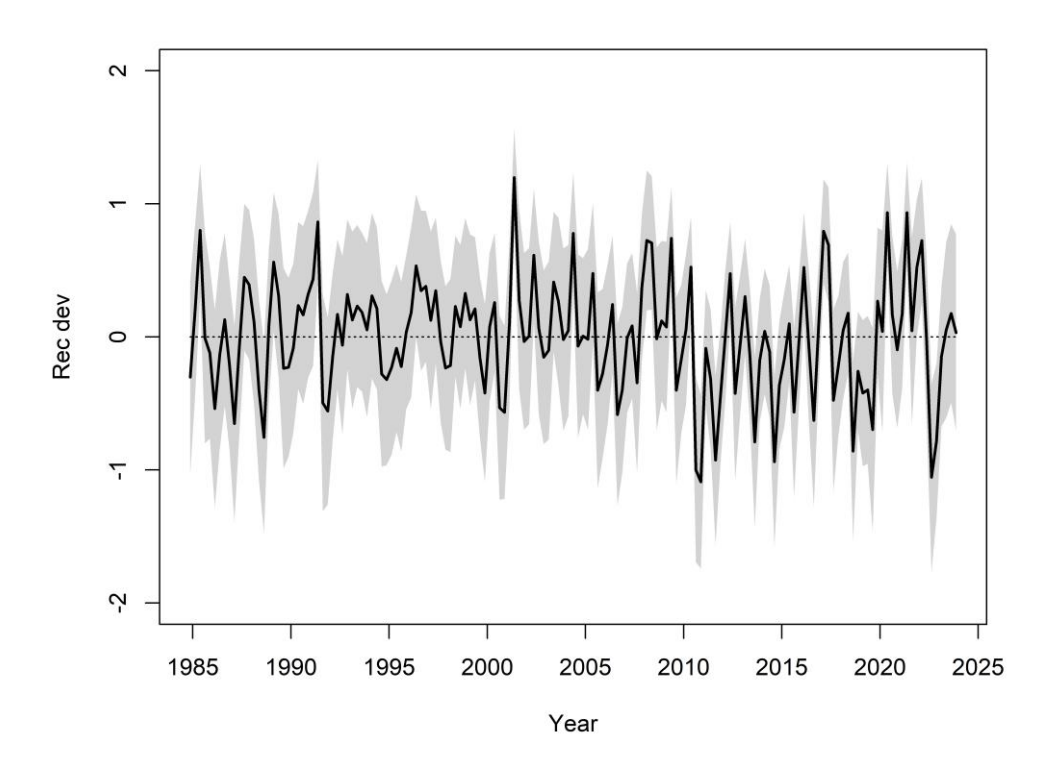


Figure 23: Recruitment deviates from the SRR with 95% confidence interval from the base model '6_update_bias'

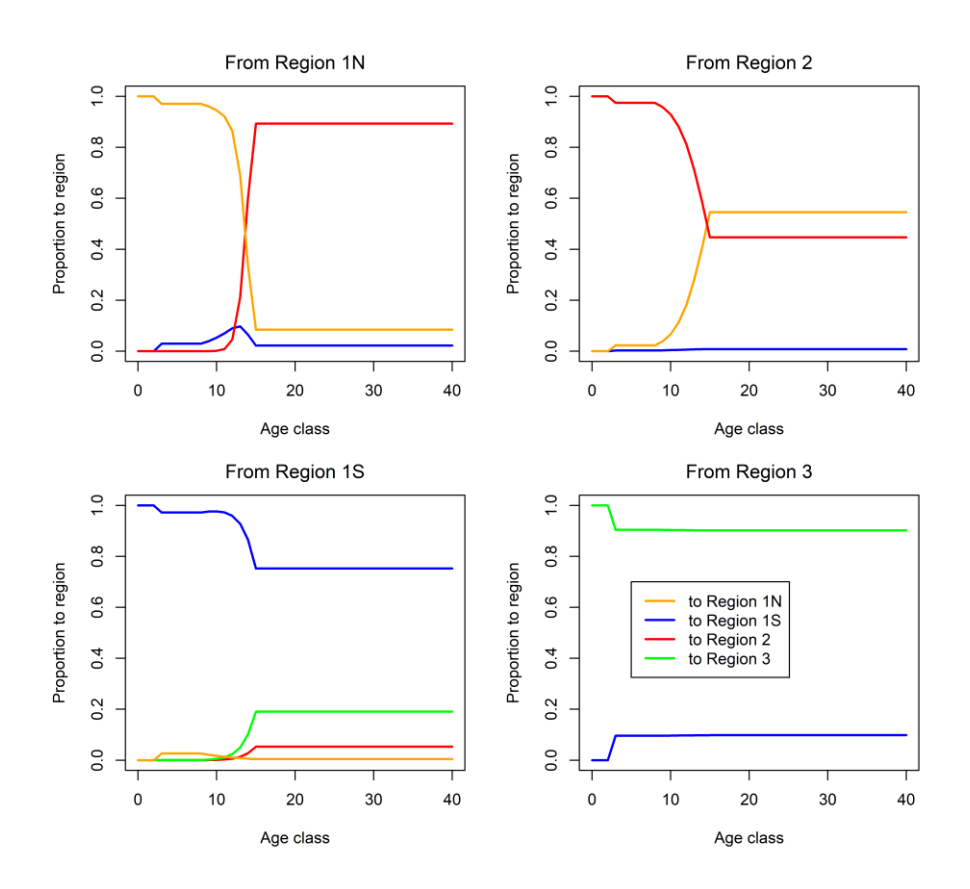


Figure 24: Estimated age specific movement parameters for the base model '6_update_bias'

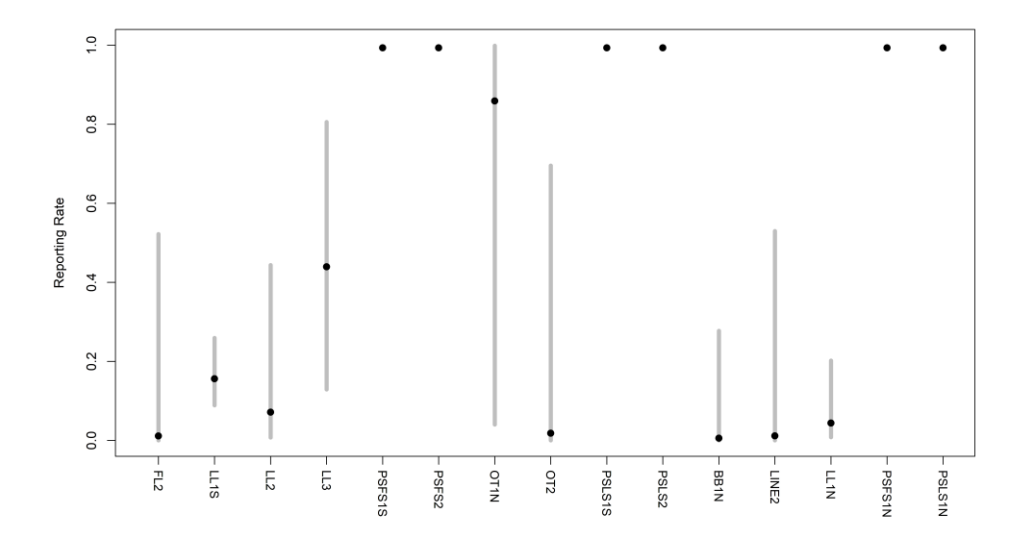


Figure 25: Tag reporting rates for each fishery from the base model '6_update_bias'. Purse seine reporting rates were fixed at a value of 1.0. Reporting rates for the other fisheries were estimated. The grey lines represent the 95% confidence interval for the estimated values.

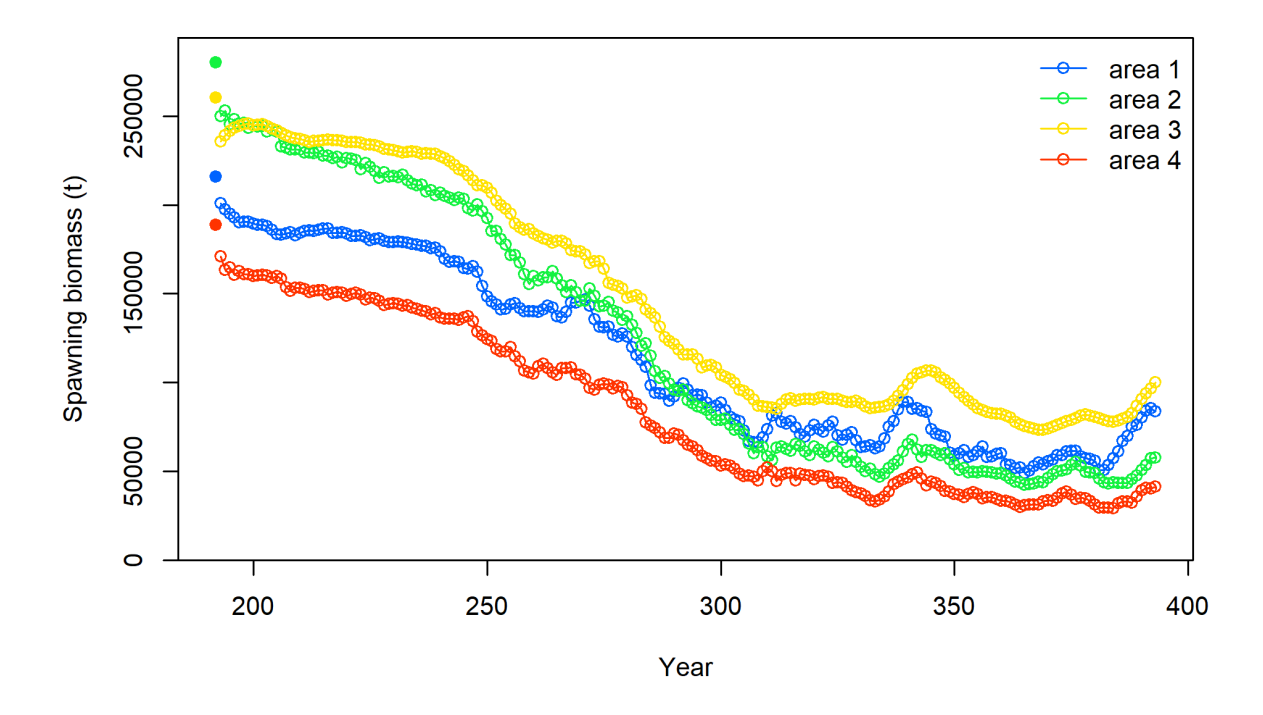


Figure 26: Estimated spawning biomass trajectories for the individual model regions from the base model '6_update_bias'.

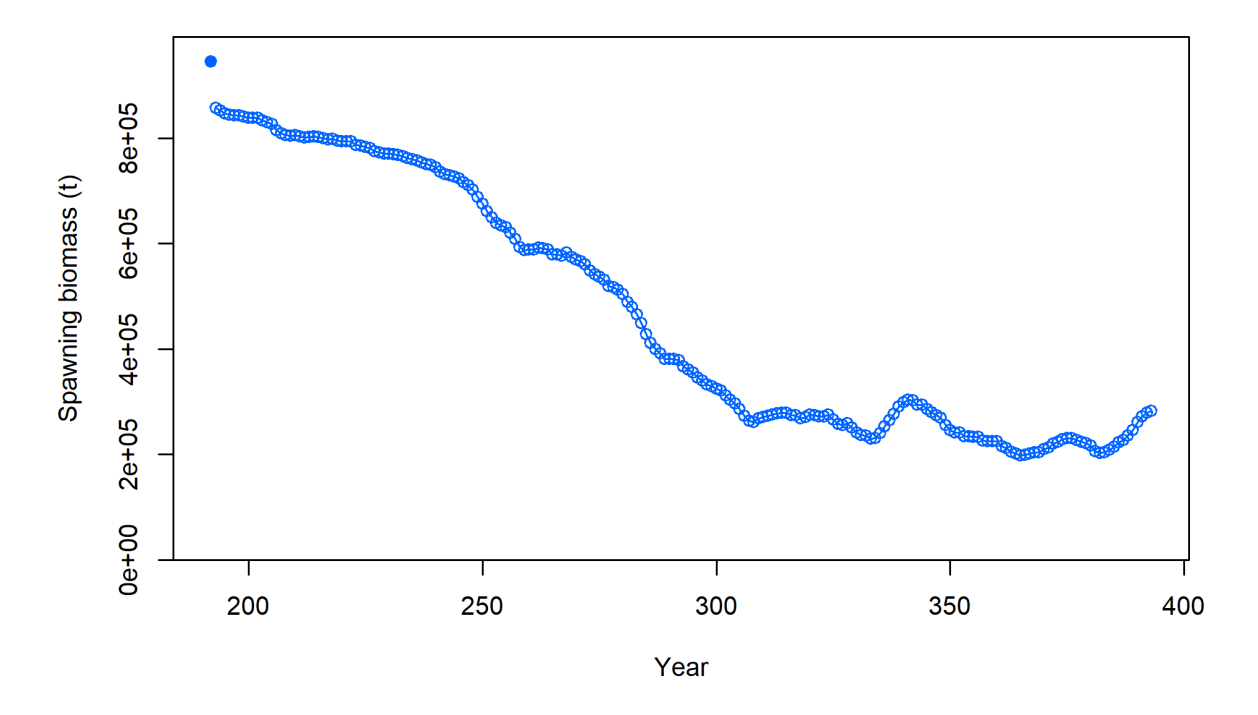


Figure 27: Estimated spawning biomass trajectories for the whole stock from the base model '6_update_bias'.

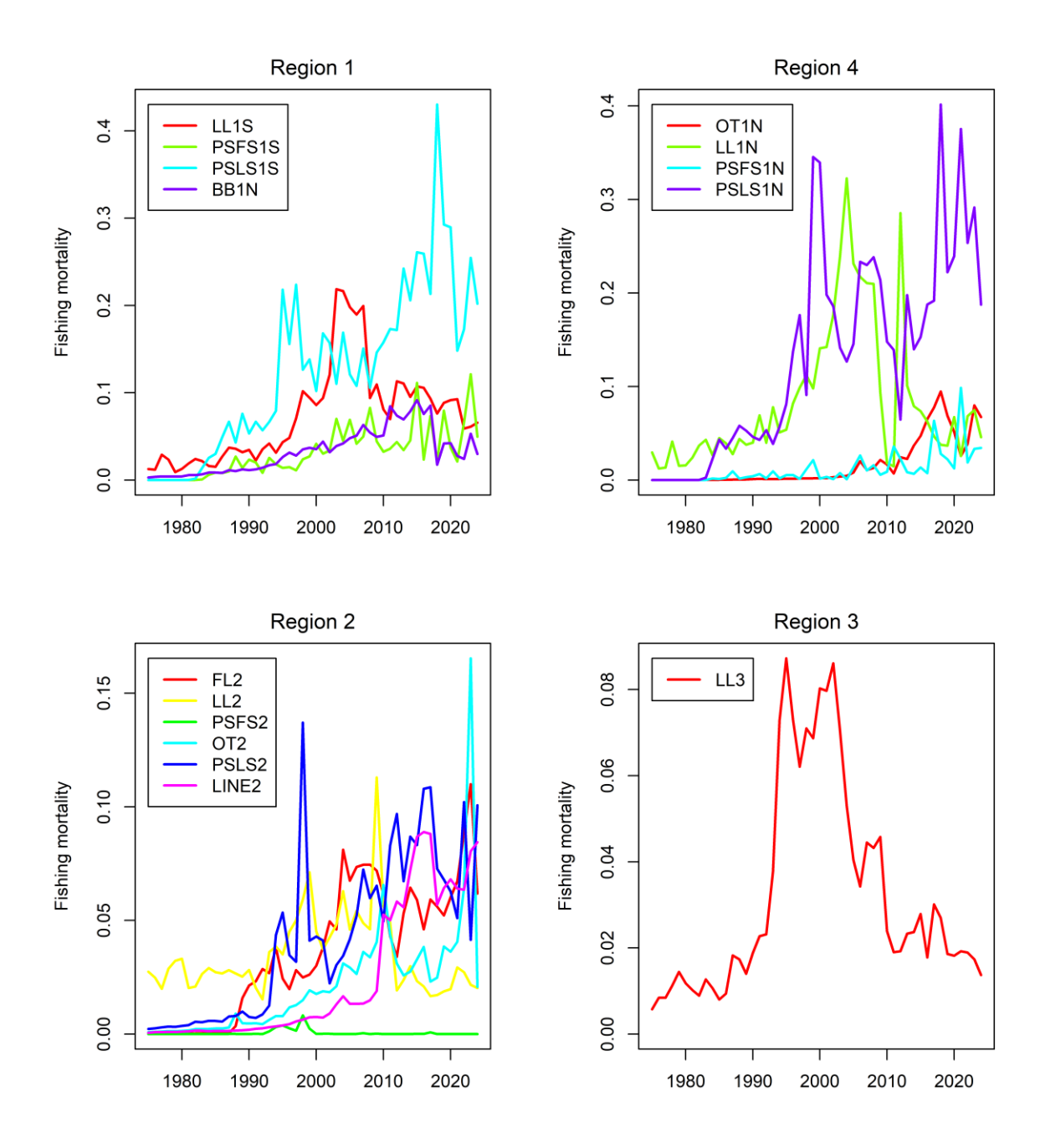


Figure 28: Trends in fishing mortality (yearly) by fleet for the base model '6_update_bias'.

6.4. Diagnostics

Some diagnostic tools were run for both base models, including running an age structured production model for both base models a retrospective analysis, and a hindcasting analysis.

6.4.1. ASPM analysis

The Age Structured Production Model (ASPM) analysis (Maunder & Piner, 2015) was used to illustrate the main drivers of the population trend, and to understand whether the composition data has an undue influence on the estimates of abundance. The ASPM analysis involved running two variations of the reference models: *ASPMfixed* where length composition data were removed from the model (by fixing selectivity parameters) and recruitment deviates were fixed at zero; and *ASPMrec* where fixed recruitment deviates (estimates from the reference model) were added back into the model (and selectivity remained fixed).

The estimated spawning stock biomass from both ASPM model runs for the base model is shown in Figure 29. The analyses indicated that the catches and abundance indices for the bigeye tuna stock generally agree, suggesting that the catch by itself may adequately explain the overall degree of stock depletion seen in the historical CPUE indices.

The stock would be expected to fall at a slower rate (but from a lower starting point) and then increase from around 2000 to present (quarter 300) with no variation in recruitment (ASPMFixed). All ASPM models provided similar estimates of relative abundance. To account for changes in the CPUE indices (abundance indices), the model requires variation in recruitment. For all other diagnostics the ASPM analysis provided similar results for the SS3 model, the ASPMFixed and ASPMrec, suggesting there is no undue influence of the length frequency data on the model outputs.

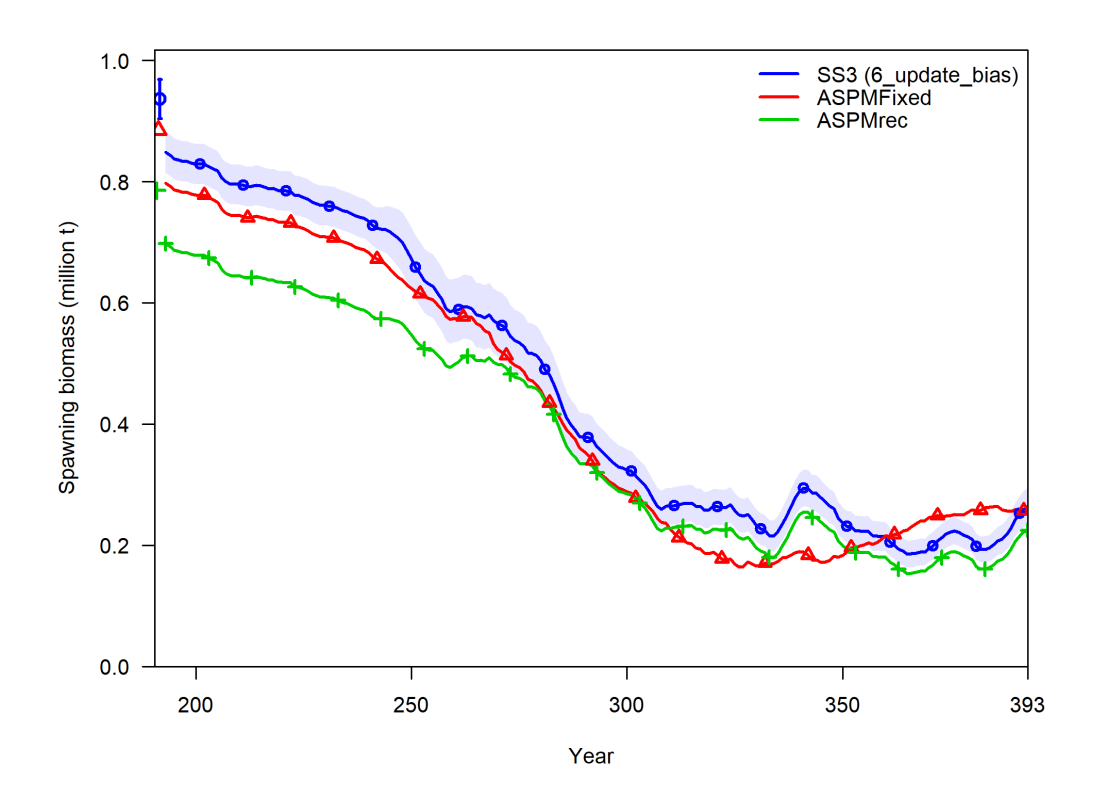


Figure 29: ASPM analysis for the base model '6_update_bias': ASPMfixed (no recruitment deviations), and ASPMrec (recruitment deviates from the reference model added back). Both runs excluded the length composition data and fixed the selectivity parameters.

6.4.2. Retrospective analysis

Retrospective analysis is a diagnostic approach to evaluate the reliability of parameter and reference point estimates and will allow the revelation of systematic bias in the model estimation. It involves fitting a stock assessment model to the full dataset, and then sequentially removing data from the inputs from the most recent years. The analysis was conducted using the two base models, and the last 5 years (20 quarters) of data were removed in 4-quarter increments to evaluate whether there were any notable changes to the model results. The selected period mirrors that of previous assessments and was intended to avoid removing any tag recovery data. The analysis of the impact of data removal was conducted on the outputs of estimated spawning stock biomass (SSB) and the ratio of SSB_{current} to SSB₀.

There were no apparent retrospective patterns in the estimates for SSB (Figure 30), fishing mortality (Figure 31), or recruitment (Figure 32), and Mohn's rho was within acceptable bounds (< 0.20). These results provide significant confidence in the robustness of the model with respect to inclusion of recent observational data.

6_update_bias

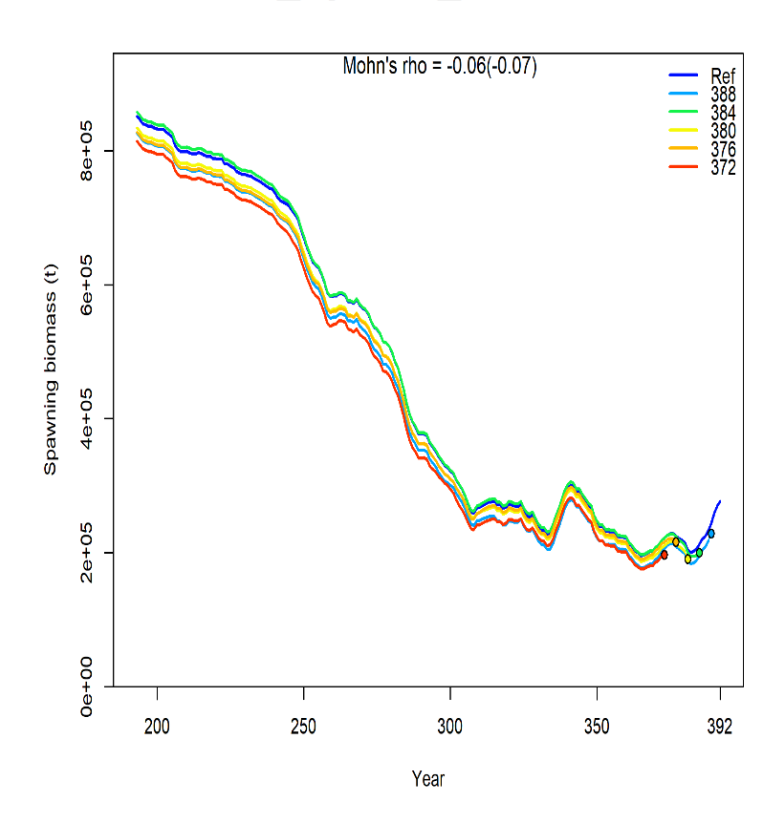


Figure 30: Retrospective analysis summary for SSB estimates (t) from the base model '6 update bias'.

6_update_bias

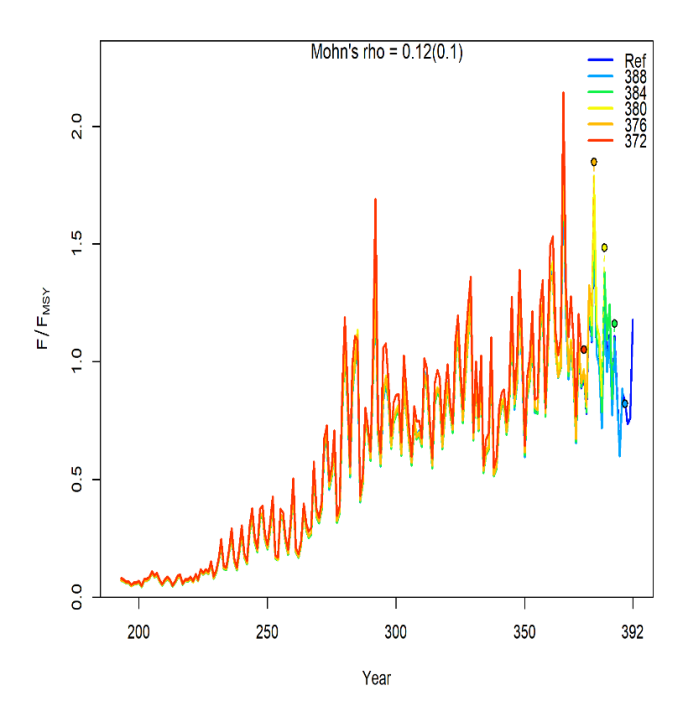


Figure 31: Retrospective analysis summary for fishing mortality estimates from the base model '6_update_bias'.

6_update_bias

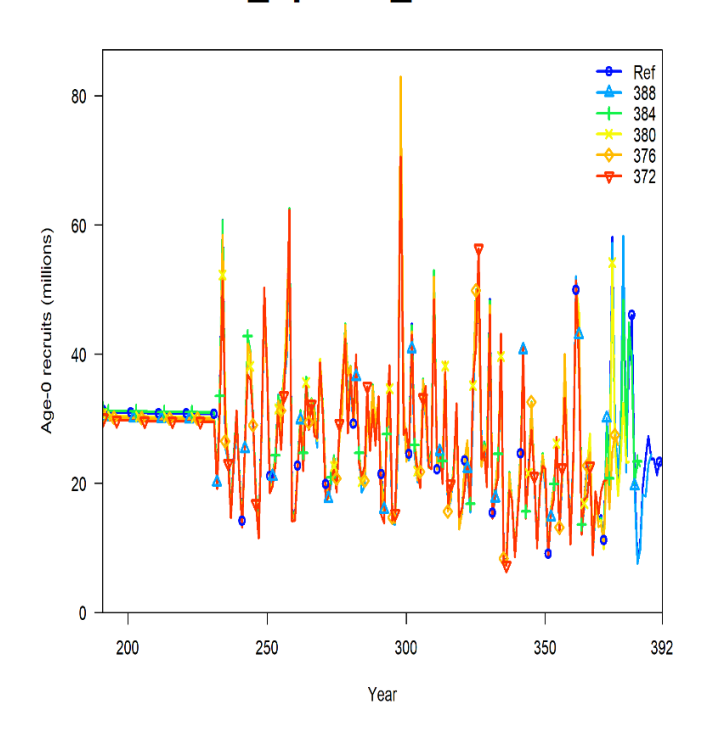


Figure 32: Retrospective analysis summary for recruitment estimates from the base model '6_update_bias'.

7. SENSITIVITY RUNS

The exploration of the model's sensitivity to input parameters aimed to identify potential revisions to the base models, and to guide the assessment group in choosing the most appropriate values for running the grid or ensemble of models that encapsulates the uncertainty within the model. Key results for the sensitivity runs are provided in Appendix A and summarised below. In previous iterations of the model, a full range of sensitivity runs were conducted among a range of input parameters (see rev2). In this final round of sensitivity runs, the following runs were conducted:

- 1) A range of values for natural mortality (M) based on the Lorenzen age-varying curve
 - a. M = 0.30, 0.38, 0.45 (low; a second 'med' value (called 'shelt'); high)
 - b. M estimated internally, with starting value of 0.37 (med, in base model)
 - c. M estimated internally, with starting value of 0.37, using a prior as outlined in Hamel & Cope (2022)
- 2) Addition of Somalia's catch data submitted for 2024 (representing an additional ~ 4000 t in the terminal year (across 4 quarters) of the model).
- 3) Variable recruitment between the four quarters of the model (not time-varying)

The final two scenarios (2 and 3) were decided at the end of the WPTT(AS) and as such were not included in the grid of models used for stock status. The results are included here for completeness, and to ensure that the next running of the bigeye tuna assessment takes these results into account prior to configuration of the 2028 assessment.

A summary plot of SSB estimates and SSB status are shown in Figure 33 and Figure 34 for all sensitivity runs. Full diagnostic tables for the sensitivity runs encompassing the range of M values are provided in Appendix C, from code developed and run by G. Correa.

7.1. Non-biological parameters

7.1.1. Addition of Somalia's catch data

The catch data for Somalia was omitted from the reference model, as agreed by the 27thWPTT(AS). Data were submitted for only 2024 and comprise the following amounts, under the "SOM" fleet:

- 1) Gear = GILL; catch = 406 t
- 2) Gear = HAND; catch = 534 t
- 3) Gear = LLCO; catch = 3,160 t
- 4) TOTAL catch = 4,100 t

Including the catch data increased the estimate of biomass (Table 10), and the depletion estimate but this was within the range of uncertainties that are included in the grid run for 2025. These increases are presumably the model's response to an increase in F (fishing mortality) in the terminal year, that must be accounted for by increased biomass in the population (compared to the reference model). This result highlights the importance of accurate catch submissions, as inclusion or exclusion of various data impacts estimated model outputs.

Estimates of selectivity were similar, and the models still fit well to the CPUE indices (Figure A1, A2). Fits to the length composition data (aggregated) were similar to when the data were not included (e.g. compared to the base/reference model) (Figure A3).

As discussed in the 27thWPTT (AS), it would be advisable to work with Somalia to ensure that data submissions continue, so that a good timeline of data can be established for inclusion into the assessment models for all tropical tuna species. This may include some historical catch reconstruction estimates, if required.

7.2. Biological parameters

7.2.1. Natural mortality

Changing the instantaneous rate of natural mortality (M) in the model had significant impacts on the estimates of biomass, and the scale of the biomass estimates (Figure 33, Figure 34, Table 9). Three

different methods of incorporating M were tested in the sensitivity analyses – three values of M fixed, implemented using the Lorenzen age-varying option in SS3 (option 6) (M = 0.30, 0.38, 0.45), and two options of M estimated internally in the model (once with a prior, and once without). For the estimates of M: the maximum age was set to 14.7 yr (as agreed at the DP meeting), and adults were assumed to be fully matured between 4 – 10 yrs, based on the maturity curve from Shono et al. (2009), and the growth curve provided by Eveson et al., (2025). Three starting values of M were used in the internal estimation – a "low" (M=0.30), "Shelton" (M=0.38), and "high" (M=0.45) estimate, based on the 50th quantiles of the probability distribution of values of M (the 0.38 value was chosen as a value between 0.37 and 0.45 that due to the lognormal distribution ends up being very close to the value within the base model (0.37)). Estimates were weighted, the weightings were estimated from the density function assuming lognormal distribution of M with SD=0.31 (also in the code provided). The prior was estimated from the method outlined in Hamel and Cope (2022), and results in a value of -1 in the SS3 input file.

When estimated internally in the model ([...]'est' and [...]'estprior'), estimates of biomass changed significantly (Figure 33; Table 9) compared to models with fixed M. The high starting estimate of M (M = 0.45) resulted in a much lower estimate of initial biomass, and a lower estimate of fishing mortality.

Retrospectives on SSB (Figure 35), fishing mortality (Figure 36), and recruitment estimates (Figure 37) revealed models with fixed M have internal consistency, whereas estimating M causes retrospective patterns to emerge, suggesting model instability, however the Mohn's rho was only outside acceptable bounds when the 'prior' method was used (6d PSshort MLorHam6Qestprior).

Likelihood profiling on M using one of the estimation models (6d_PSshort_MLorHam6Qest) suggests that estimates of M are consistent with the fixed values in the grid (Figure 38). The likelihood profile suggests that tag recapture data favour a lower value of M (\sim 0.29), whereas length data favour a higher value of M (\sim 0.36). The index data favour the mid value of M used in the reference model (0.37).

Likelihood profiling on R_0 (unfished recruitment) showed the index data to be influencing the estimate of R_0 followed by the length data (Figure 39). The models with low and middle range M showed similar patterns, and similar values of estimated R_0 , when M was lower, R_0 was also estimated to be lower, and *vice versa*.

The model is most sensitive to changes in M, and so it is recommended, in the absence of more biological data, that further research and/or focus is applied to this parameter in future assessments. For the current assessment, including three parameters for M was recommended in the grid, but not to include a model with internal estimation of M.

7.2.2. Variable recruitment between model areas

Recruitment was allowed to vary between areas for one sensitivity run, as parameterised in the 2022 base model (see Figure A4 for estimates of area-based recruitment). Allowing variable recruitment among areas of the model results in higher estimates of $SSB_{0,}$ and SSB_{2024}/SSB_{0} and lower estimates of F_{2024}/F_{MSY} .

Fits to the main CPUE indices (LL1N, LL1S) were improved by allowing for variable recruitment (Figure A5, Figure A6), but fits to the length frequency data were worse than in the reference model (Figure A7). Importantly, movement is clearly confounded with recruitment, as when recruitment is allowed to vary between the four areas in the model, movement rates of adults are reduced (Figure A8). Movement rates are lower than in the reference model, presumably due to the confounding of adult movement and recruitment within the model. Most adult movement in this model is estimated to occur between area 1 (region 1S) and area 3 (region 3, east IO) with movement of younger fish from area 4 (region 1N, and temperate regions) and area 1 (region 1S). A smaller proportion of adults move from area 3 (region 3, east IO) to area 1 (region 1S), while there is almost no adult movement between area 1 to 4 (adjacent regions 1S and 1N).

Understanding the more plausible biological scenario requires further research into the literature, and a thorough think about model fleets, and 'areas' within the model, as although they are represented as

geographical areas, some fleets (catch from country and gear) is attributed to a different geographical region from where it is caught – and grouped with other gear/vessel combinations with similar selectivity. Although tagging data in the model indicate low movement rates of tuna, it is likely that adults do move, and some may move significant distances, as has been indicated in the Pacific (Day, 2023). Interestingly the estimated movement of adults in this model does not indicate much adult movement between the adjacent regions 1N and 1S, but instead between region 1S and region 3. Both scenarios (fixed or variable area-based recruitment) provides similar estimates for SSB status (Figure 34), although estimates for SSB were higher when recruitment varied between areas (Figure 33).

As discussed in the 27thWPTT (AS), and in sections of this report, and rev1 and rev2 versions, careful thought and research should be completed prior to the final running of the 2028 model as to the optimal parameterisation of recruitment within the assessment model, given that the data do not provide good recruitment signals, and there are no fishery independent indicators of recruitment available to the model. It is preferable to have recruitment parametrised to the biological nature of the species, rather than fleet dynamics.

Table 9: Estimates of management quantities for the sensitivity testing from the base model options. Current catch (2024) in the model is 82,874 t. Base model is the first model. Internal estimation of M or having M fixed at lower values results in higher estimates of SSB₀, and SSB₂₀₂₄/SSB₀ and higher estimates of F₂₀₂₄/F_{MSY}. All models estimated C_{MSY} at values higher than current catch.

| | SSB ₀ (t) | SSB _{MSY} (t) | SSB ₂₀₂₄ (t) | SSB ₂₀₂₄ SSB ₀ | SSB ₂₀₂₄ SSB _{MSY} | F _{MSY} | F ₂₀₂₄ | F ₂₀₂₄ F _{MSY} | C _{MSY} (t) |
|------------------------------|----------------------|------------------------|-------------------------|--------------------------------------|--|------------------|-------------------|------------------------------------|----------------------|
| 6_update_bias | 945,276 | 257,728 | 264,356 | 0.2796596 | 1.0257151 | 0.2785296 | 0.2425415 | 0.8707925 | 98,594 |
| 6d_PSshort_MLorHam6Qest | 1,174,020 | 318,809 | 297,560 | 0.2534535 | 0.9333472 | 0.2805520 | 0.2532648 | 0.9027375 | 95,028 |
| 6d_PSshort_MLorHam6Qestprior | 1,194,890 | 328,158 | 299,343 | 0.2505195 | 0.9121924 | 0.2804240 | 0.2567688 | 0.9156448 | 94,946 |
| 6d_PSshort_MLorHam6Qhi | 739,034 | 183,622 | 207,981 | 0.2814224 | 1.1326570 | 0.3286656 | 0.2213562 | 0.6734997 | 107,437 |
| 6d_PSshort_MLorHam6Qlo | 1,329,780 | 371,240 | 340,590 | 0.2561249 | 0.9174382 | 0.2709748 | 0.2493903 | 0.9203450 | 94,373 |
| 6d_PSshort_MLorHam6Qshelt | 899,682 | 237,148 | 238,044 | 0.2645865 | 1.0037772 | 0.3067772 | 0.2552195 | 0.8319378 | 96,936 |

Table 10: Estimates of management quantities for the sensitivity testing from the base model options for the addition of Somalia catch, and the inclusion of variable recruitment between areas. Current catch (2024) in the model is 82,874 t. Base model is the first model. Allowing variable recruitment among areas of the model results in higher estimates of of SSB₀, and SSB₂₀₂₄/SSB₀ and lower estimates of F₂₀₂₄/F_{MSY}. Addition of the Somalia catch resulted in higher estimate of SSB₀ and SSB₂₀₂₄/SSB₀ but a similar estimate of F₂₀₂₄/F_{MSY}. All models estimated C_{MSY} at values higher than current catch.

| | SSB ₀ (t) | SSB _{MSY} (t) | SSB2024 (t) | SSB2024SSB0 | SSB2024SSBMSY | FMSY | F ₂₀₂₄ | F2024FMSY | C _{MSY} (t) |
|---------------|----------------------|------------------------|-------------|-------------|---------------|-----------|-------------------|-----------|----------------------|
| 6_update_bias | 945,276 | 257,728 | 264,356 | 0.2796596 | 1.0257150 | 0.2785296 | 0.2425415 | 0.8707925 | 98,594 |
| 6_update_rec | 1,054,240 | 281,439 | 305,549 | 0.2898285 | 1.0856660 | 0.3172724 | 0.2130359 | 0.6714605 | 104,868 |
| 6_update_som | 986,628 | 278,056 | 313,298 | 0.3175442 | 1.1267440 | 0.2590020 | 0.2211658 | 0.8539155 | 101,861 |

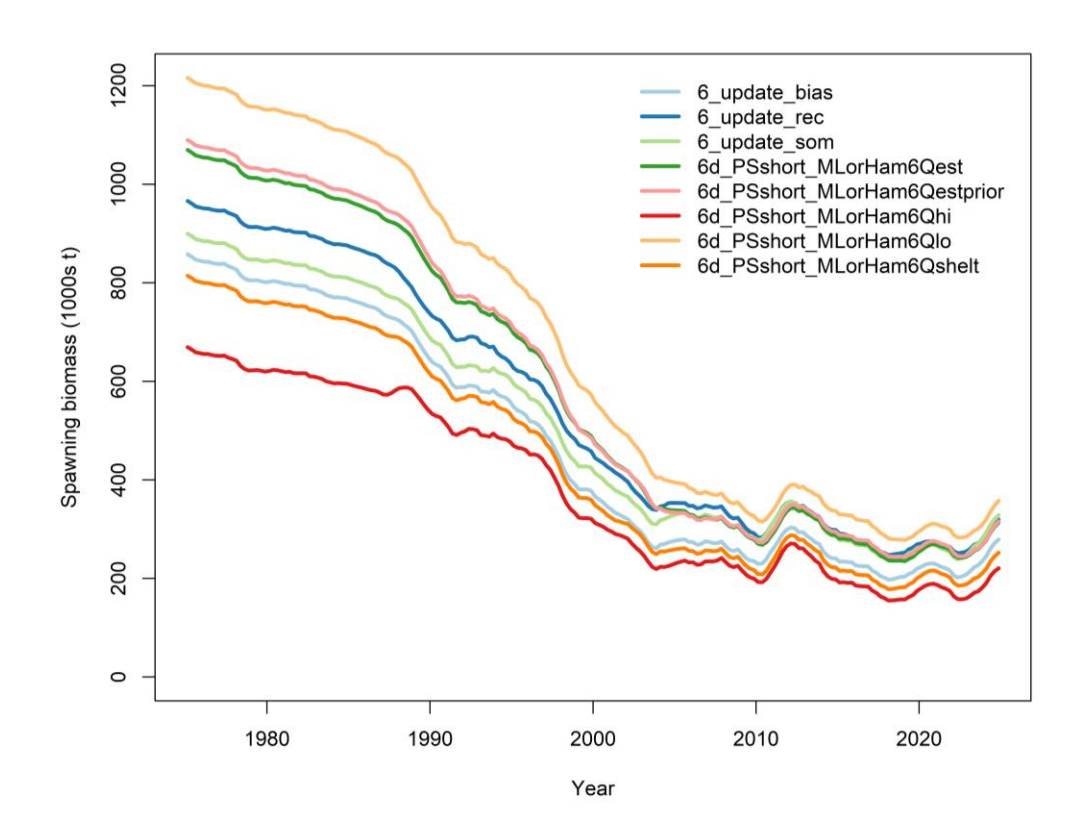


Figure 33: SSB (1000 t) estimates from all sensitivity models.

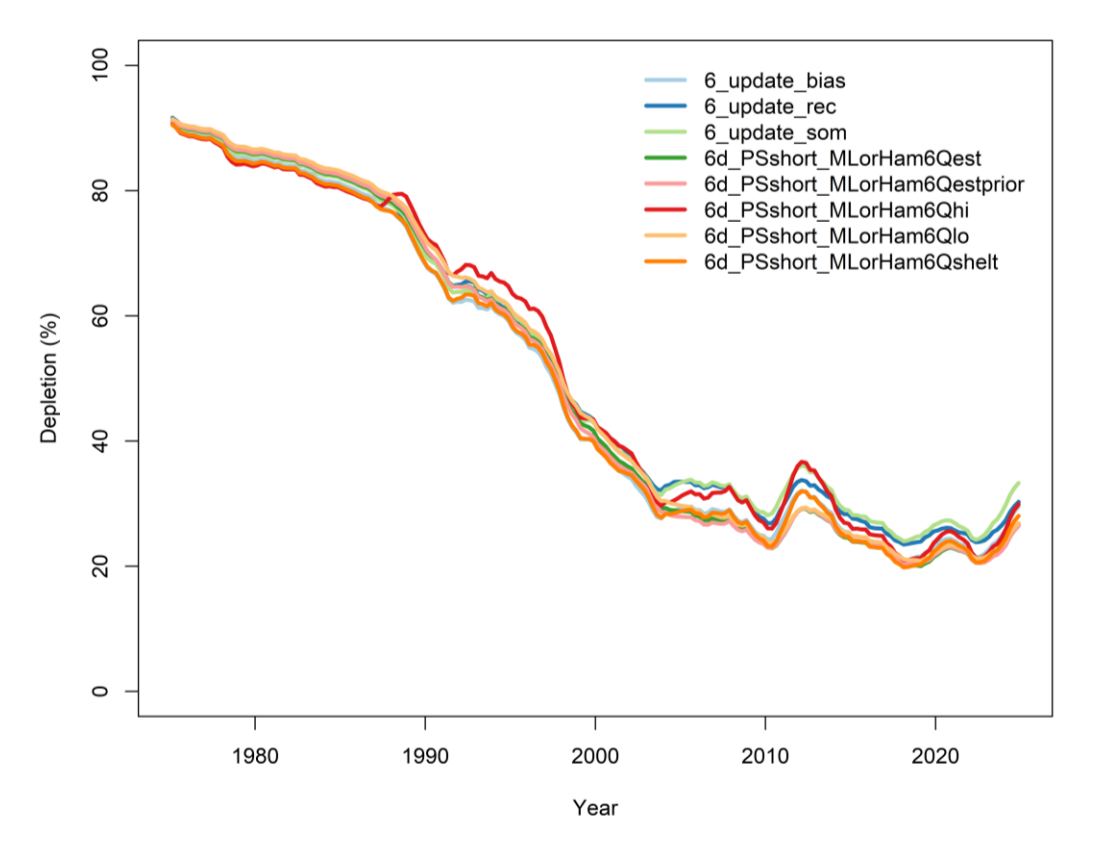


Figure 34: SSB status (% depletion) for all sensitivity models.

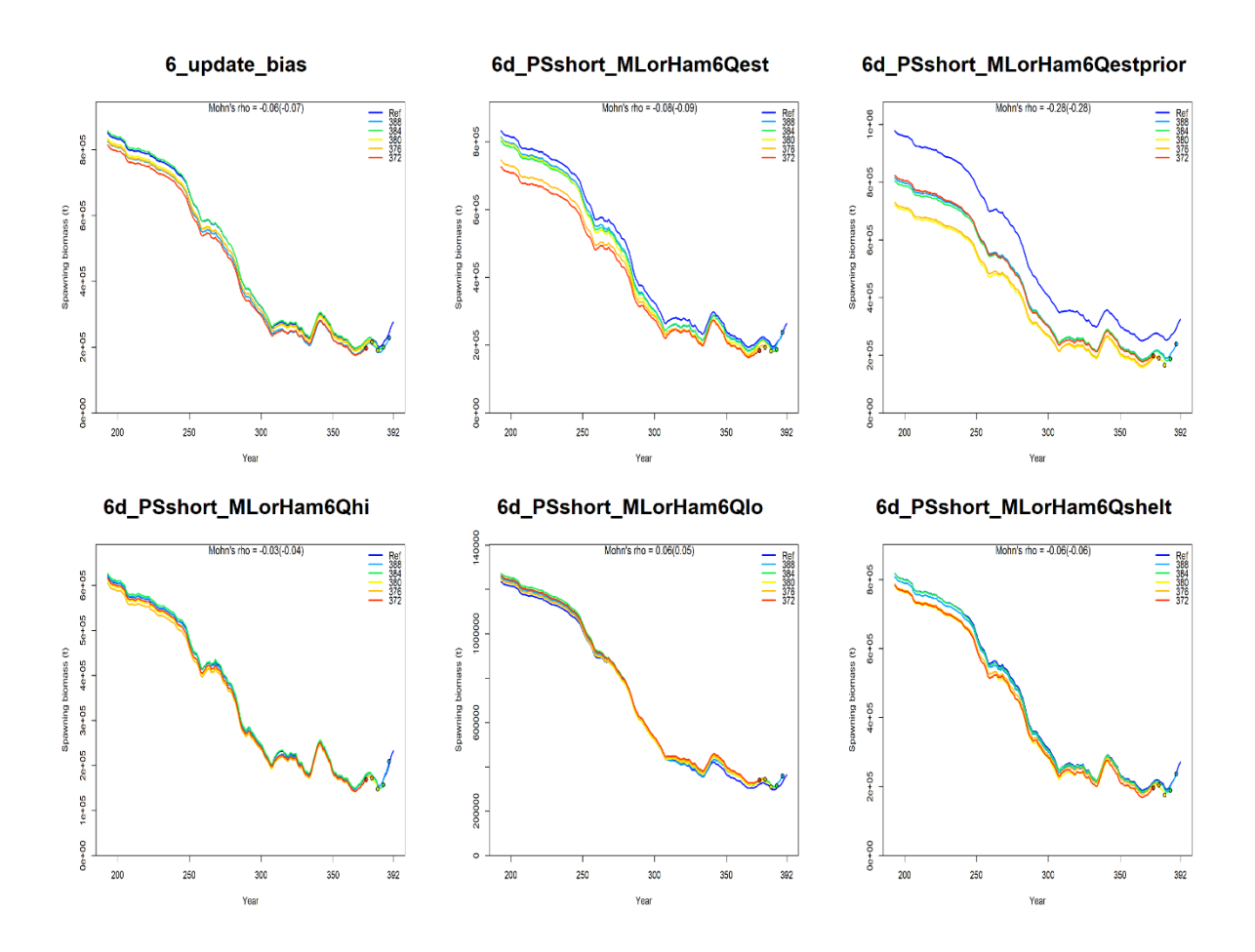


Figure 35: Retrospectives for all M sensitivity models, for estimates in spawning stock biomass (t) showing Mohn's Rho. Five years of data are removed in these analyses.

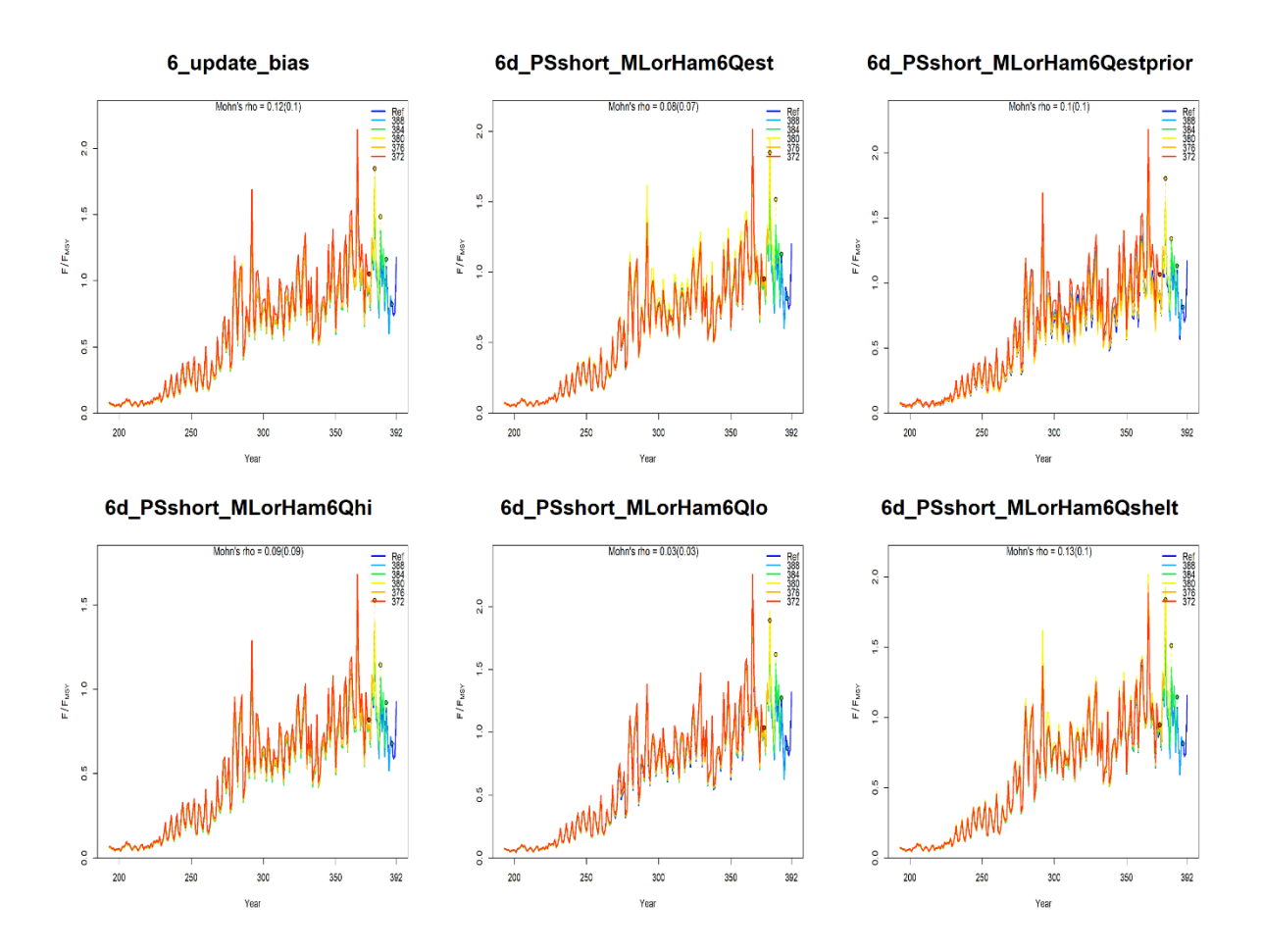


Figure 36: Retrospectives for all M sensitivity models, for fishing mortality (F), showing Mohn's Rho. Five years of data are removed in these analyses.

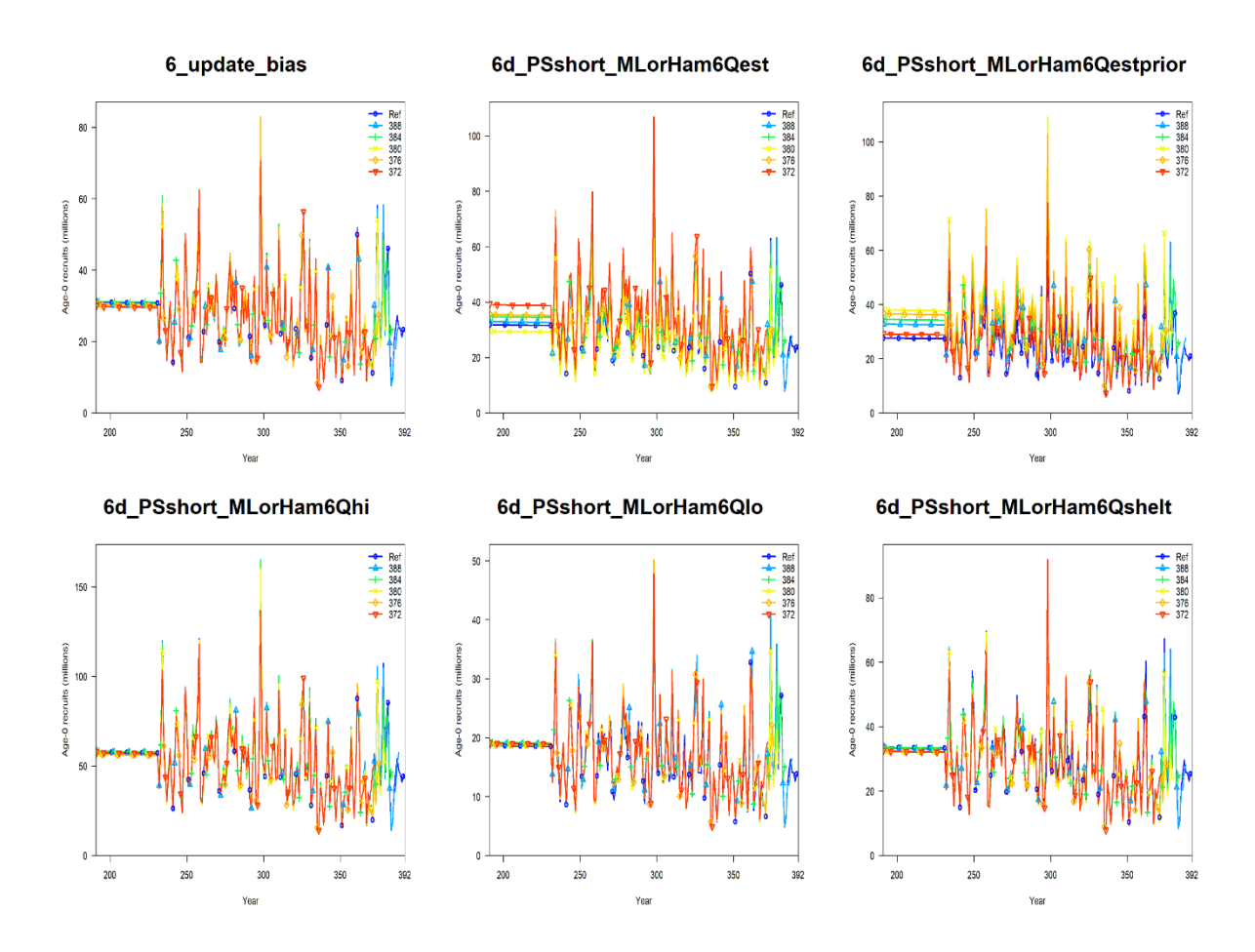


Figure 37: Retrospectives for all M sensitivity models, for estimated recruitment, showing Mohn's Rho. Five years of data are removed in these analyses.

6d_PSshort_MLorHam6Qest

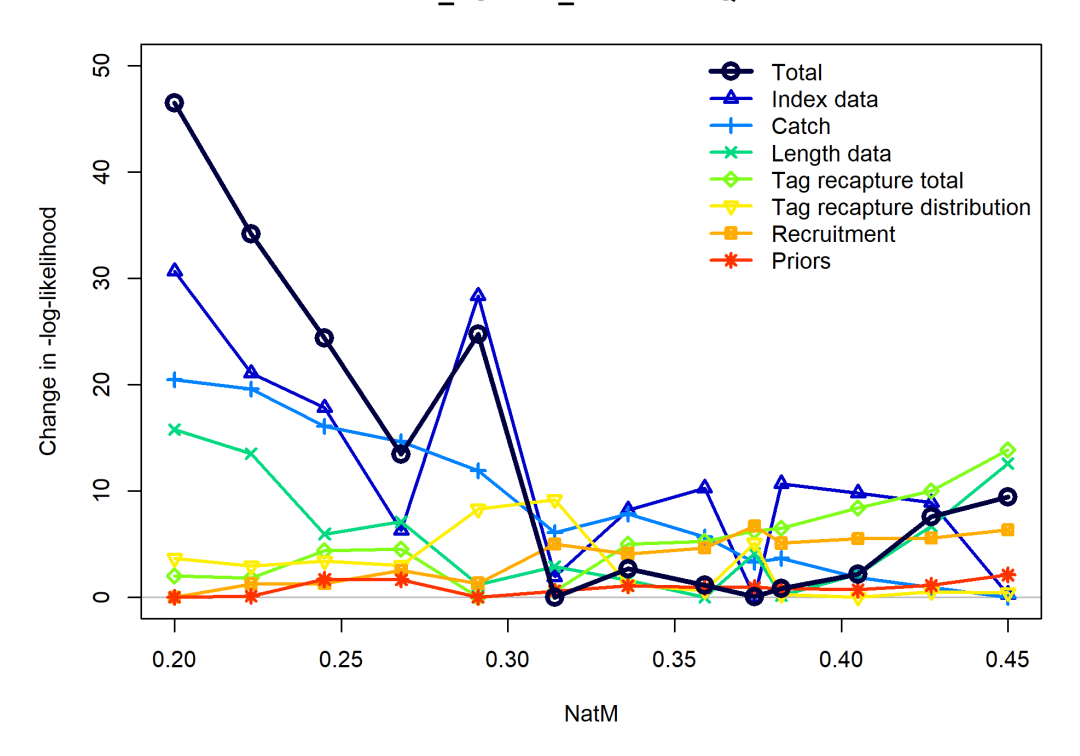


Figure 38: Likelihood profiling (change in -log(likelihood)) for M for one of the models where M was estimated.

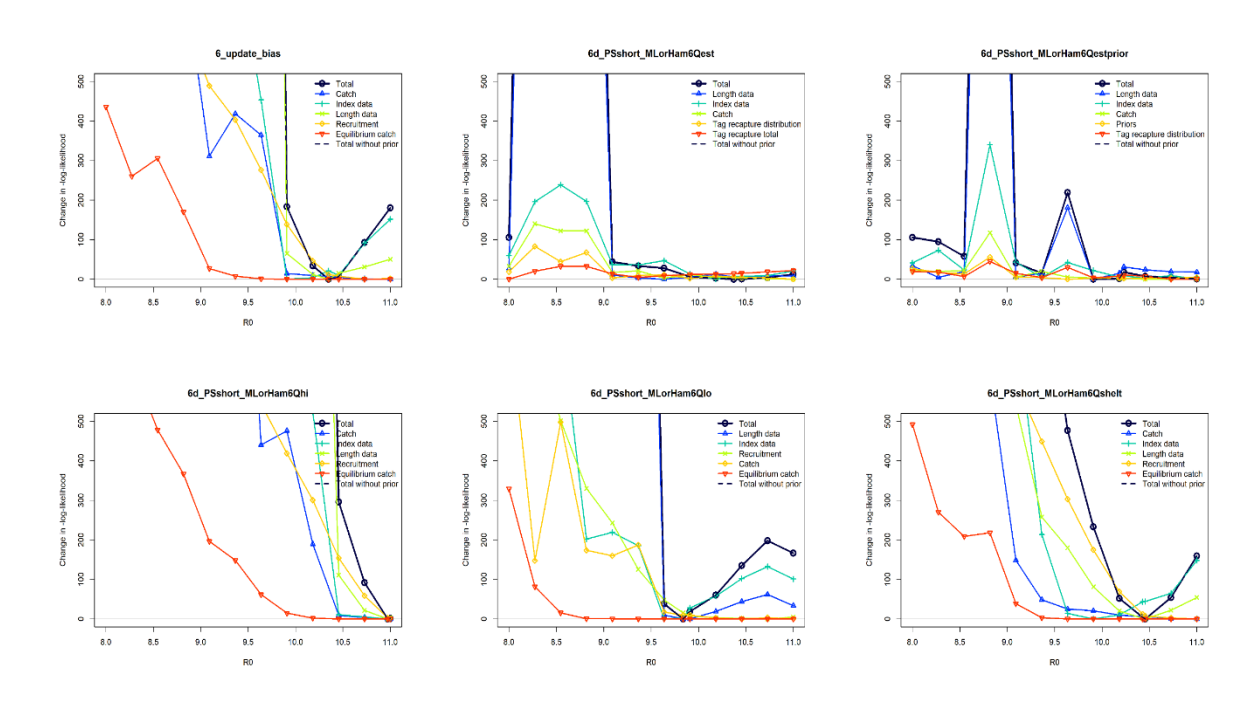


Figure 39: Likelihood profiling (change in -log(likelihood)) for unfished recruitment (R_0) for the sensitivity models where M varied. Top LH model is the reference model.

7.3. Proposed final model options for grid / ensemble

On basis of the results of sensitivity runs, and preliminary sensitivity runs completed using the previous iteration of the reference models (see rev2), final options were configured to capture the uncertainty related to assumptions on the biological parameters of natural mortality, stock-recruitment steepness, selectivity configurations, and 'gear creep' which are shown to have contributed to the main sources of uncertainty around the key model estimates.

The proposed final models involved running a combination of options on, LL 2 and 3 selectivity configurations (2 scenarios), steepness (3 values), natural mortality (3 values), and 'gear creep' on the joint longline CPUE indices (Table 8). The final model grid is, therefore almost the same as the 2022 assessment, providing a degree of continuity. Final models included the purse seine CPUE indices (short indices). The model io_h80_Gnew_MBase2025_sD_LL can be considered as a reference model in the final model ensemble. These models encompass a wide range of stock trajectories, with low steepness values generally yielding lower estimates of biomass (Table 9).

These results presented below are considered the final run of the grid for 2025, based on extensive modelling updates, and discussions at the 27thWPTT(AS).

8. STOCK STATUS

8.1. Current status and yields

MSY based estimates of stock status were determined for the final model options, including alternative assumptions on selectivity, alternative values of SRR steepness, growth, and natural mortality. Stock status was determined for individual models (Table 10), as well as for all (36) models combined incorporating uncertainty from individual models based on estimated variance-covariance matrix of parameters (Table 11).

For the selected model options, point estimates of Catch at MSY ranged from 90,984 to 114,675 t (Table 10) which are all above the current estimates of catch in 2023 and 2024 (Table 2 & Table 11). Model options with lower natural mortality generally yielded comparatively lower estimates of Catch at MSY. On average fishing mortality rates have remained well below the F_{MSY} through to 1990s and 2000s, increased significantly after 2015 (Figure 42). Biomass was estimated to have declined considerably from the late 1990s before stabilizing through the 2000s and declined again following a small increase after 2011 – 12 (Figure 40). Since 2020, the biomass is estimated to have stabilised and is now increasing, despite increasing fishing mortality.

Models that had selectivity estimated as double normal on LL2 and LL3 fleets estimate similar levels of SSB₀ compared to those with logistic selectivity (Table 10), however MSY estimates are lower with logistic selectivity, and estimates of stock status are slightly higher.

The grid encompasses a wide range of uncertainty in initial biomass estimates (Figure 41), with the rate of depletion varying between models, as current estimates of biomass are relatively similar between model options.

Diagnostic tables are provided for all models in the grid, using code developed by G. Correa in Appendix D.

Current fishing mortality (F_{2024}) was estimated to be lower than F_{MSY} for 23 out of 36 models, and current biomass (SSB_{2024}) was estimated to be between 67.1% and 157.5 % of SSB_{MSY} (Table 10). In general, current stock status relative to the MSY based benchmarks are not fundamentally different for the range of model options, although the proximity to the MSY benchmarks is sensitive to the different of model assumptions. Current spawning biomass was estimated to be below the SSB_{MSY} level ($SB_{2024}/SB_{MSY} < 1.0$) for 19 models, while 17 models estimated it to be above. Current fishing mortality (F_{2024}) is estimated to be below F_{MSY} for 23 models, and above for 13 models.

Estimates were combined across from the 36 models to generate the final KOBE stock status plot (Figure 41). For individual models, the uncertainty is characterised using the multivariate lognormal Monte-Carlo approach (Walter et al. 2019, Walter & Winker 2019, Winker et al. 2019), based on the maximum likelihood estimates and variance-covariance of the untransformed quantities F/F_{MSY} and SSB/SSB_{MSY} . Thus, estimates of stock status included both within and across model uncertainty. Combined across the model ensemble, SSB_{2024} was estimated to be of 1.02 SSB_{MSY} (0.75-1.29), and F_{2024} was estimated 0.94 F_{MSY} (0.69-1.19) (Table 11). Taking all the available information into account, the stock is **not overfished**, and **is not subject to overfishing** in 2024.

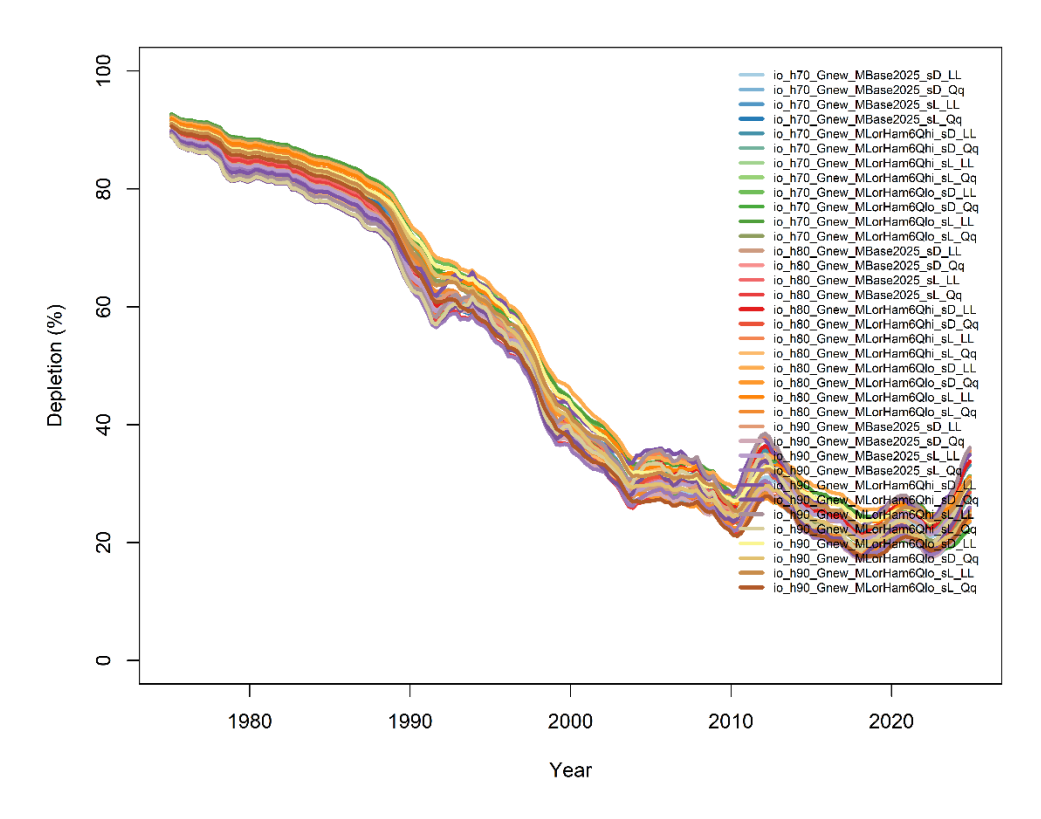


Figure 40: Spawning biomass trajectories (depletion %) from the proposed final model options in the grid

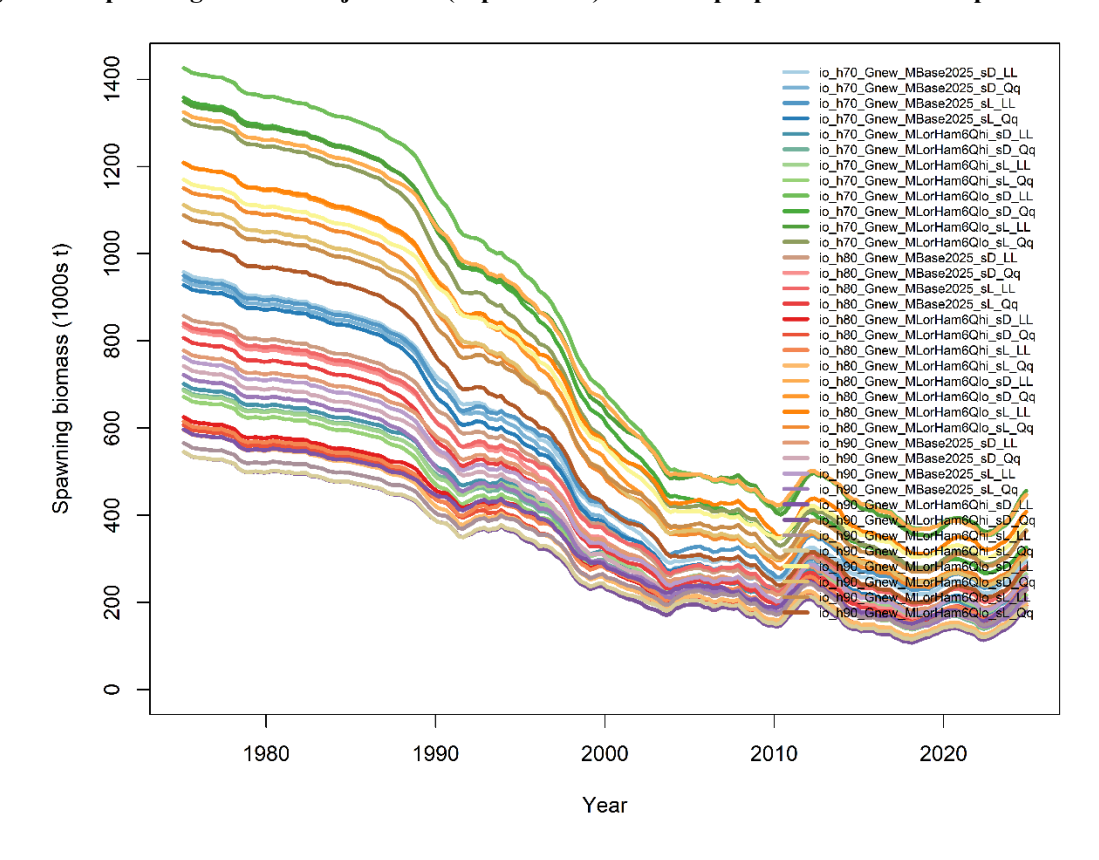


Figure 41: Spawning biomass trajectories (1000 t) from the proposed final model options in the grid

Table 10 Estimates of management quantities for the stock assessment model options. Current yield (mt) represents yield in 2024 corresponding to fishing mortality at the FMSY level.

| | SSB ₀ | SSB _{MSY} | SSB ₂₀₂₄ | SSB ₂₀₂₄ SSB ₀ | SSB ₂₀₂₄ SSB _{MSY} | F _{MSY} | F ₂₀₂₄ | F ₂₀₂₄ F _{MSY} | C _{MSY} |
|-------------------------------|------------------|--------------------|---------------------|--------------------------------------|--|------------------|-------------------|------------------------------------|------------------|
| io_h70_Gnew_MBase2025_sD_LL | 1,046,270 | 327,181 | 280,726 | 0.2683110 | 0.8580136 | 0.2179288 | 0.2372557 | 1.0886843 | 97,120 |
| io_h70_Gnew_MBase2025_sD_Qq | 1,026,110 | 315,169 | 228,504 | 0.2226896 | 0.7250205 | 0.2033628 | 0.2691715 | 1.3236025 | 98,443 |
| io_h70_Gnew_MBase2025_sL_LL | 1,034,920 | 317,099 | 304,286 | 0.2940189 | 0.9595931 | 0.2269980 | 0.2212861 | 0.9748372 | 95,596 |
| io_h70_Gnew_MBase2025_sL_Qq | 1,013,230 | 307,355 | 241,980 | 0.2388204 | 0.7872981 | 0.2175632 | 0.2573424 | 1.1828398 | 95,788 |
| io_h70_Gnew_MLorHam6Qhi_sD_LL | 770,352 | 227,629 | 241,577 | 0.3135924 | 1.0612729 | 0.2279372 | 0.2020500 | 0.8864283 | 101,745 |
| io_h70_Gnew_MLorHam6Qhi_sD_Qq | 756,608 | 221,102 | 197,652 | 0.2612347 | 0.8939415 | 0.2139224 | 0.2294719 | 1.0726878 | 101,817 |
| io_h70_Gnew_MLorHam6Qhi_sL_LL | 753,261 | 221,990 | 248,472 | 0.3298614 | 1.1192925 | 0.2326096 | 0.2030031 | 0.8727200 | 99,607 |
| io_h70_Gnew_MLorHam6Qhi_sL_Qq | 739,271 | 217,180 | 203,268 | 0.2749567 | 0.9359402 | 0.2183216 | 0.2302725 | 1.0547397 | 99,357 |
| io_h70_Gnew_MLorHam6Qlo_sD_LL | 1,539,800 | 516,848 | 425,981 | 0.2766466 | 0.8241891 | 0.1998400 | 0.2243282 | 1.1225390 | 97,704 |
| io_h70_Gnew_MLorHam6Qlo_sD_Qq | 1,470,030 | 465,278 | 312,464 | 0.2125564 | 0.6715646 | 0.1987616 | 0.2823895 | 1.4207450 | 97,438 |
| io_h70_Gnew_MLorHam6Qlo_sL_LL | 1,456,120 | 455,949 | 433,194 | 0.2974990 | 0.9500937 | 0.2242984 | 0.2151367 | 0.9591538 | 91,202 |
| io_h70_Gnew_MLorHam6Qlo_sL_Qq | 1,414,290 | 440,799 | 346,075 | 0.2446986 | 0.7851078 | 0.2171064 | 0.2474439 | 1.1397358 | 90,984 |
| io_h80_Gnew_MBase2025_sD_LL | 945,276 | 266,455 | 264,356 | 0.2796596 | 0.9921206 | 0.2622152 | 0.2425414 | 0.9249707 | 99,564 |
| io_h80_Gnew_MBase2025_sD_Qq | 918,894 | 255,275 | 217,337 | 0.2365199 | 0.8513828 | 0.2488980 | 0.2752288 | 1.1057895 | 99,766 |
| io_h80_Gnew_MBase2025_sL_LL | 925,627 | 251,628 | 265,484 | 0.2868156 | 1.0550664 | 0.2723068 | 0.2389532 | 0.8775148 | 98,250 |
| io_h80_Gnew_MBase2025_sL_Qq | 890,561 | 244,051 | 213,199 | 0.2393980 | 0.8735818 | 0.2550876 | 0.2768714 | 1.0853975 | 97,036 |
| io_h80_Gnew_MLorHam6Qhi_sD_LL | 693,800 | 178,365 | 220,551 | 0.3178884 | 1.2365150 | 0.2842376 | 0.2087201 | 0.7343157 | 105,393 |
| io_h80_Gnew_MLorHam6Qhi_sD_Qq | 674,977 | 173,451 | 180,780 | 0.2678310 | 1.0422526 | 0.2635132 | 0.2336398 | 0.8866342 | 104,458 |
| io_h80_Gnew_MLorHam6Qhi_sL_LL | 682,131 | 176,060 | 227,289 | 0.3332043 | 1.2909747 | 0.2896388 | 0.2116922 | 0.7308835 | 103,447 |
| io_h80_Gnew_MLorHam6Qhi_sL_Qq | 663,226 | 170,661 | 184,520 | 0.2782151 | 1.0812048 | 0.2664760 | 0.2374979 | 0.8912543 | 102,617 |
| io_h80_Gnew_MLorHam6Qlo_sD_LL | 1,437,400 | 454,646 | 427,654 | 0.2975191 | 0.9406307 | 0.2336812 | 0.2192412 | 0.9382065 | 98,342 |
| io_h80_Gnew_MLorHam6Qlo_sD_Qq | 1,320,830 | 399,832 | 298,201 | 0.2257679 | 0.7458157 | 0.2333520 | 0.2851369 | 1.2219175 | 97,328 |
| io_h80_Gnew_MLorHam6Qlo_sL_LL | 1,314,920 | 370,203 | 386,905 | 0.2942420 | 1.0451151 | 0.2682196 | 0.2295334 | 0.8557668 | 94,087 |
| io_h80_Gnew_MLorHam6Qlo_sL_Qq | 1,256,510 | 352,182 | 301,323 | 0.2398097 | 0.8555896 | 0.2562104 | 0.2660021 | 1.0382172 | 93,070 |
| io_h90_Gnew_MBase2025_sD_LL | 863,369 | 208,328 | 242,708 | 0.2811176 | 1.1650294 | 0.3238832 | 0.2527422 | 0.7803498 | 102,701 |
| io_h90_Gnew_MBase2025_sD_Qq | 827,162 | 198,151 | 191,667 | 0.2317167 | 0.9672787 | 0.2986104 | 0.2863667 | 0.9589977 | 102,197 |
| io_h90_Gnew_MBase2025_sL_LL | 848,271 | 200,543 | 242,670 | 0.2860754 | 1.2100622 | 0.3327540 | 0.2495264 | 0.7498825 | 101,309 |

| io_h90_Gnew_MBase2025_sL_Qq | 805,375 | 192,087 | 195,513 | 0.2427596 | 1.0178331 | 0.3071344 | 0.2874472 | 0.9359005 | 99,238 |
|-------------------------------|-----------|---------|---------|-----------|-----------|-----------|-----------|-----------|---------|
| io_h90_Gnew_MLorHam6Qhi_sD_LL | 664,233 | 141,812 | 219,685 | 0.3307345 | 1.5491267 | 0.3645244 | 0.1983389 | 0.5441033 | 114,675 |
| io_h90_Gnew_MLorHam6Qhi_sD_Qq | 612,904 | 133,279 | 168,734 | 0.2753021 | 1.2660190 | 0.3454384 | 0.2366442 | 0.6850547 | 107,218 |
| io_h90_Gnew_MLorHam6Qhi_sL_LL | 633,139 | 135,830 | 214,002 | 0.3380020 | 1.5755154 | 0.3780436 | 0.2158811 | 0.5710483 | 108,659 |
| io_h90_Gnew_MLorHam6Qhi_sL_Qq | 612,632 | 131,836 | 175,900 | 0.2871218 | 1.3342334 | 0.3481380 | 0.2384701 | 0.6849873 | 107,116 |
| io_h90_Gnew_MLorHam6Qlo_sD_LL | 1,281,920 | 356,308 | 364,063 | 0.2839980 | 1.0217642 | 0.2945592 | 0.2487266 | 0.8444027 | 99,434 |
| io_h90_Gnew_MLorHam6Qlo_sD_Qq | 1,222,100 | 332,082 | 290,875 | 0.2380122 | 0.8759124 | 0.2746828 | 0.2877322 | 1.0475073 | 100,983 |
| io_h90_Gnew_MLorHam6Qlo_sL_LL | 1,194,970 | 295,803 | 344,284 | 0.2881110 | 1.1638962 | 0.3205020 | 0.2449494 | 0.7642680 | 96,484 |
| io_h90_Gnew_MLorHam6Qlo_sL_Qq | 1,133,040 | 277,093 | 262,824 | 0.2319636 | 0.9485047 | 0.3043076 | 0.2850927 | 0.9368570 | 95,330 |

Table 11: STOCK STATUS INDICATORS FROM MODEL ENSEMBLE

| Catch in 2024: | 82,874 t |
|---|------------------|
| Average catch 2020–2024: | 87,721 t |
| MSY (1000 t) (plausible range): | 100 (94-106) |
| F _{MSY} | 0.27 (0.21-0.33) |
| SSB ₀ (1000 t) (80% CI): | 985 (623-1346) |
| SSB ₂₀₂₄ (1000 t) (80% CI): | 266 (172-359) |
| SSB_{MSY} | 276 (143-409) |
| SSB ₂₀₂₄ /SSB ₀ (80% CI): | 0.27 (0.23-0.32) |
| SSB ₂₀₂₄ / SSB _{MSY} | 1.02 (0.75-1.29) |
| F_{2024}/F_{MSY} | 0.94 (0.69-1.19) |

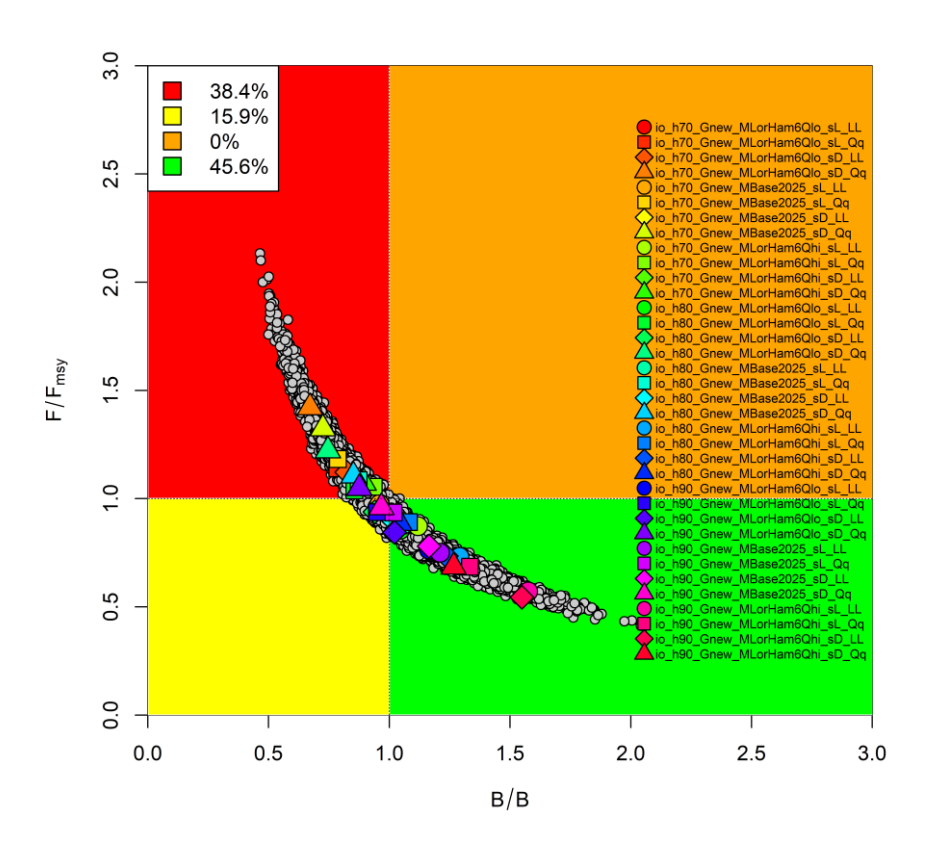


Figure 42: KOBE PLOT FROM GRID RUNS

In the 2022 assessment (using data up to 2021) the model ensemble estimated that the stock was **overfished** and **subject to overfishing** in 2021, this was a change from the 2019 assessment when the stock was estimated to be **not overfished** but subject to **overfishing**.

The estimated biomass trajectory shows a decline from exploited but equilibrium spawning stock biomass levels in 1975 to 2012 (Figure 43). Biomass levels appear to have stabilised after a decline from 2012 to 2021 and are increasing in the final years of the model, providing a more positive outlook for the stock, presumably as there are now several years of catch at or below that of MSY and fishing mortality is cycling around and above that of F/F_{MSY}. As there is a significant lack of representative biological data (length data, and representative ages), the model is forced to fit closely to the main abundance indices from the longline fleets. As there have been increases in these indices in the three most recent years (2022-2024 inclusive), alongside decreased catches, the CPUE indices alongside lower catches are driving the increase in estimated biomass in the model.

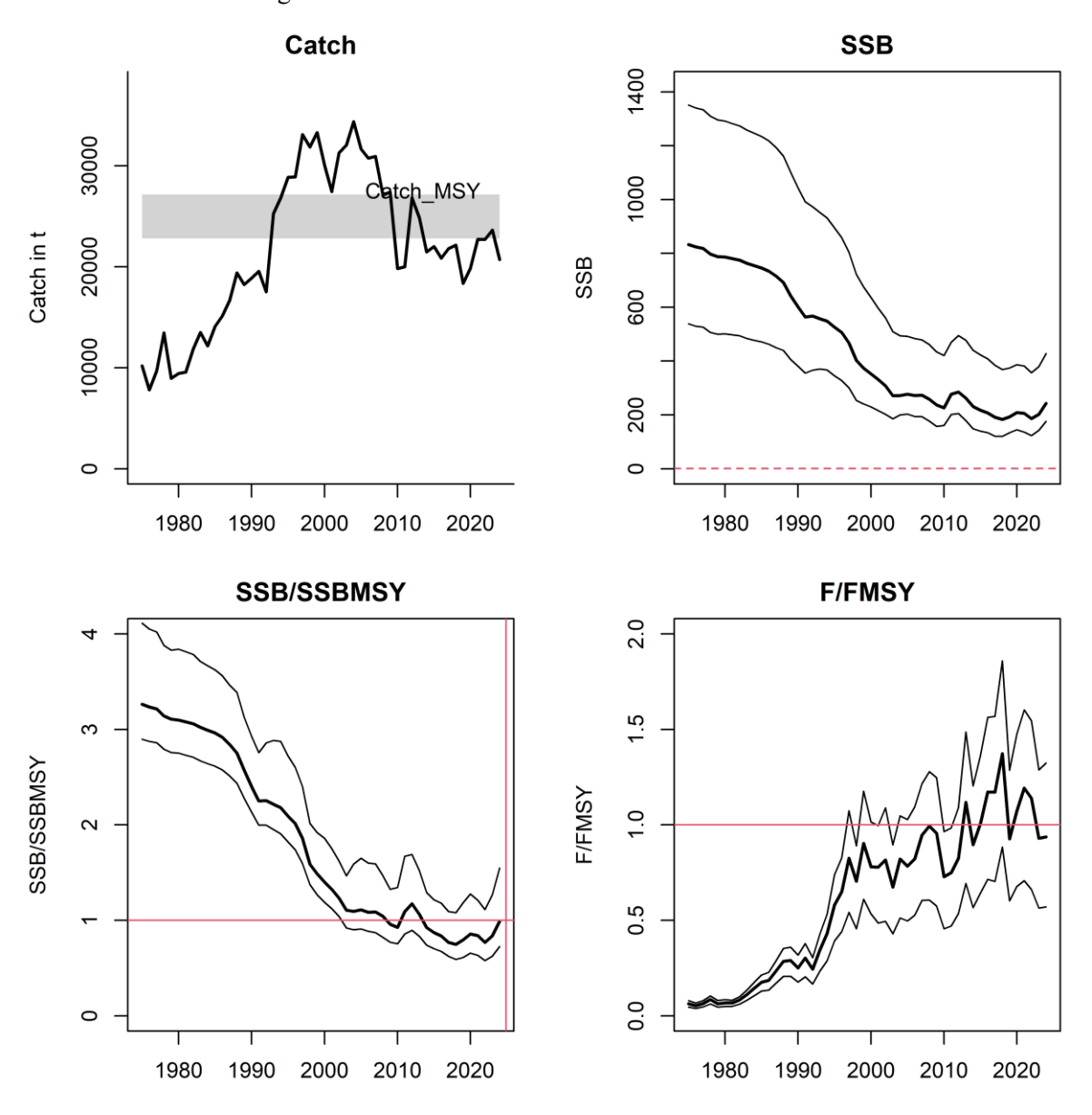


Figure 43: Management outputs from the ensemble of models (grid) used in 2024. Bounds around the main darker line represent the highest and lowest values from the grid of models. The grey band on the catch graph represents estimated optimal catch at MSY (80 % confidence interval). The horizontal red lines indicate limit or reference points for SSB/SSB_{MSY} and F/F_{MSY}.

9. DISCUSSION

This report presents a preliminary stock assessment for Indian Ocean bigeye tuna using a spatially explicit, age structured model. It represents an update and revision of the 2022 assessment model with newly available information. There are no fundamental changes in the structure of the current assessment models compared to the previous assessment, with most revisions concerning observational data, e.g., the inclusion of revised regional LL CPUE indices, and the incorporation newly available biological information including growth and natural mortality. A range of exploratory models are also presented to explore the impact of key data sets and model assumptions.

The overall stock status estimates obtained from a range of model options is similar to the previous assessment: current spawning biomass remained to be just above SSB_{MSY} ($SSB_{2024}/SSB_{MSY} = 1.02$), but fishing mortality is estimated to be below F_{MSY} ($F_{2024}/F_{MSY} = 0.94$). (Current SSB was estimated to be above SSB_{MSY} in the 2019 assessment, but at 0.90 in the 2022 assessment). This has been mostly caused by changes in CPUE indices for all regions, which have showed increases in the most recent years, and relatively stable catches in the last 5 years, that are below estimates of C_{MSY} .

The scale of the abundance indices can be found in both CPUE and length composition. The two data sources frequently include contradictory information. The best practice is to place greater focus on the CPUE data because it is more direct, whereas length composition often suffers from sampling problems, and it is impossible to eliminate the influence of biased length samples. In this assessment, only length composition from major fisheries (i.e., longlines, purse seine, and longlines for fresh tuna) is incorporated into the model. Following Hoyle et al. (2021), the longline fishery excludes Taiwanese and Seychelles length data due to sampling bias, and size data from the bait boat, line, and other fisheries are not used because the samples are of poor quality and representativeness, even though these fisheries' selectivity is linked to fisheries with a similar pattern of selection. By doing so, the impact of these length samples on estimates of the abundance is lessened.

Growth is one major source of uncertainly. The otolith aging approach utilized in the growth study of Farley et al. (2025) is supported by age validation work. The new growth curve is quite different from the integrated VB-logK curves of Eveson et al. (2012) used in the 2022 and 2019 assessments. Estimates of growth curves using the conditional-age-at-length methods of internal estimation showed that these growth curves may be well-specified. However, there are only 253 aged fish used in the model, over a short time period (2017-2024), that is not spatially- or temporally-representative of the fish within the entire Indian Ocean stock.

The assessment model adopted a 4-region spatial structure. Movement rates between regions were estimated to be much higher than in 2022, presumably due to the removal of variable recruitment between regions. As in 2022, There is very little information on the movement dynamics of bigeye tuna and this represents an uncertainty that should be investigated in the 2028 model.

More research and information on the movement rates of adult and sub-adult bigeye tuna in the Indian Ocean would go some way to improving our understanding of the likelihood of these estimates of movement.

9.1. Recommendations for future assessments

- Improved quality and quantity of length composition data: It is recommended that improvements in both quantity and quality of length frequency data are provided to the Secretariat prior to the next assessment of bigeye tuna in 2028, and that any length data omitted in this assessment are reassessed for suitability and inclusion in 2028. Results from a recent consultancy with Dr. Paul Medley may inform the next BET assessment, alongside other tropical tuna stock assessments. Additionally, a detailed investigation of current included length frequency data, particularly those in the purse seine fisheries may provide a better understanding of why the model is underfitting to the mean length data in these fisheries.
- Further development of additional abundance indices: as with other tuna assessments in the IOTC, the abundance indices are not representative of the total extent of the tuna fishery and associated catch data used in the assessment. There is additional concern regarding the contracting spatial extent of Korean and Japanese frozen longline fleets. It is recommended that other CPCs develop CPUE series for consideration in stock assessment of bigeye tuna. Standardised CPUE indices can either be included in an integrated modelling platform or contribute to overall knowledge of various components of the stock. Development of appropriate CPUE standardisations can be supported by the Secretariat or completed by the Secretariat (if appropriate operational data are provided).
- Ageing data: Currently there are a total of 253 data points for BET within the assessment model. This represents a minute percentage of the fish being caught. The samples cover only a few years of fishing, all within the last 10 years. It is strongly recommended that more fish are aged, encompassing both male and female fish, from all length-bins across the spatial extent of the fishery, to build a reasonable timeseries of biologically informative data. Age data should be accompanied by detailed information on the source of the fish (e.g. time, date, location, sex, fishing gear, vessel flag etc.) if the data are to be used to either estimate age-at-length within the model (as data need to be allocated to appropriate timesteps, model areas, and model fleets) or to account for changes in age-at-length over time or space (due to population dynamics, environmental factors, such as climate change or high fishing effort).
- Research into recruitment variability: In this iteration of the BET stock assessment model, area-based recruitment was fixed (not estimated by the model), resulting in high estimates of adult movement between the areas. It is unlikely that recruitment is equal in all areas, but further research (and/or analyses of published research) is required to ensure that parameterisation of area-based recruitment is based on biological information, and not on the longline CPUE indices (as in previous models), which are unlikely to be an index of recruitment.
- Characterisation of model fleets: Over time, the gear types and catch composition have changed, possibly resulting in model fleets that contain inconsistent selectivity and/or targeting practices. This was identified in particular for the BB1N fishery during the 27th WPTT(AS), and the 2028 assessment would benefit from investigating model fleet composition.

10.REFERENCES

- Aires-da Silva, A. M., Maunder, M. N., Schaefer, K. M., and Fuller, D. W. (2015). Improved growth estimates from integrated analysis of direct aging and tag-recapture data: An illustration with bigeye tuna (Thunnus obesus) of the eastern Pacific Ocean with implications for management. Fisheries Research, 163:119–126.
- Akia, S., Guery, L., Grande, M., Kaplan, D., Baéz, J.C., Ramos, M. L., Uranga, J., Abascal, F., Santiago, J, Merino, G., Gaertner, D. 2022. European purse seiners CPUE standardization of Big Eye tuna caught under dFADs. IOTC-2022-WPTT24-12.
- Appleyard SA, RD Ward, PM Grewe. 2002. Genetic stock structure of bigeye tuna in the Indian Ocean using mitochondrial DNA and microsatellites. J. Fish Biol. 60: 767-770.
- Cadrin, C.A., D.R. Goethel, A. Berger, E. Jardim. 2023. Best practices for defining spatial boundaries and spatial structure in stock assessment. Fisheries Research: 262: 106650. https://doi.org/10.1016/j.fishres.2023.106650.
- Carvalho, F., Winker, H., Courtney, D., Kapur, M., Kell, L., Cardinale, M., Schirripa, M., Kitakado, T., Yemane, D., Piner, K.R., Maunder, M.N., Taylor, I., Wetzel, C.R., Doering, K., Johnson, K.F., Methot, R.D., 2021. A cookbook for using model diagnostics in integrated stock assessments. Fish. Res. 240, 105959. https://doi.org/https://doi.org/10.1016/j.fishres.2021.105959
- Chassot E, Assan C, Esparon J,, Tirant A, Delgado d, Molina A, Dewals P, Augustin E, Bodin N. 2016. Length-weight relationships for tropical tunas caught with purse seine in the Indian Ocean: Update and lessons learned. IOTC-2016-WPDCS12-INF05.
- Chow, S., Okamoto, H., Miyabe, N., Hiramatsu, K., and Barut, N. (2000). Genetic divergence between Atlantic and Indo-Pacific stocks of bigeye tuna (Thunnus obesus) and admixture around South Africa. Molecular Ecology, 9(2):221–227.
- Cope, J.M., Hamel, O.S. (2022). Upgrading from M version 0.2: An application-based method for practical estimation, evaluation, and uncertainty characterisation of natural mortality. *Fisheries Research* 256.
- Correa, G.M., Kaplan, D.M., Uranga, J., Grande, M., Imzilen, T., Merino, G., Ramos Alonso, M.L. 2025. Standardised catch per unit effort of bigeye tuna in the Indian Ocean for the European purse seine fleet operating on floating objects. IOTC-2025-WPTT27DP-14.
- Day, J., Magnusson, A., Teears, T., Hampton, J., Davies, N., Castilo Jordan, C., Peatman, T., Scott, R., Phillips, J.S., McKechnie, S., Scott, F., Yao, N., Natadra, R., Pilling, G., Williams, P., Hamer, P. 2023. Stock assessment of bigeye tuna in the western and central Pacific Ocean: 2023. WCPFC-SC19-2023/SA-WP-05.
- Díaz-Arce, N., Grewe, P., Krug, I Artetxe, I., Ruiz, J., et al. (2020). Evidence of connectivity of bigeye tuna (Thunnus obesus) throughout the Indian Ocean inferred from genome-wide genetic markers. IOTC-2020-WPTT22(AS)-16.
- Eveson, P., Million, J., Sardenne, F., Le Croizier, G. 2012. Updated growth estimates for skipjack, yellowfin and bigeye tuna in the Indian Ocean using the most recent tag-recapture and otolith data. IOTC-2012-WPTT14-23.
- Eveson, P., Million, J., Sardenne, F., Le Croizier, G. 2015. Estimating growth of tropical tunas in the Indian Ocean using tag-recapture data and otolith-based age estimates. Fisheries Research 163, 58–68,
- Eveson, P., Farley, J., 2021. Investigating growth information for yellowfin and bigeye tuna from the IOTTP tag-recapture data.
- Eveson, P., Luque, P.L, Farley, J., Krusic-Golub, K., Artetxe-Arrate, I., Clear, N., Fraile, I., Duparc, A., Faucheux, C., Juan-Jorda, M.J., Mattlet, A-F., Nunes Alves, A.M., Silva Sousa, R.J., Guerreiro, A.C.S.G., Diaha, C., Murua, H., Zudaire, I. (2025) Updating the estimation of age and growth of bigeye tuna (*Thunnus obesus*) in the Indian Ocean from counts of daily and annual increments in otoliths. IOTC-2025-WPTT27DP-08.

- Farley, J.H., Clear, N.P., Leroy, Bruno., Davis, T.L.O., McPherson, G. 2004. Age and growth of bigeye tuna (Thunnus obesus) in the eastern and western AFZ.
- Farley, J., Krusic-Golub, K., Eveson, P., Clear, N., Luque, P.L., Artetxe-Arrate, I., Fraile, I., Zudaire, I., Vidot, A., Govinden, R., Ebrahim, A., Romanov, E., Chassot, E., Bodin, N., Murua, H., Marsac, F., Merino, G. 2021. Estimating the age and growth of bigeye tuna (*Thunnus obesus*) in the Indian Ocean from counts of daily and annual increments in otoliths. IOTC-2021-WPTT23-BET growth.
- Fonteneau, A., Pallares, P. 2004. Tuna natural mortality as a function of their age: the bigeye tuna case. IOTC-2004-WPTT-INF02.
- Fonteneau, A., Ariz, R., Delgado, A., Pallares, P., Pianet, R. 2004. A comparison of bigeye stocks and fisheries in the Atlantic, Indian and pacific oceans. IOTC-2004-WPTT-INF03.
- Francis, R.C. and Hilborn, R. 2011. Data weighting in statistical fisheries stock assessment models. Canadian Journal of Fisheries and Aquatic Sciences 68(6): 1124–1138. doi:10.1139/f2011-025.
- Fu, D. 2017. Indian ocean skipjack tuna stock assessment 1950-2016 (stock synthesis). IOTC-2017-WPTT19-47 rev1.
- Fu, D. 2019. Preliminary Indian Ocean Bigeye Tuna Stock Assessment 1950-2021 (Stock Synthesis). IOTC-2019-WPTT21-61.
- Fu, D., Merino, G., Winker, H. 2022. Preliminary Indian Ocean Bigeye Tuna Stock Assessment 1950-2021 (stock synthesis). IOTC-2022-WPTT24-10.
- Fu, D., Langley, A. Merino, G., Ijurco, A.U. 2018. Preliminary Indian ocean yellowfin tuna stock assessment 1950-2017 (Stock Synthesis). IOTC-2018-WPTT20-33.
- Gaertner, D., Hallier, J.P. 2015. Tag shedding by tropical tunas in the Indian Ocean and other factors affecting the shedding rate. Fisheries Research. 2015/163.
- Grewe, P. M., Wudianto, C., Proctor, C. H., Adam, M. S., Jauhary, A. R., Schaefer, K., Itano, D. G., Evans, K., Killian, A., Foster, S. D., Gosselin, T., Feutry, P., Aulich, J., Gunasekera, R. M., Lansdell, M., and Davies, C. R. (2019). Population Structure and Connectivity of Tropical Tuna Species across the Indo Pacific Ocean Region. Technical Report WCPFC-SC15-2019/SA-IP-15. Hampton. J. 2000. Natural mortality rates in tropical tunas: size really does matter. Can. J. Fish. Aquat. Sci. 57: 1002–1010 (2000).
- Hamel, O.S. 2015. A method for calculating a meta-analytical prior for the natural mortality rate using multiple life history correlates. ICES J. Mar. Sci. 72, 62–69.
- Hamel, O.S., and Cope, J.M. (2022) Development and considerations for application of a longevity-based prior for the natural mortality rate. *Fisheries Research* 256: 106477.
- Hamel, O.S., Ianelli, J.N., Maunder, M.N, Punt, A.E. (2023) Natural mortality: Theory estimation, and application in fishery stock assessment models. *Fisheries Research* 261: 106638.
- Hamer, P., Potts, J., Macdonald, J., and Senina, I. (2023). Review and analyses to inform conceptual models of population structure and spatial stratification of bigeye and yellowfin tuna assessments in the Western and Central Pacific Ocean. Technical Report SC19-SA-WP-02, Palau.
- Harley, S.J. 2011. Preliminary examination of steepness in tunas based on stock assessment results. WCPFC SC7 SA IP-8, Pohnpei, Federated States of Micronesia, 9–17 August 2011.
- Hillary, R.M., Eveson, J.P., 2015. Length-based Brownie mark-recapture models: derivation and application to Indian Ocean skipjack tuna. Fish. Res. 163, 141–151.
- Hillary, R.M., Million, J., Anganuzzi, A., Areso, J.J. 2008a. Tag shedding and reporting rate estimates for Indian Ocean tuna using double-tagging and tag-seeding experiments. IOTC-2008-WPTDA-04.
- Hillary, R.M., Million, J., Anganuzzi, A., Areso, J.J. 2008b. Reporting rate analyses for recaptures from Seychelles port for yellowfin, bigeye and skipjack tuna. IOTC-2008-WPTT-18.

- Hoyle, S.D., Leroy, B.M., Nicol, S.J., Hampton, J. 2015. Covariates of release mortality and tag loss in large-scale tuna tagging experiments. Fisheries Research 163, 106-118.
- Hoyle, S.D., Kitakado, T., Matsumoto, T., Kim, D.N., Lee, S.I., Ku, J.E., Lee, M.K., Yeh,Y., Chang, S.T., Govinden, R., Lucas, J., Assan, C., Fu, D. 2017a. IOTC-CPUEWS-04 2017: Report of the Fourth IOTC CPUE Workshop on Longline Fisheries, July 3th-7th, 2017. IOTC-2017-CPUEWS04-R. 21 p.
- Hoyle, S., Satoh, K., Matsumoto, T. 2017b. Exploring possible causes of historical discontinuities in Japanese longline CPUE. IOTC–2017–WPTT19–33 Rev1.
- Hoyle, S.D., Okamoto, H. (2015). Descriptive analyses of the Japanese Indian Ocean longline fishery, focusing on tropical areas. IOTC-2015-WPTT17-INF08.
- Hoyle, S.D., Langley, A. 2018. Indian Ocean tropical tuna regional scaling factors that allow for seasonality and cell areas. IOTC-2018-WPM09-13.
- Hoyle, S., Chang, ST., Fu, D., Geehan, J., Itoh, T., Lee, S.I., Matsumoto, T., Yeh, Y.M., Wu, R.F. 2021. IOTC-2021-WPTT(DP)23-08: Review of size data from Indian Ocean longline fleets, and its utility for stock assessment.
- Hoyle 2022. Natural mortality ogives for the Indian Ocean bigeye tuna stock assessment. IOTC–2022-WPTT24(DP)-17.
- IOTC 2016. Report of the 18th Session of the IOTC Working Party on Tropical Tunas. Seychelles, 5–10 November 2016. IOTC–2016–WPTT18–R. 126 pp.
- IOTC 2018a. Report of the 20th Session of the IOTC Working Party on Tropical Tunas. Seychelles, 29 October 3 November 2018. IOTC–2018–WPTT20–R. 127 pp.
- IOTC 2018b. Review of the statistical data and fishery trends for tropical tunas. IOTC-2018-WPTT20-07 Rev 1. IOTC-2004-WPTT-INF04.
- IOTC 2019a. Report of the 21st Session of the IOTC Working Party on Tropical Tunas. Seychelles, 21 26 October 2019. IOTC-2019-WPTT21-R: 146 pp.
- IOTC 2019b Report of the 15th Session of the IOTC Working Party on Data Collection and Statistics. IOTC, Karachi, Pakistan, 27-30 November 2019.
- IOTC 2021. Report of the 23nd Session of the IOTC Working Party on Tropical Tunas. Online, 22 24 June 2020. IOTC-2021-WPTT23(DP)-R[E]: 35 pp.
- IOTC 2022. Report of the 24th Session of the IOTC Working Party on Tropical Tunas, Data Preparatory Meeting. Online, 30-May 03 June 2022. IOTC–2022–WPTT24(DP)–R. 37 pp.
- ISSF (2011). Report of the 2011 ISSF stock assessment workshop. Technical Report ISSF TechnicalReport 2011-02, Rome, Italy, March 14-17, 2011.
- Kell, L.T., Kimoto, A., Kitakado, T., 2016. Evaluation of the prediction skill of stock assessment using hindcasting. Fisheries research, 183, pp.119-127.
- Kitakado, T., Wang, S.P., Matsumoto, T., Lee, S.I., Satoh, K., Yokoi, H., Okamoto, K., Lee, M.K., Lim, J.H., Kwon, Y., Tsai, W.P., Su, N.J., Chang, S.J., Chang, F.C. 2022. Joint CPUE indices for the bigeye tuna in the Indian Ocean based on Japanese, Korean and Taiwanese longline fisheries data up to 2020. IOTC–2022-WPTT24(DP)-15
- Kitakado, T., Wang, S-P., Lee, S.I., Tsuda, Y., Park, H., Lim, J-H., Nirazuka, S., Tsai, W-P. 2025. Update of joint CPUE indices for bigeye tunas in the Indian Ocean based on Japanese, Korean and Taiwanese longline fisheries data (up to 2024). IOTC-2025-WPTT27DP-09.
- Kolody, D., Herrera, M., Million, J., (2010). Exploration of Indian Ocean Bigeye Tuna Stock Assessment Sensitivities 1952-2008 using Stock Synthesis (updated to include 2009). IOTC-2012-WPTT10-4.
- Kolody, D. 2011. Can length-based selectivity explain the two stage growth curve observed in Indian Ocean YFT and BET. IOTC-2011-WPTT13-33.

- Langley, A.; Herrera, M.; Sharma, R. 2013a. Stock assessment of bigeye tuna in the Indian Ocean for 2012. IOTC-2013-WPTT15-30.
- Langley, A.; Herrera, M.; Sharma, R. 2013b. Stock assessment of bigeye tuna in the Indian Ocean for 2012. IOTC-2013-WPTT15-30-Rev 1.
- Langley, A. 2016. Stock assessment of bigeye tuna in the Indian Ocean for 2016 model development and evaluation.
- Matsumoto, T. 2016. Consideration on the difference of average weight by estimation method for tunas caught by Japanese longline in the Indian Ocean. IOTC-2016-WPDCS12-16.
- Maunder, M.N., Piner, K.R., 2015. Contemporary fisheries stock assessment: many issues still remain. ICES J. Mar. Sci. 72, 7–18.
- Maunder. A concise guide to developing fishery stock assessment models.
- Methot, R.D., Taylor, I.G. 2011. Adjusting for bias due to variability of estimated recruitments in fishery assessment models. Can. J. Fish. Aquat. Sci. 68: 1744–1760.
- Methot, R.D. 2013. User manual for Stock Synthesis, model version 3.24f.
- Methot, R.D., Wetzel, C.R. 2013. Stock synthesis: A biological and statistical framework for fish stock assessment and fishery management. Fisheries Research 142 (2013) 86–99.
- Merino, G., Urtizberea, A., Fu, D., Winker, H., Cardinale, M., Lauretta, M. V., Murua, H., Kitakado, T., Arrizabalaga, H., Scott, R., Pilling, G., Minte-Vera, C., Xu, H., Laborda, A., Erauskin-Extraminiana, M., Santiago, J., 2022. Investigating trends in process error as a diagnostic for integrated fisheries stock assessments. Fish. Res. 256, 106478.
- Moore, B. R., Lestari, P., Cutmore, S. C., Proctor, C., and Lester, R. J. G. (2019). Movement of juvenile tuna deduced from parasite data. ICES Journal of Marine Science, 76(6):1678–1689.
- Nishida, T., Rademeyer, R. (2011). Stock and risk assessments on bigeye tuna (*Thunnus obesus*) in the Indian Ocean based on AD Model Builder implemented Age-Structured Production Model (ASPM). IOTC-2011-WPTT-42.
- Okamoto, H. 2005. Recent trend of Japanese longline fishery in the Indian Ocean with special reference to the targeting. Is the target shifting from bigeye to yellowfin? IOTC-2005-WPTT-11.
- Preece, A., Williams, A. 2025. An update on Consideration of Exceptional Circumstances for the Bigeye Tuna MP 2025. IOTC-2025-WPM16-MSE-04.
- Punt A.E., Castillo-Jordan, C., Hamel, O.S., Cope, J.M., Maunder, M.N., Ianelli, J.N. (2021) Consequences of error in natural mortality and its estimation in stock assessment models. *Fisheries Research* 233 (105759).
- Schaefer, K., Fuller, D., Hampton, J., Caillot, S., Leroy, B., and Itano, D. (2015). Movements, dispersion, and mixing of bigeye tuna (1t Thunnus obesus) tagged and released in the equatorial Central Pacific Ocean, with conventional and archival tags. *Fisheries Research*, 161:336–355
- Shono, H., K. Satoh, H. Okamoto, and T. Nishida. (2009). Updated stock assessment for bigeye tuna in the Indian Ocean up to 2008 using Stock Synthesis III (SS3). IOTC-2009-WPTT-20.
- Then, A.Y.; Hoenig, J.M.; Hall, N.G.; Hewitt, D.A. Evaluating the predictive performance of empirical estimators of natural mortality rate using information on over 200 fish species. ICES Journal of Marine Science. 72:82-92; 2015
- Thorson, J.T., Johnson, K.F.,Methot, R.D., and Taylor, I.G. 2017. Model-based estimates of effective sample size in stock assessment models using the Dirichlet-multinomial distribution. Fisheries Research 192: 84–93. doi:10.1016/j.fishres.2016.06.005.
- Vincent, M. T., Pilling, G.M., Hampton, J. 2018. Incorporation of updated growth information within the 2017 WCPO bigeye stock assessment grid, and examination of the sensitivity of estimates to alternative model spatial structures. WCPFC-SC14-2018/ SA-WP-03.

- Waterhouse, L, Sampson DB, Maunder M, Semmens BX. 2014. Using areas-as-fleets selectivity to model spatial fishing: Asymptotic curves are unlikely under equilibrium conditions. Fisheries Research. 158:15-25.
- Walter, J., Hiroki, Y., Satoh, K., Matsumoto, T., Winker, H., Ijurco, A.U., Schirripa, M., 2019. Atlantic bigeye tuna stock synthesis projections and kobe 2 matrices. Col. Vol. Sci. Pap. ICCAT 75, 2283–2300.
- Walter, J., Winker, H., 2019. Projections to create Kobe 2 Strategy Matrices using the multivariate log-normal approximation for Atlantic yellowfin tuna. ICCAT-SCRS/2019/145 1–12.
- Winker, H., Walter, J., Cardinale, M., Fu, D. 2019. A multivariate lognormal Monte-Carlo approach for estimating structural uncertainty about the stock status and future projections for Indian Ocean Yellowfin tuna. IOTC–2019–WPTT21–xx.
- Waterhouse, L, David B. Sampson, D., Maunder, M., Semmens, B. 2014. Using areas-as-fleets selectivity to model spatial fishing: Asymptotic curves are unlikely under equilibrium conditions. Fisheries Research 158 (2014) 15–25.
- Williams, A., Jumppanen, P., Preece, A., Hillary, R. 2022. Running the IOTC Bigeye Tuna Management Procedure for 2022. IOTC-2022-WPM13-10.
- Williams, A., Preece, A., Hillary, R. 2022 Specifications of the IOTC Bigeye Tuna Management Procedure. IOTC-2022-WPM13-11.
- Williams, A., Preece, A. 2025. Update on running the IOTC Bigeye Tuna Management Procedure for 2024. IOTC-2025-WPM16MSE-02.
- Iker Zudaire, Iraide Artetxe-Arrate, Jessica Farley, Hilario Murua, Deniz Kukul, Annie Vidot, Shoaib Abdul Razzaque, Mohamed Ahusan, Evgeny Romanov, Paige Eveson, Naomi Clear, Patricia L. Luque, Igaratza Fraile, Nathalie Bodin, Emmanuel Chassot, Rodney Govinden, Ameer Ebrahim, Umair Shahid, Theotime Fily, Francis Marsac, Gorka Merino. Preliminary estimates of sex ratio, spawning season, batch fecundity and length at maturity for Indian Ocean bigeye tuna. IOTC-2022-WPTT24(DP)-18.

11.APPENDIX A:

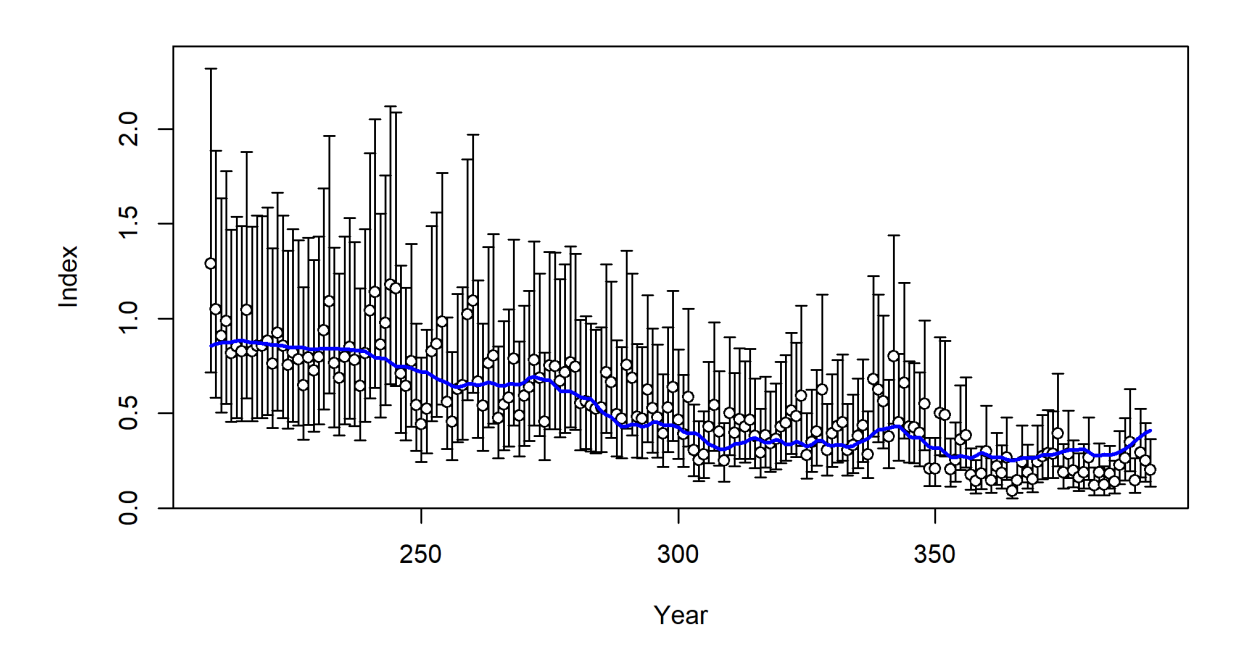


Figure A1: Fits to the LL CPUE index Region 1N from the Somalia catch edition sensitivity run

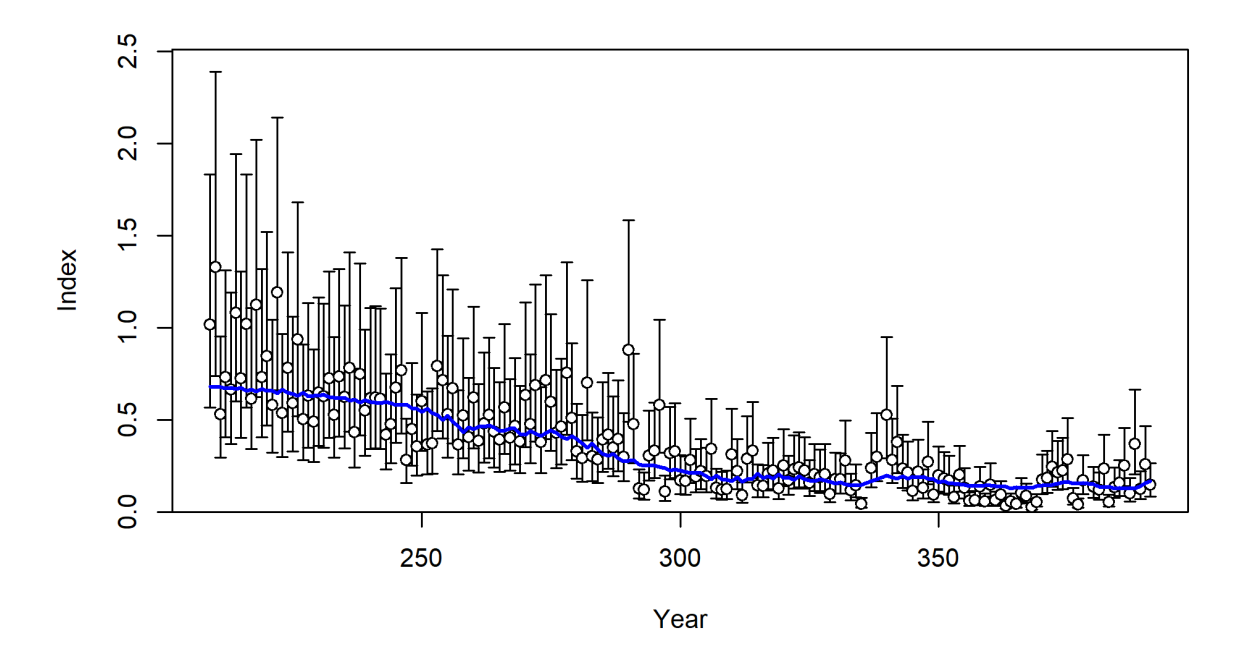


Figure A2: Fits to the LL CPUE index Region 1S from the Somalia catch edition sensitivity run

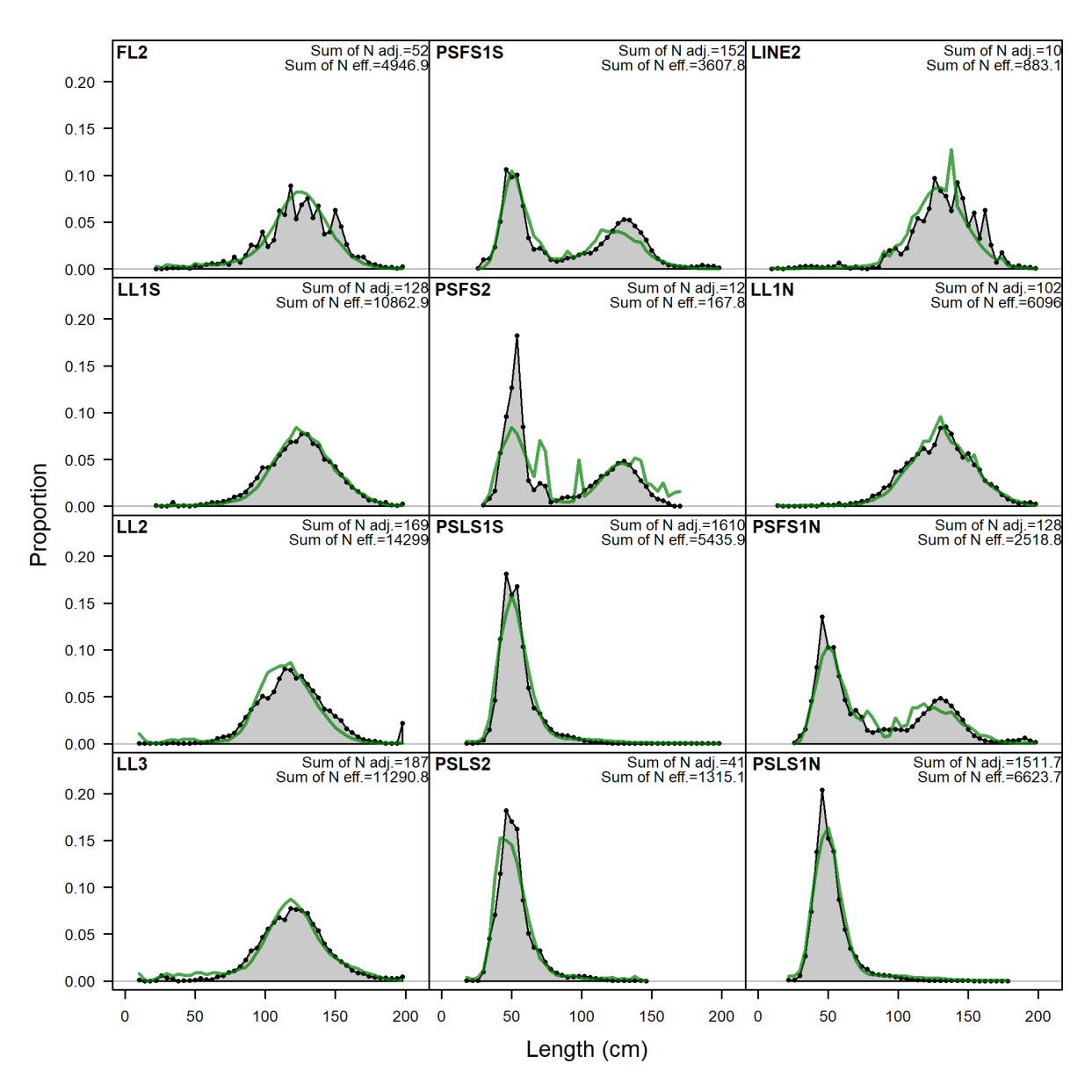


Figure A3: Fits to the length composition data when the Somalia catches are added to the model. Fits are similar to when the catch data are omitted (in the reference /base model).

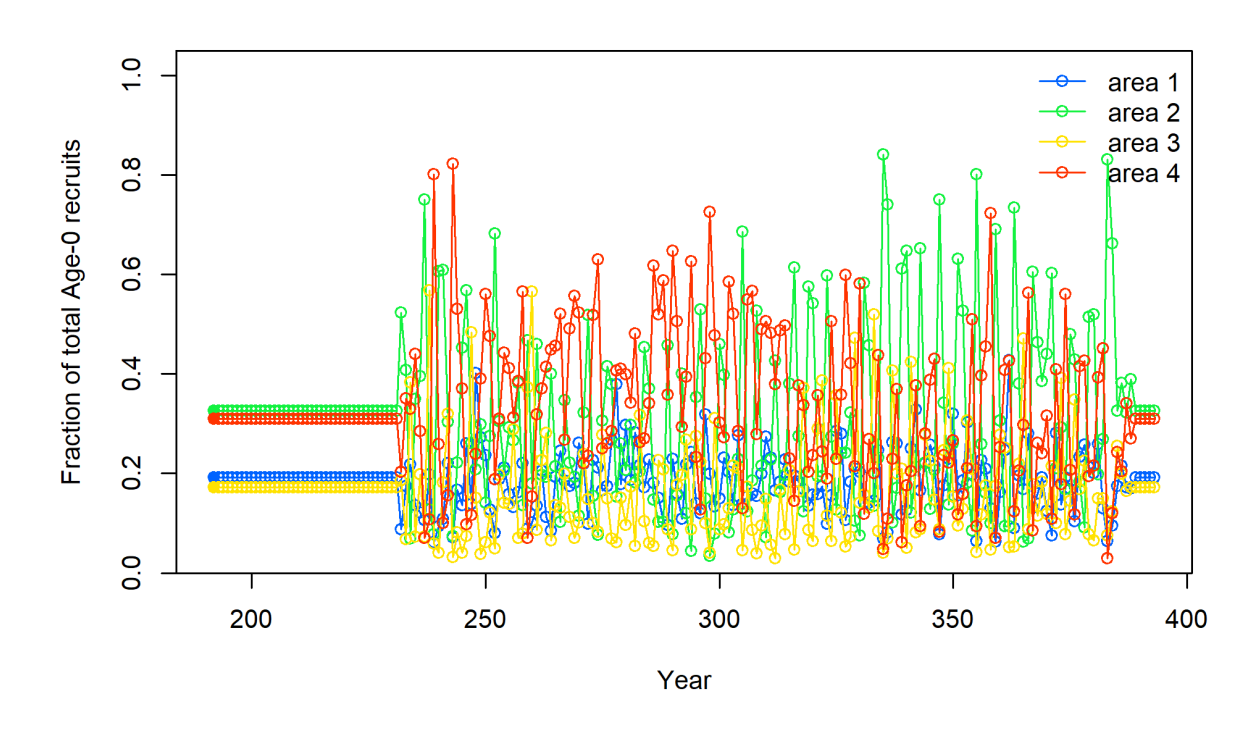


Figure A4: Estimated fraction of recruitment by area from the sensitivity run where recruitment is allowed to vary between areas (as opposed to being fixed in the reference model). Areas 2 and 4 (region 2 and region 1N) have proportionally higher estimated recruitment than area 1 (region 1S) and area 3 (region 3).

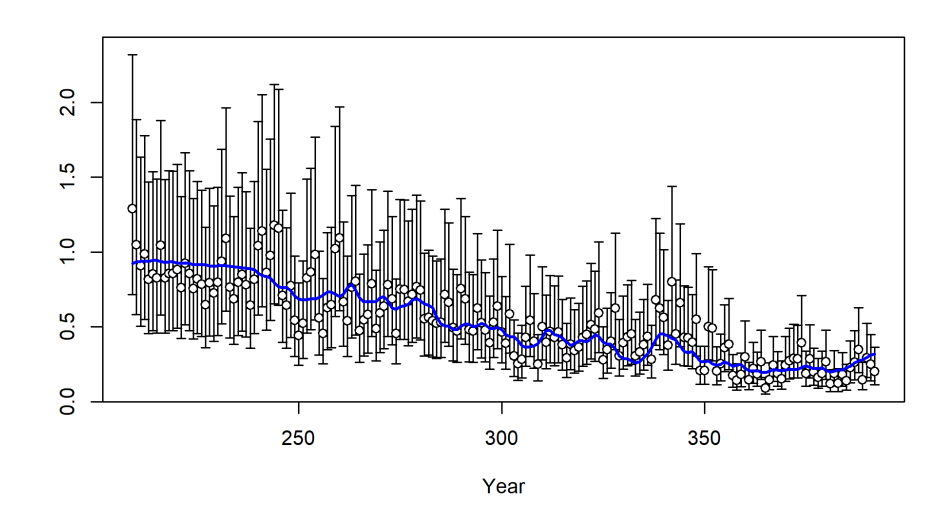
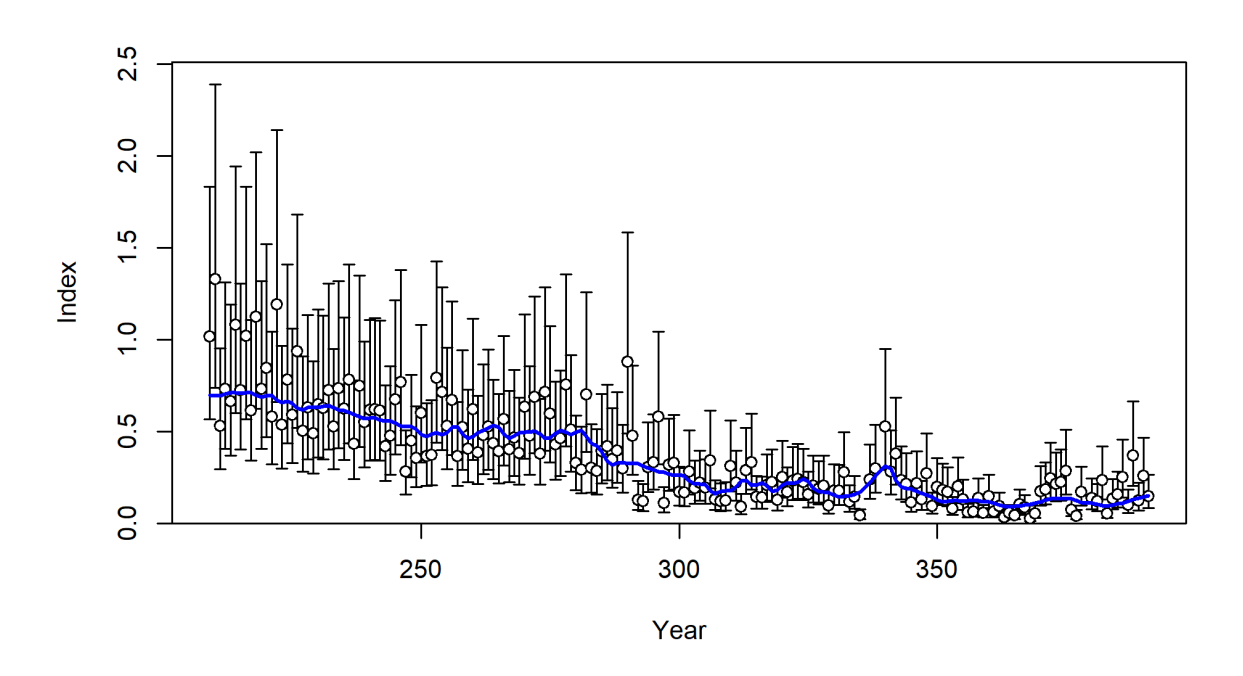
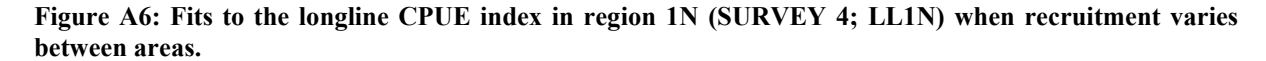


Figure A5: Fits to the longline CPUE index in region 1S (SURVEY 1; LL1S) when recruitment varies between areas.





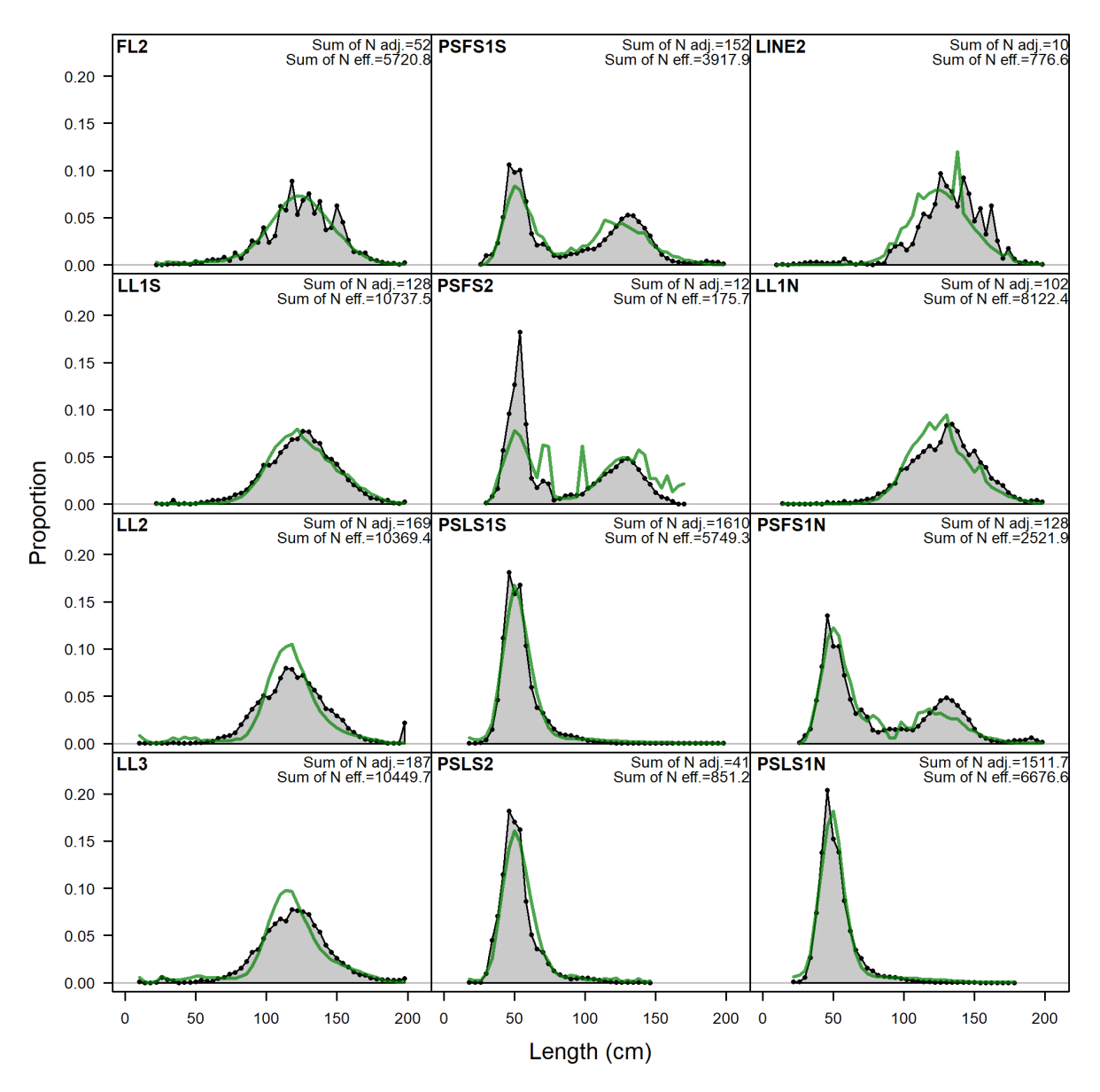


Figure A7: Fits to the aggregated length composition data when recruitment varies between areas. Fits to the LL1N, LL2, LL3 and LINE2 fisheries are worse than in the reference model.

Movement rates (fraction moving per year in season 1)

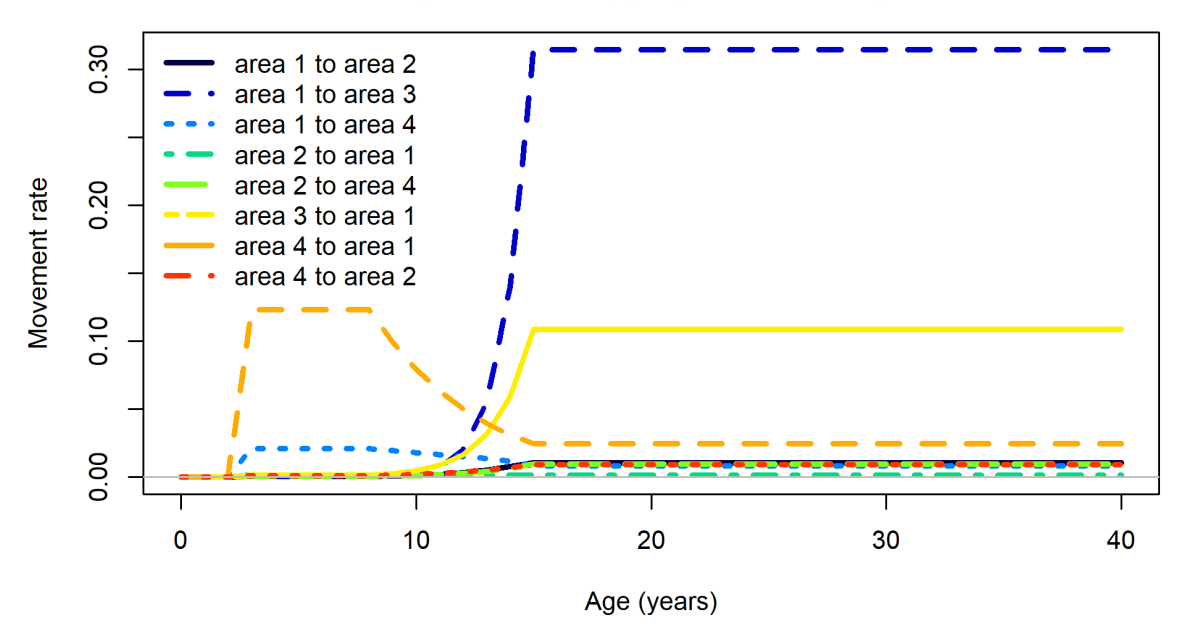


Figure A8: Movement rates of different aged fish between areas when recruitment is allowed to vary between areas. Movement rates are lower than in the reference model, presumably due to the confounding of adult movement and recruitment within the model. Most adult movement in this model is estimated to occur between area 1 (region 1S) and area 3 (region 3) with movement of younger fish from area 4 (region 1N) and area 1 (region 1S). A smaller proportion of adults move from area 3 (region 3, east IO) to area 1 (region 1S), while there is almost no adult movement between area 1 to 4 (adjacent regions 1S and 1N).

12.APPENDIX B: CPUE COMPARISON

Analysis of Indian Ocean CPUE - 2025 Bigeye Tuna Assessment

Genevieve Phillips (genevieve.phillips@fao.org), Joel Rice (ricemarineanalytics@gmail.com)

2025-06-26

12.1. Introduction

This document presents a comparison of the six catch per unit of effort (CPUE) series submitted for consideration in the 2025 IOTC bigeye tuna (*Thunnus obesus*) assessment in the Indian Ocean using methods developed for CPUE comparisons for a stock assessment model within ICCAT (Rice et al., 2025). The goals of this analysis are 1) to investigate any relative differences between model inputs so that data conflict is not introduced into the model via indices of abundance (CPUE series) that imply different, conflicting states of nature (i.e. do alternative indices of abundance indicate that the stock is increasing or the stock is decreasing); and 2) to understand whether it is reasonable to include the purse seine indices of abundance in the stock assessment (pending sensitivity runs on the assessment model).

12.2. Data and methods

12.3. Catch and effort data

Within the fisheries landing bigeye tuna in the Indian Ocean, data are aggregated into four regional longline fleets (which in turn are comprised of several fisheries, aggregated by gear type and fishing behaviour), and two regional purse seine fleets. In total, there are six abundance indices (catch per unit effort (CPUE) series) which together span the Indian Ocean, however each index is related to a different region of the ocean. Four of the CPUE series are based on catch and effort data from three nations (JAP, TWN,China, and KOR), forming four joint CPUE indices. For more detail on the methods, please see Kitikado et al. (2025) and the paper presented to the data preparation meeting for Tropical Tuna in June 2025.

The purse seine CPUE series considered have been submitted by EU,Spain and in this analysis the regional (R1N and R1S split) 'long' indices have been used (time period 1991-2023). During WPTT09-DP there were discussions around whether these indices should be included within the stock assessment, as they are based on indices that are not considered to be highly accurate representations of fish biomass. The reasons behind this are that these indices are based on purse seine fisheries that use drifting fish aggregating devices (DFADs) to aggregate fish, and therefore increase the effectiveness of fishing operations. When using such CPUE indices, if there is little difference between the nominal and standardised CPUE indices (as in the case of the supplied indices) there are likely to be other variables impacting the CPUE that are not included within the model (for example fish behaviour, fish habitat availability, whether the fleet is targeting bigeye tuna or not). See Correa et al (2025) for further information regarding the purse seine CPUE indices.

For all the CPUE indices in the 2025 bigeye tuna stock assessment, there is uncertainty around the CPUE indices as accurate reflections of the population biomass. This is because bigeye tuna are not a primary target species throughout the Indian Ocean. They are often caught as bycatch when fishers are targeting yellowfin or skipjack tuna, as the three species often school together when individuals are smaller. This also causes identification issues as juvenile or sub-adult yellowfin tuna closely resemble

bigeye tuna. These issues are somewhat accounted for in both the purse seine and joint longline CPUE indices, by the use of clustering analyses and / or 'hooks between floats' in the longline (prior to 2025) to attempt to identify data that relates to targeted fishing of bigeye tuna as opposed to opportunistic fishing or bycatch data.

12.4. Methods

The CPUE time series for bigeye tuna (*Thunnus obesus*) in the Indian Ocean are plotted (**Figure 1**) along with a lowess smoother fitted to the CPUE each year using a general additive model (GAM) to compare trends for the submitted CPUEs. Residuals from the smoother fits to CPUE are compared to identify deviations from the overall trends. This allows conflicts between indices (e.g. highlighted by patterns in the residuals) to be identified.

Correlations between indices are evaluated in **Figure 3** via pairwise scatter plots for CPUE indices where they overlap. The lower triangle shows the pairwise scatter plots between indices with a regression line, the upper triangle provides the correlation coefficients, and the diagonal provides the range of observations along with a linear model fit between them.

A hierarchical cluster analysis was used to evaluate the indices using a set of dissimilarities and the results are plotted in **Figure 4**. This analysis can identify similar and dissimilar trends. If indices represent the same stock components, then it is reasonable to expect them to be correlated. If indices are not correlated or are negatively correlated, i.e. they show conflicting trends, then this may result in poor fits to the data and bias in the parameter estimates obtained within a stock assessment model. Therefore, the correlations can be used to select groups of indices that represent a common hypothesis about the evolution of the stock (Rice 2022, ICCAT 2017).

Cross-correlations for the region are plotted with a lag from -10 to 10 in **Figure 5** (i.e., the correlations between series when they are lagged by -10 to 10 years) which can help determine whether there is relationship between two time-dependent variables at different time lags. This approach can be particularly useful when comparing indices of abundance for bycatch species derived from fleets targeting diff species (i.e. tropical vs temperate tunas), or aggregated at different levels (trips vs sets).

If all CPUE series are thought to represent the overall dynamics of the stock, careful examination of how one index may lead or lag another, temporal shifts or delays in population dynamics may become apparent (e.g. migration patterns, or the effects of environmental drivers). For example, a strong correlation at a positive lag might indicate that changes in one index precedes changes in another, possibly suggesting sampling of separate part of the stock (e.g. juvenile vs adult).

Conversely, correlations at negative lags may reflect delayed responses in one component of the population to changes in another. Overall, lagged cross-correlation helps clarify potential lead-lag relationships between datasets, offering insights into the relative similarity of the CPUE series. Careful interpretation of the results is suggested given the potential bycatch nature of this stock and the changes fleet dynamics and potential gear or technological creep within the purse seine fisheries.

The diagonals in **Figure 5** show the auto-correlations of an index lagged against itself. This can help identify whether a relationship exists between the CPUE series and earlier years, which would be identified by a large correlation, with the correlations on both sides that quickly become small.

All analyses were conducted using R and FLR, including the *diags* package which provides a set of common methods for reading these data into R, plotting and summarising them (e.g., see: http://www.flr-project.org/).

13. 3. Results and conclusions

The overall trend for the indices is an overall decreasing trend from the 1980s to the present day. The variation in the CPUE indices has reduced slightly over time, more so in the purse seine fisheries, possibly indicating improved efficiency relating to DFAD use, or overall improved knowledge of fish behaviour over time. Over the last 15-20 years, there has been little overall change in the CPUE indices, with the exception of a marked increase in the longline region 2 index in the last year (4 quarters of data; **Figure B1**).

Overall **Figures B1 and B2** indicate that the series follow the overall trend, and may provide some evidence of a potential recruitment pulse in 2004 (as seen by an increase in CPUE in the purse seine fisheries), followed by a subsequent increase in CPUE in the longline fisheries (particularly in region 1 south) in 2008-2009 approximately four years later.

Differences in the size, sign and trend in the residuals be evidence of a more rapidly decreasing trend in the stock trajectory in recent years in region 1 south, potentially lead by increases in efficiency in purse seine fisheries that capture juvenile fish, leading to fewer adult fish reaching maturity, and reproducing, and fewer adult fish available for the longline fishery in this key region. However, it is important to consider the potential that bigeye tuna are often considered a bycatch species, and decreases in CPUE may indicate a shift in targeting preferences to the main tropical tuna species. This requires further species identification data, and observer data for verification.

Correlations between indices are evaluated in **Figure B3**. The lower triangle shows the pairwise scatter plots between indices with a regression line, the upper triangle provides the correlation coefficients, and the diagonal provides the range of observations. The strongest correlation is between LL_R1S and LL_R1N (Corr: 0.782), suggesting a strong positive relationship. This indicates that these two fleets are sampling the same components of the stock, which is reassuring as they are both longline indices from the joint CPUE from TWN,China, KOR, and JAP. A strong positive correlation is also evident between PS_R1S and PS_R1N (Corr: 0.719), indicating similar spatiotemporal dynamics and/or operational practices, and likely sampling the same population. Only one pairing (PS_R1N vs. LL_R3) shows a near-zero correlation (Corr: 0.037), suggesting these indices may be relatively independent or reflect uncorrelated processes. This could be due to the inherent differences in gear type (PS vs LL), target species (if other tropical tuna are targeted), region (R3 vs R1), aggregation scale, or the different size classes caught by the gear (sub-adult vs adult).

All indices showed positive correlations, with only the LL_R3 index having non-significant correlations (although positive trends) with the purse seine indices. This is likely due to the different regions being sampled by these fisheries.

The hierarchical cluster analysis (**Figure 4**) identified two groupings of time-series. The first group includes the purse seine CPUE indices. The second group includes the longline CPUE indices, showing strong correlations between the LL CPUE indices in all regions.

Lagged cross-correlations are plotted in **Figure 5** and the analysis revealed that the longline CPUE indices are likely targeting the same portion of the population, with little lag observed between the

datasets. The longline CPUE index from R2 (region 2) shows some lag between that index and the purse seine indices, suggesting that these two indices are sampling distinct components of the population (highly likely as the purse seine fisheries are targetting smaller individuals than the longline fleets), and also that these regions *may* have asynchronous abundance signals (driven by the differential portions of the population). Along with the positive correlations between these indices, this provides some evidence that the purse seine indices may reflect ontogenetic behaviour within the population dynamics of bigeye tuna (e.g. smaller subadults targeted by the purse seine fisheries potentially moving into region 2 as they get larger, where they are caught by the longline fleets.)

13.1. References

Indian Ocean Tuna Commission (IOTC) (2025). IOTC-2025-WPTT27(DP): Report of the 27th Meeting of the Working Party for Tropical Tunas - Data Preparatory Meeting. (Online, June 11-13 2025).

Correa, G.M., Kaplan, D.M., Uranga, J., Grande, M., Imzilen, T., Merino, G., Alonso, M.L.R. (2025). Standardised catch per unit effort of bigeye tuna in the Indian Ocean for the European purse seine fleet operating on floating objects. 27th Working Party for Tropical Tunas - Data Preparatory Meeting. (Online, June 11-13 2025).

Kitakado, T., Wang, S-P., Lee, S.I., Tsuda, Y., Park, H., Lim, J-H., Nirazuka, S., Tsai, W-P. (2025). IOTC-2025-WPTT27(DP)-09: Update of joint CPUE indices for bigeye tunas in the Indian Ocean based on Japanese, Korean and Taiwanese longline fisheries data (up to 2024). 27th Working Party for Tropical Tunas - Data Preparatory Meeting. (Online, June 11-13 2025).

Rice, J., Sant'Ana, R., Kikuchi, E., Gustavo Cardoso, L. (2025). Analysis and comparison and of Catch Per Unit Effort Series submitted for the 2025 South Atlantic shortfin make shark assessment in the ICCAT region.

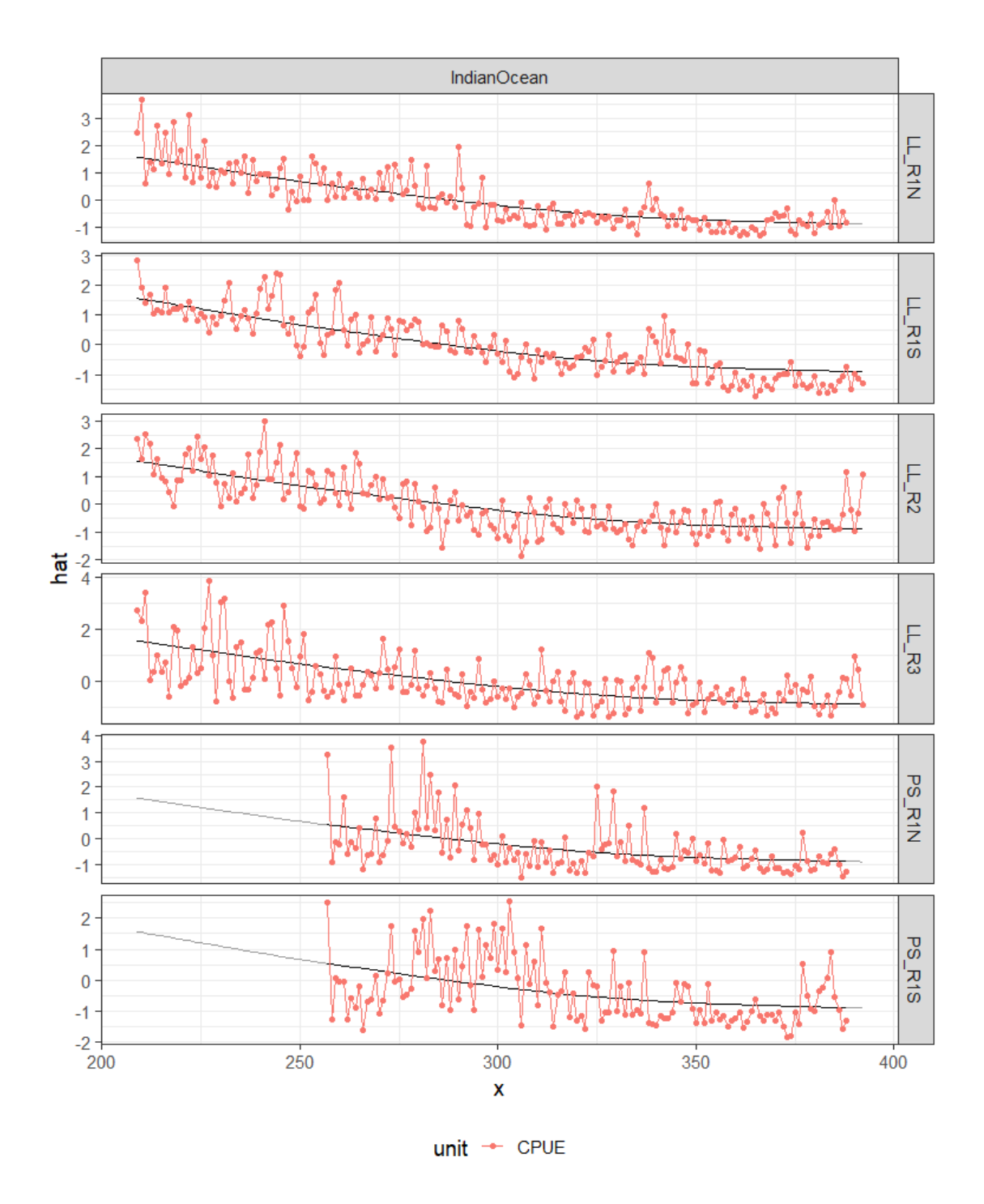


Figure B1. Indian Ocean time series of CPUE indices; Points are the standardized values, continuous black lines are a lowess smoother showing the average trend by area (i.e. fitted to year for each area with series as a factor). X-axis is time, Y-axis are the scaled indices.

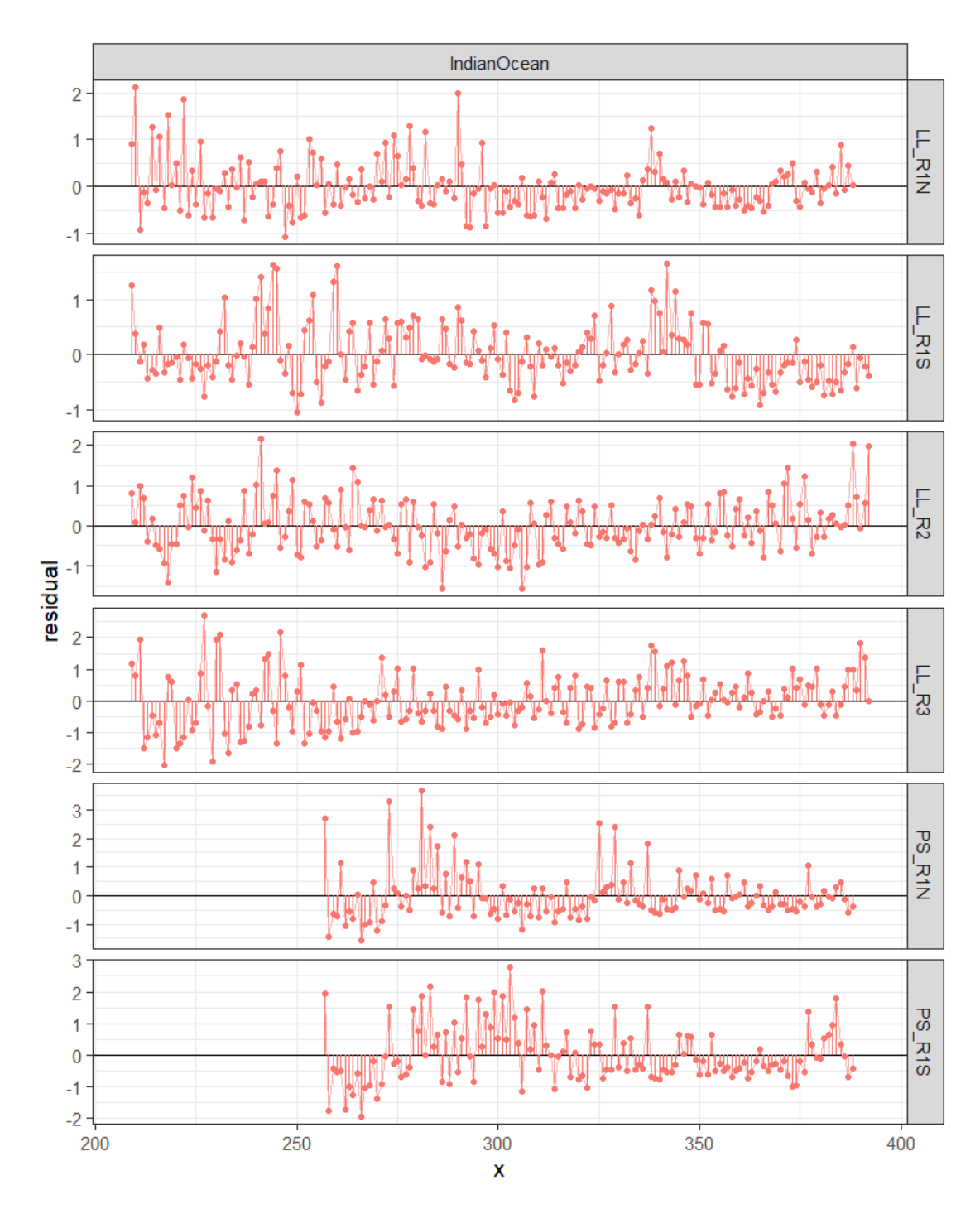


Figure B2. Time series of residuals from the smooth fit to CPUE indices. X-axis is time, Y-axis are the scaled indices.

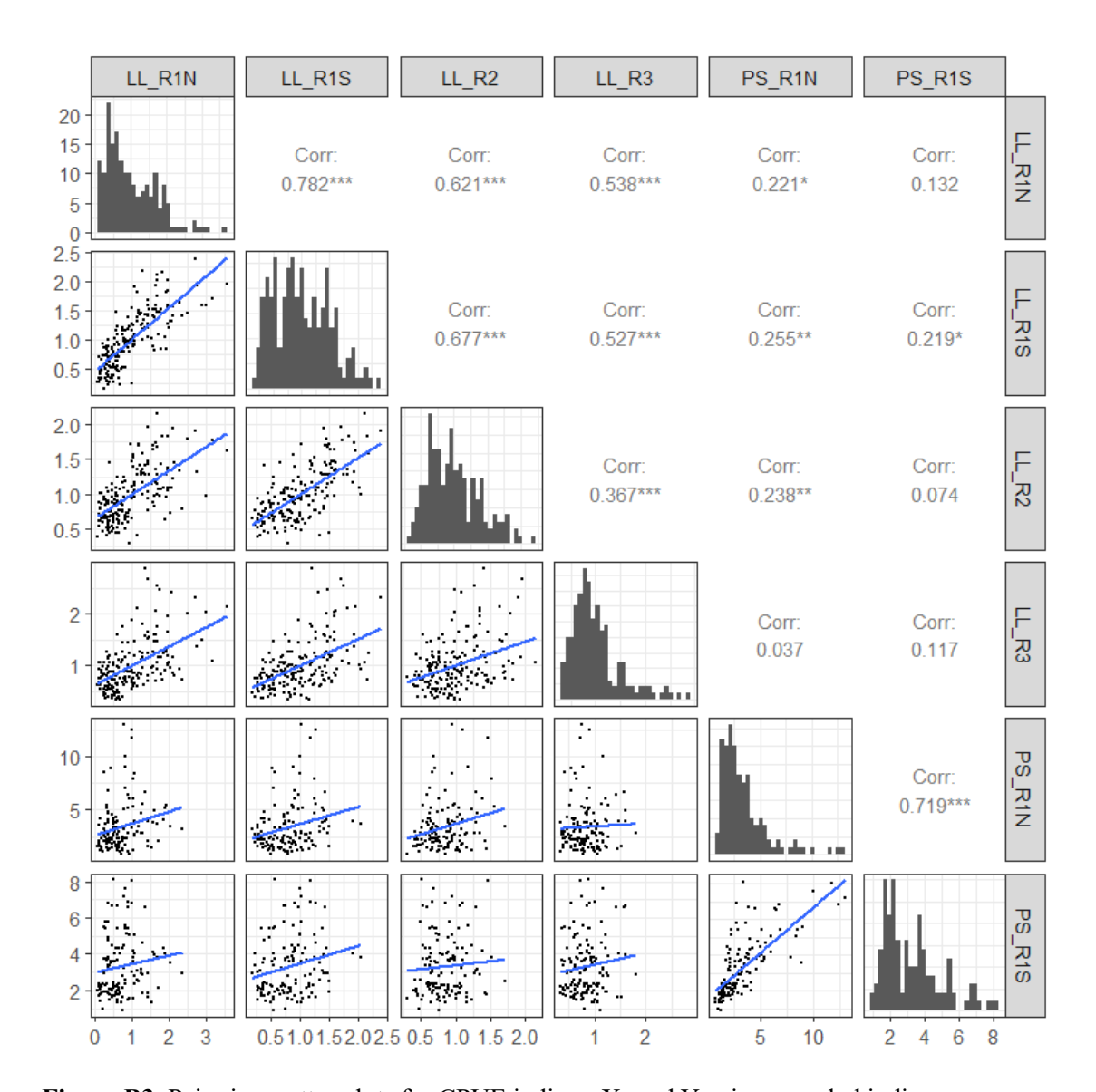


Figure B3. Pairwise scatter plots for CPUE indices. X- and Y-axis are scaled indices.

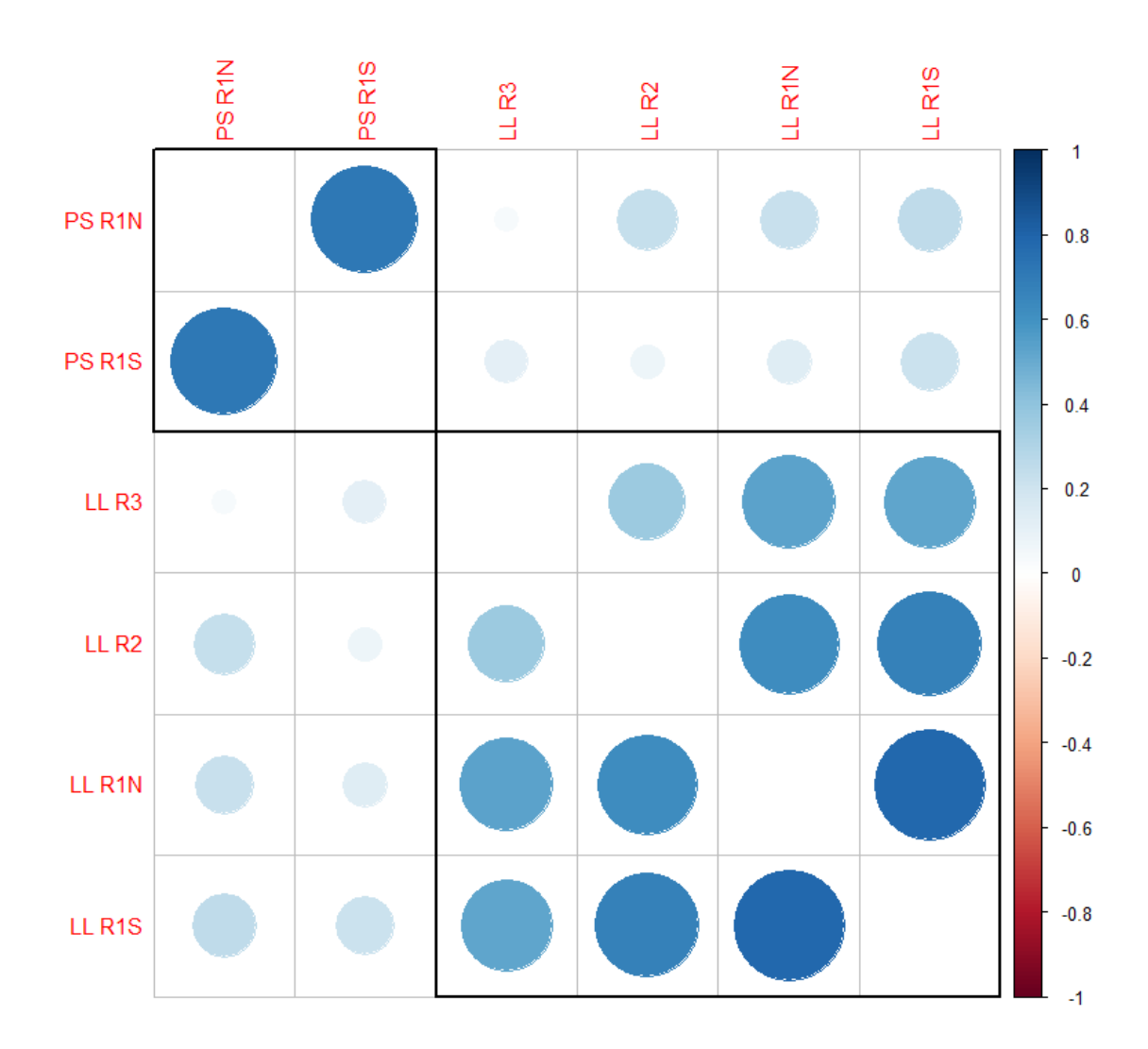


Figure B4. Correlation matrix for CPUE indices; blue indicates positive and red negative correlations, the order of the indices and the rectangular boxes are chosen based on a hierarchical cluster analysis using a set of dissimilarities.

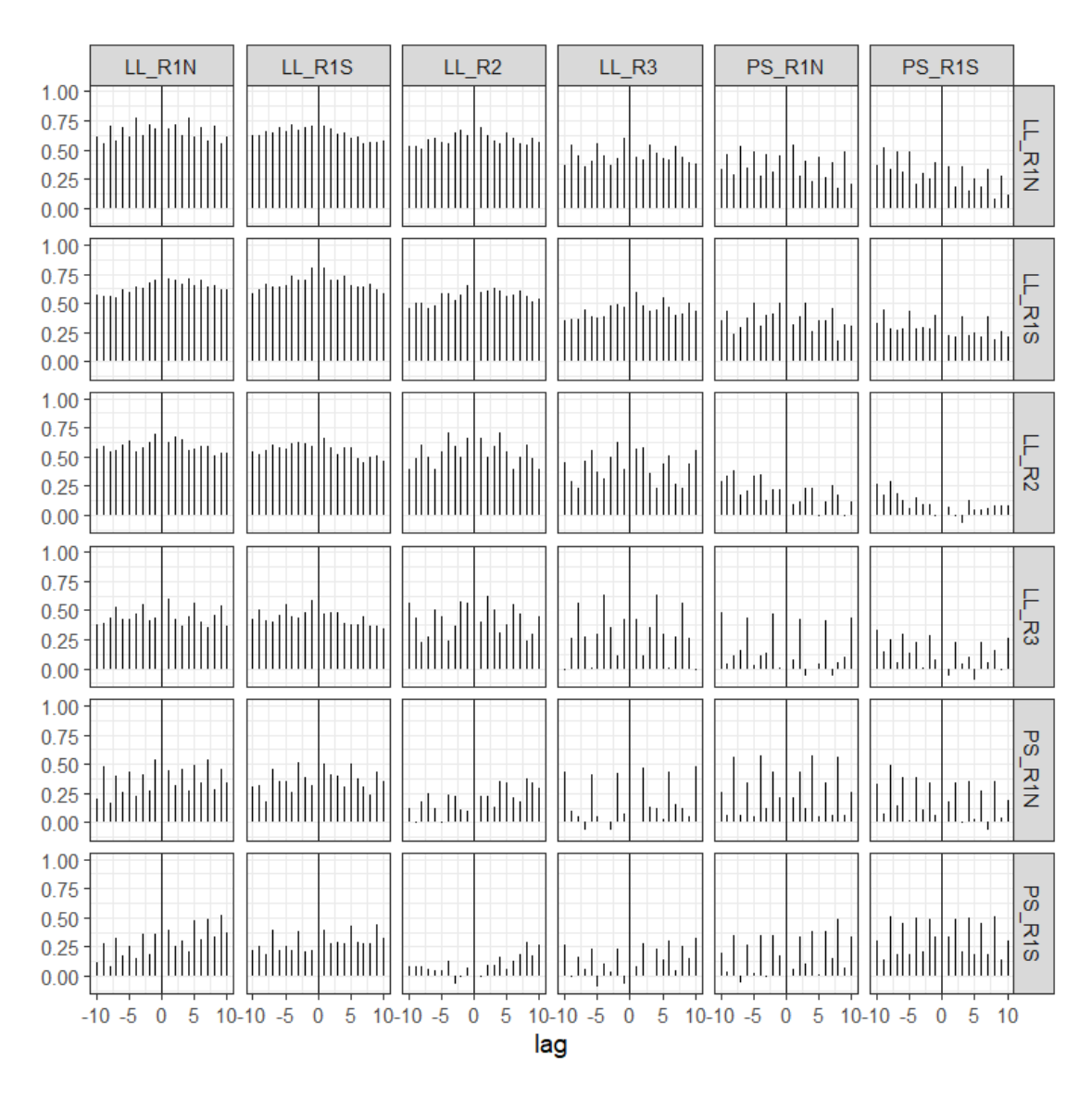


Figure B5 Cross-correlations between CPUE indices to identify lagged correlations (e.g., due to year-class effects). X-axis is lag number, and y-axis is cross-correlation.

APPENDIX C: DIAGNOSTIC TABLE FOR M SENSITIVITY RUNS

| Model | No. pars | Max gradient | Hessian invertible? | NLL | No. pars on bounds | Mohn rho SSB | Mohn rho F | Mohn rho Rec | Mohn rho Bratio | Trend in recdevs? |
|------------------------------|----------|-----------------|---------------------|---------|--------------------------|-----------------|---------------|-----------------|-----------------------|-------------------|
| 6_update_bias | 313 | < 1e-04 | FALSE | 1033.31 | 2 | -0.06 | 0.12 | 0.16 | -0.04 | FALSE |
| 6d_PSshort_MLorHam6Qest | 314 | < 1e-04 | FALSE | 1032.59 | 3 | -0.08 | 0.08 | 0.33 | -0.01 | FALSE |
| 6d_PSshort_MLorHam6Qestprior | 314 | < 1e-04 | FALSE | 1060.41 | 3 | -0.28 | 0.1 | 0.53 | -0.07 | FALSE |
| 6d_PSshort_MLorHam6Qhi | 313 | < 1e-04 | FALSE | 1041.93 | 2 | -0.03 | 0.09 | 0.3 | -0.02 | FALSE |
| 6d_PSshort_MLorHam6Qlo | 313 | < 1e-04 | FALSE | 1039.95 | 2 | 0.06 | 0.03 | 0.38 | -0.01 | FALSE |
| 6d_PSshort_MLorHam6Qshelt | 313 | < 1e-04 | FALSE | 1044.83 | 4 | -0.06 | 0.13 | 0.2 | -0.03 | FALSE |

APPENDIX D: DIAGNOSTIC TABLE FOR GRID MODELS

| Model | No. | Max | Hessian | NLL | No. pars | Mohn | Mohn | Mohn | Mohn | Trend in |
|-------------------------------|------|----------|-------------|---------|--------------|------------|-------|------------|---------------|----------|
| | pars | gradient | invertible? | | on bounds | rho SSB | rho F | rho Rec | rho Bratio | recdevs? |
| io_h70_Gnew_MBase2025_sD_LL | 313 | < 1e-04 | FALSE | 1042.3 | 3 | -0.01 | 0.11 | 0.09 | -0.01 | FALSE |
| io_h70_Gnew_MBase2025_sD_Qq | 313 | < 1e-04 | FALSE | 1027.25 | 2 | -0.03 | 0.11 | 0.2 | -0.03 | FALSE |
| io_h70_Gnew_MBase2025_sL_LL | 309 | < 1e-04 | FALSE | 1077.62 | 3 | -0.03 | 0.06 | -0.05 | -0.01 | FALSE |
| io_h70_Gnew_MBase2025_sL_Qq | 309 | < 1e-04 | FALSE | 1069.17 | 4 | 0.01 | 0.04 | 0.09 | 0.01 | FALSE |
| io_h70_Gnew_MLorHam6Qhi_sD_LL | 313 | < 1e-04 | FALSE | 1035.96 | 2 | -0.06 | 0.1 | 0.14 | -0.04 | FALSE |
| io_h70_Gnew_MLorHam6Qhi_sD_Qq | 313 | < 1e-04 | FALSE | 1033.81 | 2 | -0.03 | 0.05 | 0.27 | -0.03 | FALSE |
| io_h70_Gnew_MLorHam6Qhi_sL_LL | 309 | < 1e-04 | FALSE | 1057.06 | 2 | -0.04 | 0.09 | -0.08 | -0.02 | FALSE |
| io_h70_Gnew_MLorHam6Qhi_sL_Qq | 309 | < 1e-04 | FALSE | 1048.01 | 3 | -0.01 | 0.04 | 0.03 | -0.01 | FALSE |
| io_h70_Gnew_MLorHam6Qlo_sD_LL | 313 | 2.00E-04 | FALSE | 1049.71 | 1 | -0.02 | 0.05 | 0.19 | -0.01 | FALSE |
| io_h70_Gnew_MLorHam6Qlo_sD_Qq | 313 | 1.00E-04 | FALSE | 1033.3 | 3 | 0.04 | 0.02 | 0.43 | -0.03 | FALSE |
| io_h70_Gnew_MLorHam6Qlo_sL_LL | 309 | < 1e-04 | FALSE | 1109.85 | 4 | -0.01 | 0.03 | 0.18 | -0.01 | FALSE |
| io_h70_Gnew_MLorHam6Qlo_sL_Qq | 309 | < 1e-04 | FALSE | 1106.45 | 3 | 0.01 | 0 | 0.38 | 0.01 | FALSE |
| io_h80_Gnew_MBase2025_sD_LL | 313 | < 1e-04 | FALSE | 1031.34 | 2 | -0.04 | 0.08 | 0.18 | -0.03 | FALSE |
| io_h80_Gnew_MBase2025_sD_Qq | 313 | < 1e-04 | FALSE | 1034.75 | 3 | -0.08 | 0.12 | 0.28 | -0.07 | FALSE |
| io_h80_Gnew_MBase2025_sL_LL | 309 | < 1e-04 | FALSE | 1075.97 | 4 | -0.01 | 0.06 | -0.02 | -0.02 | FALSE |

| io_h80_Gnew_MBase2025_sL_Qq | 309 | < 1e-04 | FALSE | 1069.83 | 4 | 0 | 0.04 | 0.12 | -0.01 | FALSE |
|-------------------------------|-----|---------|-------|---------|---|-------|-------|------|-------|-------|
| io h80 Gnew MLorHam6Qhi sD LL | 313 | < 1e-04 | FALSE | 1076.81 | 4 | -0.11 | 0.11 | 0.3 | -0.07 | TRUE |
| | | | | | | | | | | |
| io_h80_Gnew_MLorHam6Qhi_sD_Qq | 313 | < 1e-04 | FALSE | 1045.2 | 4 | -0.02 | 0.04 | 0.43 | -0.02 | FALSE |
| io_h80_Gnew_MLorHam6Qhi_sL_LL | 309 | < 1e-04 | FALSE | 1055.88 | 2 | -0.01 | 0.07 | 0.02 | 0 | FALSE |
| io_h80_Gnew_MLorHam6Qhi_sL_Qq | 309 | < 1e-04 | FALSE | 1050.74 | 3 | 0.01 | 0.01 | 0.18 | 0 | FALSE |
| io_h80_Gnew_MLorHam6Qlo_sD_LL | 313 | < 1e-04 | FALSE | 1047.71 | 3 | -0.21 | 0.18 | 0.13 | -0.12 | FALSE |
| io_h80_Gnew_MLorHam6Qlo_sD_Qq | 313 | 0.0078 | FALSE | 1046.85 | 3 | -0.04 | 0.17 | 0.33 | -0.06 | FALSE |
| io_h80_Gnew_MLorHam6Qlo_sL_LL | 309 | < 1e-04 | FALSE | 1109.23 | 4 | 0.01 | 0.01 | 0.28 | 0 | FALSE |
| io_h80_Gnew_MLorHam6Qlo_sL_Qq | 309 | < 1e-04 | FALSE | 1106.5 | 3 | 0.03 | -0.02 | 0.41 | 0.01 | FALSE |
| io_h90_Gnew_MBase2025_sD_LL | 313 | < 1e-04 | FALSE | 1037.94 | 3 | -0.05 | 0.08 | 0.28 | -0.05 | FALSE |
| io_h90_Gnew_MBase2025_sD_Qq | 313 | < 1e-04 | FALSE | 1036.72 | 2 | -0.01 | 0.02 | 0.41 | -0.03 | FALSE |
| io_h90_Gnew_MBase2025_sL_LL | 309 | < 1e-04 | FALSE | 1075.93 | 4 | -0.01 | 0.05 | 0.01 | -0.01 | FALSE |
| io_h90_Gnew_MBase2025_sL_Qq | 309 | < 1e-04 | FALSE | 1065 | 2 | 0 | 0.04 | 0.14 | -0.02 | FALSE |
| io_h90_Gnew_MLorHam6Qhi_sD_LL | 313 | < 1e-04 | FALSE | 1086.08 | 3 | -0.08 | 0.09 | 0.44 | -0.05 | TRUE |
| io_h90_Gnew_MLorHam6Qhi_sD_Qq | 313 | < 1e-04 | FALSE | 1053.09 | 3 | 0.01 | 0.03 | 0.57 | 0.02 | TRUE |
| io_h90_Gnew_MLorHam6Qhi_sL_LL | 309 | < 1e-04 | FALSE | 1057.76 | 2 | -0.03 | 0.07 | 0.14 | -0.02 | TRUE |
| io_h90_Gnew_MLorHam6Qhi_sL_Qq | 309 | < 1e-04 | FALSE | 1056.09 | 4 | 0.01 | 0.02 | 0.35 | 0 | TRUE |
| io_h90_Gnew_MLorHam6Qlo_sD_LL | 313 | < 1e-04 | FALSE | 1042.18 | 2 | -0.08 | 0.16 | 0.23 | -0.07 | FALSE |
| io_h90_Gnew_MLorHam6Qlo_sD_Qq | 313 | < 1e-04 | FALSE | 1053.93 | 2 | -0.03 | 0.11 | 0.43 | -0.09 | FALSE |

| io_h90_Gnew_MLorHam6Qlo_sL_LL | 309 | < 1e-04 | FALSE | 1109.46 | 3 | 0.02 | 0 | 0.27 | 0.01 | FALSE |
|-------------------------------|-----|---------|-------|---------|---|------|-------|------|------|-------|
| io_h90_Gnew_MLorHam6Qlo_sL_Qq | 309 | < 1e-04 | FALSE | 1107.13 | 3 | 0.04 | -0.03 | 0.39 | 0.01 | FALSE |